学位論文

Study of the photosystem II photoinhibition: Analyses of repair processes

（光化学系 II 光阻害の研究：修復過程の精査）

平成 26 年 7 月　博士（理学）　申請

東京大学大学院理学系研究科

生物科学専攻

宮田　一範

Abstract

Light is indispensable to plants as energy source for photosynthesis. However, strong light inhibits photosynthesis. This phenomenon is called photoinhibtion. Kok (1956), the pioneer of photoinhibition studies, defined photoinhibition as the reduction of photosynthetic capacity induced by exposure to visible light. This definition is commonly used for photoinhibition in various photosynthetic organisms. The central feature of photoinhibition is inactivation of photosystem II (PSII) by light energy. Various mechanisms of the PSII photoinhibition have been propounded. Currently, the most plausible hypotheses are the excess energy hypothesis and two-step hypothesis. According to the excess energy hypothesis, excess light energy damages D1 protein in PSII. By the two-step hypothesis, ultra-violet or visible light inactivates the Mn cluster in the oxygen-evolving center (OEC) in PSII and subsequently light energy damages D1 protein. Studies based on these two hypotheses have been conducted actively. However, the arguments have not been settled yet. The consensus features of these hypotheses are as follows. The D1 protein possessing the PSII reaction center is damaged by light energy. The damaged D1 protein is replaced with D1 protein synthesized *de novo*. This repair activity is high. Therefore, a balance between the rate of photodamage to D1 protein and the rate of D1 protein turnover cycle determines the extent of net PSII photoinhibition. D1 protein turnover determines the PSII repair rate. The repair is not induced in the dark. It is also known that there is optimal light intensity for the repair. When incident light is low, apparent photoinhibition is not observed because the PSII repair rate matches the PSII damage rate.

The PSII photoinhibition occurs in plants, algae and cyanobacteria. Photosynthetic organisms cannot avoid the PSII pohotoinhibition and have the repair mechanisms. The repair processes in the chloroplast require light. Expression level of *psbA* mRNA increases in high light. Light-induced ΔpH across the thylakoid membrane is required to form the FtsH hexamer that is

involved in degradation of the D1 protein, and import of the D1 protein into the thylakoid membrane. Because, both the D1 protein degradation and its *de novo* synthesis require ATP. I estimated the amount of ATP for the repair of the D1 protein and other components. The amount of ATP needed for the PSII repair corresponded to 0.1-2% of the ATP produced by the photophosphorylation.

The rate constant of photodamage, k_{pi}, appears to depend on intensity of the incident light or the excess energy. While, the rate constants of repair, k_{rec}, is influenced by the incident PPFD as well as by the daily PPFD in the growth light environment. The energy used for recovery of the photoinhibited PSII can be saved by the decreasing excess energy. One of the processes that decrease excess energy is non-photochemical quenching (NPQ). The capacity for NPQ is different depending on the growth light environments. However, in many studies, plants grown in growth chambers have been used. In this study, I used cucumber plants grown in a growth chamber and some plant species from the field. k_{pi} and k_{rec} values in the field-grown plants showed strong dependences on the daily PPFD as was the case for the chamber-grown plants. When compared at a given daily PPFD level, the field-grown plants had higher NPQ and lower photochemical quenching coefficient than the chamber-grown plants. This was probably because the field-grown plants experienced stronger irradiance levels many times, while, the chamber-grown plants did not have such the experience.

The D1 protein turnover requires ATP, whereas, the repair process of Mn cluster does not. For the free manganese to be incorporated into the Mn cluster, light energy is needed. This process is called photoreactivation of the Mn cluster. In cucumber leaves, the Mn cluster loses Mn ions and is inactivated by dark-chilling treatment. The inactivated Mn cluster is reactivated by light energy. The light triggers an electron transfer in the PSII core complex. Especially, D1 protein is a key factor.

I hypothesized that the photoreactivation would depend on visible light wavelength. Actually, inactivated leaves were photoreactivated depending not only on light intensity but also on wavelength. The photoreactivation was most effective in weak light at 5-10 μmol m^{-2} s^{-1} irrespective of the wavelengths, blue, red or green. However, the extent of the photoreactivation differed depending on wavelength. The efficiency of reactivation of OEC was lowest in blue light while highest in green light. At middle or high PPFDs, the trends depending on wavelength were similar. At high PPFDs, there was hardly no reactivation of OEC in blue light, while considerable reactivation was observed in green light.

The repair process according to the two-step hypothesis is still unclear because the complete story of the repair process of the photoinhibition has not been clarified. Clarification of the actual state of the Mn cluster during the repair process in the photoinhibition is an important issue in the future.

Table of contents

Acknowledgements

I would like to express my sincere gratitude and appreciation to Professor Ichiro Terashima (The University of Tokyo), who gave thoughtful advice and continuous guidance throughout the study. I also wish to express my special thanks to Associate Professor Ko Noguchi for kind support and valuable guidance in statistics.

I am grateful to Associate Professor Hiroshi Ikeda (The University of Tokyo) for giving me a chance to study wild plants in the Himalayas. This study was supported by a Grant-in-Aid for Scientific Research, Research Project Number: 23255005. I am very indebted to the valuable comments and helps by Japanese and Nepali colleagues in the Himalayas.

I thank Dr. Akio Takenaka (National Institute for Environmental) and Dr. Kazukiyo Yamamoto (Nagoya University) for programming CanopOn 2 and LIA32, respectively. Without their software, this study would not have been possible.

I would thank Professor Masahiko Ikeuchi (The University of Tokyo), Professor Hajime Wada (The University of Tokyo) and Professor Tatsuru Masuda (The University of Tokyo) for critically examining my doctoral study and providing invaluable comments.

I am also grateful to Professor Takaaki Ono (Ibaraki University), Professor Kouki Hikosaka (Tohoku University), Assistant Professor Riichi Oguchi (Tohoku University), Assistant Professor Yukifumi Uesono (The University of Tokyo), Assistant Professor Haruhiko Taneda (The University of Tokyo), Mr. Masaru Kono (The University of Tokyo) and the members of Laboratory of Plant Ecology in The University of Tokyo for their kind helps.

I would like to acknowledge my family for their support throughout my education career.

Finally, I wish to extend my appreciation to Emeritus Professor Yoshimichi Hori (Ibaraki University), who triggered my ambition for plant physiological ecology.

Abbreviations

a	fraction of active PSII
a_t	a at a given time point
Abs_{leaf}	light absorptance of the leaf
ASL	above sea level
ATP	adenosine triphosphate
B_{photo}	difference in the CO_2 assimilation rate, expressed as ATP equivalents
b6f	cytochrome b_6f complex
C_{D1}	rate of ATP use per leaf area for the repair of D1 protein
C_{photo}	ATP production rate by the thylakoid reaction
$C_{photo14}$	ATP production rate by the thylakoid reaction in case of $14H^+$ / 3ATP
$C_{process}$	cost of turnover of one photodamaged D1 protein
C_{PSII}	rate of ATP use per leaf area for the repair of PSII
C_{resp}	ATP production rate per leaf area by the dark respiration
Chl	chlorophyll
Chl a	chlorophyll *a*
Chl b	chlorophyll *b*
$D1_{leaf}$	a number of D1 protein per leaf area
DCIP	dichlorophenol indophenol
DPC	diphenylcarbazide
E	east longitude
e^-	electron
E_{photon}	average photon energy of PAR
E_X	rate of excess energy transfer to closed PSII
E_Y	quantum yield of excess energy to closed PSII
F_o	minimal fluorescence
F_m	maximal fluorescence
F_s'	steady-state fluorescence in light
F_v / F_m	quantum yield of the open PSII of the dark-treated leaves
F_v' / F_m'	quantum yield of the open PSII in light
Fdx	ferredoxin
G	gain of photosynthesis rate
H^+	proton
HL	high light
I	intensity of light

I_0	assuming maximum PPFD
J_t	electron transfer rate
k_{pi}	rate constant of photodamage
k_{rec}	rate constant of repair
LED	light emitting diode
LHCI	light harvesting chlorophyll-protein complex I
LHCII	light harvesting chlorophyll-protein complex II
LL	low light
N	north latitude
NADP	oxidized form of nicotinamide adenine dinucleotide phosphate
NADPH	reduced form of nicotinamide adenine dinucleotide phosphate
NPQ	non-photochemical quenching
OEC	oxygen-evolving complex
OSR	open sky ratio
P	photosynthesis rate
P_{max}	maximum photosynthesis rate
PAR	photosynthetically active radiation
PC	plastocyanin
Pheo	pheophytin *a*
PPFD	photosynthetically active photon flux density
$PPFD_{cs}$	PPFD of the campsite
$PPFD_{LIAcs}$	maximum PPFD at the campsite, estimated with LIA32
$PPFD_{LIAos}$	imaginary completely open site at the same geographical location, estimated with LIA32
$PPFD_{LIAos\text{-}sample}$	imaginary completely open site at the same location of the sampling site, estimated with LIA32
$PPFD_{LIAsample}$	PPFD at the sampling site, estimated with LIA32
$PPFD_{os}$	PPFD at the completely open site
$PPFD_{sample}$	PPFD of the sampling site
PQ	plastoquinone
PSI	photosystem I
PSII	photosystem II
$PSII_{leaf}$	content of PSII reaction center
PSII-RC	PSII reaction center
qL	photochemical quenching coefficient according to the lake model
qP	photochemical quenching coefficient according to the puddle model

R_d	dark respiration rate
RC	reaction center
ROS	reactive oxygen species
t	time
TSR	daily total shortwave radiation
UV	ultra-violet
Y(NO)	yields of non-photochemical energy dissipation in closed PSII
Y(NPQ)	yields of non-photochemical energy dissipation
Y(PSII)	quantum yield of PSII photochemistry
Yz	tyrosine residue of the D1 protein
Δa	changes in *a*
Δt	changes in t
ϕ	initial slope
Φ_{ExC}	excess energy parameter
Φ_{PSII}	quantum yield of PSII photochemistry
Φ_{PSII}'	quantum yield of PSII electron transport in light
φ_{PSII}	ratio of absorbed light energy allocated to the PSII core
θ	curvature coefficient

General introduction

Plants transform physical energy of light to chemical energy

Ultimate energy source for plants is light. Plants can transform physical energy of light to chemical energy of ATP (adenosine triphosphate) and NADPH (nicotinamide adenine dinucleotide phosphate) and then the energy is stored in the form of carbohydrate. The process in which the light energy is captured and stored is defined as photosynthesis (Blankenship 2002). The organisms that are able to photosynthesize are called photosynthetic organisms, which include cyanobacteria, purple bacteria, green sulfur and non-sulfur bacteria, heliobacteria, various algae and plants. The photosynthetic organisms capture light energy with photosynthetic pigments. A photosynthetic pigment excited by the light energy relays its excitation energy to neighbouring pigments and eventually to the reaction center (RC), where the electron transport starts. The electron transport produces reducing equivalents such as NADPH and the gradient of electrochemical potential of proton (H^+) across the thylakoid membrane. The H^+ gradient is used in production of ATP. By these processes, light energy is converted to chemical energy of NADPH and ATP. The electron transport systems differ depending on the photosynthetic organisms. However, the basics of the process are conserved. In this study, I used angiosperms (a taxon of the land plants). In the plants, the electron transport is operated by thylakoid membrane intrinsic proteins, photosystem II (PSII), cytochrome b_6f complex (b6f) and photosystem I (PSI), and some intersystem electron carriers in the chloroplast.

Photosynthetic electron transport and ATP synthesis

To drive the electron transport, the plants need to capture light and relay the light energy to the RC. In PSII and PSI, the light energy is captured by the light harvesting chlorophyll-protein complex II (LHCII) and the light harvesting chlorophyll-protein complex I (LHCI), respectively.

The LHCII and LHCI possess chlorophyll *a* (Chl a) and chlorophyll *b* (Chl b), which absorb light and excited. The light energy (the excitation energy) is relayed in the LHCII or LHCI. Finally, the excitation energy is passed to RC in the PSII or PSI via chlorophylls in the PSII or PSI core complex.

In the PSII, light is captured mainly by the LHCII. The LHCII relays the light energy as the excitation energy, and passes it to chlorophylls in the core complex and eventually to the PSII-RC. The PSII-RC is P680 that is a special pair of Chl a molecules. P680 is excited by the excitation energy and becomes to $P680^*$, which has strong reducing power. The $P680^*$ immediately transfers electrons to pheophytin *a* (Pheo), and $P680^+$ thus formed is reduced by an electron from H_2O via the tyrosine residue in the D1 protein (Yz). In this event, the manganese (Mn) cluster in the oxygen-evolving complex (OEC) pulls out electrons from $2H_2O$ and releases O_2 and four protons into the thylakoid lumen. Pheo transfers electrons to a quinone electron acceptor, Q_A and then the electrons are transferred from Q_A to the second quinone electron acceptor, Q_B. Q_B transfers electrons to b6f via the plastoquinone (PQ) pool. PQs pump protons from the stroma to thylakoid lumen. The b6f transfers the electron to the PSI via plastocyanin (PC). The PSI reaction center, P700 is a special pair of Chl a molecules in the PSI and the light energy is provided by the LHCI, via PSI core complex. $P700^*$ reduces to electron carrier in the PSI. Finally, the electrons in the PSI are transferred to ferredoxin (Fdx) and the Fdx reduces $NADP^+$ ($+H^+$) to NADPH by Fdx-NADP oxidoreductase. The gradient of electrochemical potential of H^+ thus formed across the thylakoid membrane by the electron transport drives CF_0-CF_1 ATP synthase to produce ATP. The linear electron transport is driven by these two light dependent processes.

Photoinhibtion

As described above, light is the essential energy source for photosynthesis. However, strong incident light inhibits the photosynthesis. The inhibition is called photoinhibition. Kok, the pioneer of photoinbition studies, defined photoinhibition as the reduction of photosynthetic capacity induced by exposure to visible light (Kok 1956, Powles 1984). This definition is commonly used for photoinhibition of various photosynthetic organisms. The primary cause of photoinhibition is inactivation of PSII by light energy. Various mechanisms of the PSII photoinhibition have been propounded. Currently, popular hypotheses are the excess energy hypothesis (Ögren *et al*. 1984, Vass *et al*. 1992) and the two-step hypothesis (Hakala *et al*. 2005, Ohnishi *et al*. 2005). According to the excess energy hypothesis, excess light energy damages D1 protein in the PSII. On the other hand, the two-step hypothesis claims that ultra violet or visible light inactivates the Mn cluster in the OEC in PSII at first and then light energy damages the D1 protein.

In vivo, both mechanisms are involved in the PSII photoinhibition (Oguchi *et al*. 2009). The degree of the photoinhibition *in vivo* reflects the balance of the photodamage and the repair of PSII (Greer *et al*. 1986, Aro *et al*. 1993a). The both reactions, the photodamage and repair, are the first-order reactions. The rate constant for the photodamage is k_{pi} and that for the repair is k_{rec} (Kok 1956). Values of k_{pi} and k_{rec} depend on the incident light intensity during the photoinhibition treatment and the growth irradiance (Tyystjärvi *et al*. 1992). Many studies showed the effects of incident light intensity and growth irradiance. However, in most of the studies, constant light from artificial light sources is used for the photoinhibition treatment and plant growth. k_{pi} and k_{rec} have been never measured using field plants.

Excess energy hypothesis of PSII photoinhibition

The excess energy hypothesis includes two scenarios. One is the acceptor side hypothesis

(Vass *et al*. 1992). An electron cannot be transferred from Q_A to PQ pool when Q_B has been already reduced. When P680 is excited by light energy in this situation, the electron cannot be transferred to anywhere. An excited Chl, Chl^* near the P680 or $P680^*$ itself changes into the triplet excited state $^3Chl^*$ or $^3P680^*$. $^3Chl^*$ and $^3P680^*$ transfer their excitation to O_2. Then, O_2 changes into singlet oxygen ($^1O_2$). $^1O_2$, one of the reactive oxygen species (ROS), damages the D1 protein. The other is the donor side hypothesis (Callahan *et al*. 1986, Aro *et al*. 1993a). The electron transport from the Mn cluster to P680 delays when the thylakoid lumen is acidified. In this situation, when P680 and Yz change into $P680^+$ and Yz^+ the portion between $P680^+$ and Yz^+ is damaged. Because $P680^+$ plucks out an electron from its surrounding (a part of the D1 protein). This damage occurs even in the absence of O_2 (Jegerschöld and Styring 1991, Shipton and Barber 1991).

Two-step hypothesis of PSII photoinhibition

The two-step hypothesis (Hakala *et al*. 2005) includes the first step being proportional to H^+ irradiance and the second step by excess energy. The first step is the release of Mn ion from the Mn cluster induced by the light absorbed by a Mn(III) in the Mn cluster. The Mn(III) shows high absorbance in ultra-violet (UV) and blue regions. The second step is based on the donor side hypothesis mentioned above. The D1 protein in the PSII-RC is damaged by photosynthetically active light. Effective light is not only blue but also red because chlorophyll well absorbs light at these wavelengths.

Repair of the PSII photoinhibition by D1 protein turnover

Both of the hypotheses claim that the D1 protein possessing the PSII reaction center is damaged by light energy. The damaged D1 protein is replaced with a D1 protein synthesized *de*

novo. This repair rate is high. Therefore, the extent of net PSII photoinhibition is determined by a balance between the rate of photodamage to D1 protein and the rate of D1 protein turnover cycle. When incident light is low, photoinhibition is not apparent because the PSII repair rate matches the PSII damage rate. D1 protein turnover is particular by rapid (Greenberg *et al*. 1987). However, the repair does not occur in the dark. There is optimal light intensity for the repair (Chow *et al*. 2005).

The repair of photoinhibited D1 protein requires the protein turnover. The PSII photoinhibition occurs in plants, algae, cyanobacteria and photosynthetic bacteria. Photosynthetic organism cannot avoid the PSII photoinhibition. Thus, they have to evolve the repair system. The repair of photoinhibited D1 protein is constituted by degradation of photodamaged D1 protein and *de novo* synthesis, and insertion of the D1 protein. The D1 protein turnover involves various enzymes. Although these enzymes are somewhat different depending on the photosynthetic organisms, basic mechanisms are conserved. In this study, as noted above, I used angiosperms. Therefore, I summarize the turnover processes of angiosperms, below.

The electron transport through PSII does not occur when the photodameged D1 protein blocks the electron flow. Consequently, the photodameged D1 protein is needed to be removed from the inactivated PSII. The PSII forms a complex with the LHCII (PSII-LHCII). First of all, D1 protein, D2 protein and CP43 in the PSII are phosphorylated by STN8 (Vainonen *et al*. 2005). The phosphorylation of the PSII plays a role in identification of the inactivated PSII and separation of the inactivated PSII from the PSII-LHCII complex (Yokthongwattana and Melis 2006). When the phosphorylation is limited, the degradation rate of the photodamaged D1 protein is limited (Aro *et al*. 1992). The inactivated PSII is dephosphorylated and the photodameged D1 protein is degraded in the stroma thylakoid (non-appressed thylakoid)

(Rintamäki *et al*. 1996). The photodamaged PSII is degraded by ATP-dependent proteolysis by FtsH and ATP-independent proteolysis by Deg (Adam and Clarke 2002). The photodameged D1 protein is cleaved to 10 kD and 23 kD by Deg2 (Haußühl *et al*. 2001). Then, the 23 kD fragment is degraded by FtsH (Spetea *et al*. 1999, Lindahl *et al*. 2000) and the 10 kD fragment is degraded by Deg1, Clp etc. (Kato and Sakamoto 2009, Kato *et al*. 2012). In this regard, FtsH plays a major role in degradation of the photodamaged D1 protein and Degs may play subsidiary roles, because a Deg2 deficient mutant did not show any phenotype in relation to the photoinhibition (Huesgen *et al*. 2006, Kato *et al*. 2012).

After the photodameged D1 protein is removed from the PSII, the PSII requires a D1 protein synthesized *de novo*. The D1 protein is encoded in a chloroplast gene and synthesised by the chloroplast ribosome from the *psbA* mRNA. The newly-synthesised D1 protein is inserted into the PSII during the *de novo* D1 protein synthesis by the chloroplast gene coded translocon, cpSecY (Zhang *et al*. 2000, Zhang *et al*. 2001). The newly-synthesised D1 protein is matured by CtpA with processing on its C-terminal part (the peptide bond between 344 and 345 amino acids) (Inagaki *et al*. 2001). The processing is necessary for reassembly with CP43 and OEC (Diner *et al*. 1988, Baena-González and Aro 2002, Roose and Pakrasi 2004). The repaired PSII forms the PSII-LHCII complex and joins the electron transport in the grana thylakoid. The last process requires some proteins. However the precise roles of these proteins are unknown (Mulo *et al*. 2008).

The expression level of *psbA* mRNA increases in high light (Kettunen *et al*. 1997). Light-induced ΔpH formation of the thylakoid membrane is required for the formation of the FtsH hexamer and import of a newly-synthesised D1 protein into the thylakoid membrane (Yoshida and Yamamoto 2011, Zhang *et al*. 2000). The D1 protein degradation and biosynthesis processes require ATP. On the other hand, translation of *psbA* mRNA is prevented

by ROS (Nishiyama *et al*. 2001, Nishiyama *et al*. 2011). As a result, the repair of photodamaged D1 protein is inhibited at strong light probably because the ROS are readily formed (shown in CHAPTER 2). The energy needed for the recovery of PSII photoinhibition can be decreased through avoiding exposure to strong light (Raven 1989) and/or decreasing excess energy. One of the processes for decreasing excess energy is non-photochemical quenching (NPQ). Raven (2011) calculated the cost of photoinhibition including the strong light avoidance and the NPQ. The avoidance restricts temporal availability of light energy, however, the resources paid for the cost are shared by other processes. While the main scheme of NPQ is a xanthophyll cycle, the cost of non-photochemical excitation energy dissipation using the xanthophyll cycle is unknown. It is not yet possible to accurate calculation of the cost.

Repair of the PSII photoinhibition by Mn cluster photoreactivation

The D1 protein turnover requires ATP and ΔpH. However, the repair process of the Mn cluster requires neither of these. In this regard, incorporation of free manganese ion to the Mn cluster requires light energy (Ono and Inoue 1987, Tamura and Cheniae 1987). This process is called the photoreactivation of the Mn cluster. The Mn cluster loses Mn ions by the treatment with Tris or NH_2OH *in vitro*. The inactivated Mn cluster requires three factors for its reactivation (Ono 2001). Mn ion and Ca ion are needed (Tamura and Cheniae 1987). These are important constituents of the Mn cluster: Mn_4CaO_5 (Umena *et al*. 2011). Another important factor is visible light. In the dark, reactivation of the inactivated Mn cluster does not occur (Ono and Inoue 1982). The light triggers an electron transfer in the PSII core complex. This electron transfer oxidizes the PSII-RC. Then, a loosely associated Mn ion provides an electron to the PSII-RC and simultaneously the Mn ion is incorporated into the OEC (Tamura *et al*. 1991). These processes have been studied *in vitro*. However, Terashima *et al*. (1989) and Shen *et al*.

(1990) indicated that the photoreactivation can be studied in cucumber leaves. Lastly, D1 protein is a key factor. Yz and a number of amino acid residues of the D1 protein have roles in maintaining structure and function of the Mn cluster (Diner 2001, Debus 2001, Kimura and Ono 2006). Furthermore, other proteins of the PSII subserve the photoreactivation (Ishikawa *et al*. 2002). Ono (2001) summarized these processes in his review.

The photoreactivation starts by the process that a free Mn^{2+} unsteadily bounds to some acid residues of the D1 protein associated with the Mn cluster lacking in Mn ions. When electron transport occurs in the PSII by photosynthetically active light, the D1 protein losing electron plucks out electron from Mn(II) (it is originally from the free Mn^{2+}). Mn(II) is oxidized into Mn(III). Then, Mn(III), thus formed, bounds to the other Mn ions and thereby the Mn cluster is reactivated.

The photoreactivation is inhibited by H_2O_2 (Ono and Inoue 1987). If photoinhbition occurs by the two-step hypothesis, there is a possibility that ROS produced by the strong light inhibits the photoreactivation.

The study aims

In this study, I aimed at addressing three questions. First, can the photophosphorylation in the chloroplast well cover the amounts of ATP required to recover from the photoinhibition? I estimated the amount of ATP needed for repairing D1 protein and other components. Second, I examined effects of light during the photoinhibition treatment and the light environment during plant growth on the rate constants for photodamage and repair in the PSII photoinhibition. In such studies, researchers mainly use plants that are grown in continuous light provided by artificial light sources like fluorescent tubes. Do the field plants show the rate constant of photodamage and repair, different from those of growth-chamber grown plants? Thus, I used

not only the growth-chamber grown plants but also some field plants. According to the two-step hypothesis of the photoinhibition, the inactivation of the Mn cluster depends on light wavelength. Third, I examined light conditions for photoreactivation. I used cucumber leaves that had been chilled in the dark to deactivate the Mn clusters and examined the conditions for photoreactivation of the Mn cluster.

CHAPTER 2

Cost and benefit of the repair of photodamaged photosystem II in spinach leaves: Roles of acclimation to growth light.

Introduction

The energy cost of photoinhibition was estimated in some algae (Raven and Samuelsson 1986) and in vascular plants (Raven 1989, 2011). Raven (1989) calculated the extents of the photoinhibition and the cost of recovery from the photoinhibion for several forest-understory conditions including sunflecks. In Raven (2011), he considered not only the repair of the photodamaged D1 protein (including a lesser extent of D2 protein) but also costs of various mechanisms for avoidance of photoinhibition or photodamage. Furthermore, he estimated the comprehensive cost of the photoinhibition with repair and avoidance of the photodamage taking account of the various mechanisms. In this study, I aimed at providing more specific estimation of the cost of the turnover of D1 and some other proteins in PSII and the benefit from maintenance of the high photosynthetic activity brought about by the repair in higher plants. The method for determining the rate constant for photoinhibition and that for repair was developed and has been known for a long time (Kato *et al*. 2002a, Kok 1956, Wüschmann and Brand 1992). Kato *et al*. (2002a) showed that the sensitivity to photoinhibition, expressed as the rate constants of photodamage and repair, depended on growth light environments. I therefore examined effects of photosynthetic photon flux density (PPFD) during the plant growth on the sensitivity to photoinhibition.

In my study for the master's dissertation, the energy required for the repair of the photodamaged D1 protein (cost) was determined quantitatively. I detected photodamaged PSII by measuring the quantum yield of PSII using the chlorophyll fluorescence technique (Demmig and Björkman 1987). In the present study, I assessed the increase in the photosynthetic capability brought about by the repair of the photodamaged PSII (benefit) through the measurement of the photosynthesis rate. I compared the cost and the benefit quantitatively, because plants should benefit from the repair. As already mentioned above, I also examined

effects of growth PPFD on these rate constants, the cost, and benefit to know somewhat overlooked aspects in light acclimation of leaf photosynthesis. Furthermore, I discuss why the plants need to pay the cost of the repair of the photodamaged PSII, running a simple simulation of daily photosynthesis using the parameters obtained in this study.

Materials and methods

Plant materials

One-week-old seedlings of spinach (*Spinacia oleracea* L. 'Torai', Takii, Kyoto, Japan), germinated in vermiculite (Nittai vermiculite GL 30L, Nittai, Osaka, Japan) were transferred to containers (9.5 L in volume), each containing 8 L of the Hoagland's standard hydroponic solution. Plants were grown in a growth chamber, 8 h light / 16 h dark cycle at an air temperature of 23°C for at least one month. Mature leaves harvested from the plants grown for one to two months. PPFD just above the plants was adjusted either at 300 (high light, HL) or 120 (low light, LL) μmol m^{-2} s^{-1}. For the lower growth irradiance for LL plants, the plants were covered with black shade cloth (neutral shading). The light was supplied by a bank of cool white fluorescent tubes (FPR-96EXNA, Panasonic, Osaka, Japan). The Hoagland's standard hydroponic solution contained 4 mM KNO_3, 4mM $Ca(NO_3)_2$, 1.5 mM $MgSO_4$, 1.33 mM NaH_2PO_4, 0.05 mM Fe-EDTA, 0.01 mM $MnSO_4$, 1 μM $ZnSO_4$, 1 μM $CuSO_4$, 0.05 mM H_3BO_3, 0.5 μM Na_2MoO_4, 0.1 mM NaCl, and 0.2 μM $CoSO_4$. pH of the solution was adjusted to 6.0 (Epstein 1994). The solution was continuously aerated and was renewed every week.

Chlorophyll fluorescence measurements

Chlorophyll (Chl) fluorescence was measured with a PAM-101 fluorometer (Walz, Effetrich, Germany). The leaf was cut at the base of the petiole, and the petiole was cut in deionized water again to avoid embolism in the xylem. The leaves with their petioles in water in containers were kept in the dark for 30 min or more prior to the measurements of the minimal (F_o) and maximal (F_m) fluorescence. A saturating pulse at PPFD of 5000 μmol m^{-2} s^{-1} was given for 0.8 s to obtain F_m. The maximum photochemical efficiency of PSII photochemistry of the dark-treated leaves, Φ_{PSII}, were evaluated as F_v / F_m, where $F_v = F_m - F_o$ (Kitajima and Butler 1975, Krause and Weis

1991). The quantum yield of the open PSII in the light was determined as F_v' / F_m', where $F_v' = F_m' - F_o'$ (Genty *et al*. 1989). The prime (') indicates the fluorescence signal in the light. The photochemical quenching coefficient, qP, was calculated as $(F_m' - F_s')/(F_m' - F_o')$, where F_s' is the steady-state fluorescence in the actinic light (Schreiber *et al*. 1994). The quantum yield of PSII electron transport in the light (Φ_{PSII}') was calculated as $(F_m' - F_s')/(F_m')$ (Genty *et al*. 1989). The quantum yield of non-photochemical quenching, NPQ, was estimated as $(F_m - F_m')/(F_m')$ (Bilger and Björkman 1990). The quantum yield of excitation transfer to closed PSII in the light, defined as the excess energy (E_Y), was calculated as $(1 - qP) \times (F_v' / F_m')$ (Demmig-Adams *et al*. 1996, Stefanov and Terashima 2008). The rate of the linear electron transport, J_t, is expressed as:

$$J_t = \Phi_{PSII}' \times \varphi_{PSII} \times Abs_{leaf} \times I, \quad (1)$$

where φ_{PSII} is the ratio of absorbed light energy allocated to the PSII core. Abs_{leaf} is leaf absorptance (Genty *et al*. 1989). φ_{PSII} was assumed to be 0.5 and Abs_{leaf} was determined with a hand-made integrating sphere. I is PPFD of the white actinic light (400 − 3000 μmol m^{-2} s^{-1}). PPFD was measured with a quantum sensor (LI-190SA and LI-1000, LI-COR, Lincoln, NE, USA). A halogen lamp (KL1500LCD, Schott, Mainz, Germany) was used as continuous white actinic light. The rate of excess energy transfer to closed PSII, E_X, was estimated as:

$$E_X = E_Y \times \varphi_{PSII} \times Abs_{leaf} \times I \text{ (Kato } \textit{et al}\text{. 2003).} \quad (2)$$

Photoinhibitory treatments

The leaves were exposed to PPFD at 400, 800, 1600, or 3000 μmol m^{-2} s^{-1} to induce photoinhibition. Air temperature around the leaves was kept at 25°C using a fan. Light was

provided by a slide projector with a halogen lump (JC24V-250W; Kahoku Lighting Solutions, Miyagi, Japan). For PPFD of 3000 μmol m^{-2} s^{-1}, light was provided by a halogen lamp (KL1500LCD, Schott). The JC24V-250W and KL1500LCD measured in the laboratory showed almost identical light spectra (Fig. 1). PPFD was adjusted using neutral density filters (Toshiba, Tokyo, Japan). Heat was cut using a heat-ray cut filter (Cold filter; Optical Coatings Japan, Tokyo, Japan). The leaf temperature during the photoinhibition treatment at 1600 μmol m^{-2} s^{-1} for 2 h, measured with a thermocouple was around 26°C. After the photoinhibitory treatment, the leaves were placed in the dark for 30 min or more and then the quantum yield of PSII photochemistry was estimated as F_v / F_m. The repair process of the damaged PSII requires light and, thus, it hardly proceeds during the dark treatment (Chow *et al*. 2005).

To inhibit the repair process, I used lincomycin, an inhibitor of the chloroplast-encoded protein synthesis by 70S ribosome. Leaves were fed with 1 mM lincomycin solution, via their petioles for 1.5 − 3 h in the dark at 25°C. By weighing the leaf together with the container before and after the treatment, the amount of lincomycin solution absorbed was calculated. I used the leaves that had absorbed more than 1 mL of the 1 mM lincomycin solution / g leaf fresh weight. A preliminary study confirmed that the amount and concentration were sufficient to inhibit the D1 repair cycle (Fig. 2).

The rate constants of photodamage (k_{pi}) and repair (k_{rec})

The maximum quantum yield of PSII photochemistry (Φ_{PSII}) decreased depending on both duration of light treatment and irradiance. I calculated the rate constants of photodamage (k_{pi}) and repair (k_{rec}) from the decreasing rate of Φ_{PSII}. I followed the model that photodamage and repair occur concurrently and are described as the first-order reactions (Kok *et al*. 1956, Tyystjärvi *et al*. 1992). Assuming that the rates of photodamage and repair are proportional to

the concentration of active and inactivated PSII, respectively, the fraction of active PSII, *a*, is expressed as:

$$a = \frac{k_{pi} + k_{rec}\ \exp[-(k_{pi} + k_{rec}) \times t]}{k_{pi} + k_{rec}}, \qquad (3)$$

where *t* is illumination time. When lincomycin is added, k_{rec} is zero. Then eqn. 3 is simplified as:

$$a = \exp(-k_{pi} \times t). \qquad (4)$$

First, I determined k_{pi} from the time course of the decrease in F_v / F_m in the presence of lincomycin. With k_{pi} thus obtained, I determined k_{rec} from the time course of the decrease in F_v / F_m in the absence of lincomycin. The best-fit curves were obtained by the least squares method.

The PSII content

The content of PSII-RC ($PSII_{leaf}$) per unit leaf area was measured with a gas-phase oxygen electrode (LD-1, Hansatech, King's Lynn, UK) and a stroboscope with a xenon lamp (Fiber strobo FS-1J10, Nissin electronic, Tokyo, Japan) driven by a pulse generator (Model 575 Digital Delay / Pulse Generator, BNC, CA, USA) according to Chow *et al*. (1989). The leaf disk (10 cm^2) cut with a leaf punch was set in the gas-phase oxygen electrode and then determined the respiration rate in the dark. Subsequently, the leaf disk was exposed to 10 Hz saturating single turnover flashes (half decay time 4 μs) for 5 min. The concentration of PSII was determined from the rate of oxygen evolution and the number of flashes, assuming that O_2 is evolved every

4 single turnover flashes (Kok *et al*. 1970). The concentrations of CO_2 and O_2 in the leaf chamber were at about 5% and 15%, respectively. The CO_2 concentration at 5% is high enough to overcome closed stomata, saturate photosynthesis and suppress oxygenation of ribulose-1,5-bisphosphate by RuBisCO in leaf discs of mesic herbaceous plants (Terashima *et al*. 1988).

Calculation of costs

The repair of photodamaged PSII via the so-called D1 repair cycle requires energy cost. To calculate this cost, I needed to know the D1 protein turnover processes and the specific energy cost of each of these processes. In this study, I modified the schemes of the repair cycle proposed by Kato and Sakamoto (2009) and by Mulo *et al*. (2008) (Fig. 3). The specific energy cost of protein synthesis was estimated according to Noguchi *et al*. (2001a), which is a modified version of Zerihun *et al*. (1998) and more suitable for plant leaves. The number of amino acids of the spinach D1 protein was assumed to be 353 according to the NCBI (http://www.ncbi.nlm.nih.gov/protein/61230125). I also assumed that the number of amino acids of D1 protein does not change when D1 protein is photodamaged. The number of peptide bonds of D1 protein is '353 − 1'. The specific costs of these processes are summarized in Table 1. To calculate the cost on leaf area basis, I needed to know the number of D1 protein per leaf area ($D1_{leaf}$). Because each PSII complex has one D1 protein, I assumed that the measured value of the PSII content per leaf area equals that of D1 protein. The rate constant of repair, k_{rec}, expresses the rate of decrease in the fraction of the inactivated PSII, $1 - a$:

$$- d(1 - a) / dt = k_{rec} \times (1 - a). \quad (5)$$

Thus, the rate of increase in the fraction of the active PSII by the repair cycle is simply expressed as:

$$da / dt = k_{rec} \times (1 - a). \quad (6)$$

Eq. 6 expresses the rate of repair under the conditions where the photodamage and repair occur simultaneously when the inactivated PSII fraction is $1 - a$. I define the rate of ATP use per leaf area for the repair of D1 protein as C_{D1} (mol ATP m^{-2} s^{-1}). The C_{D1} consists of the number of D1 proteins repaired per unit time and the cost of turnover of one photodamaged D1 protein ($C_{process}$). Consequently C_{D1} is expressed as:

$$C_{D1} = D1_{leaf} \times k_{rec} \times (1 - a) \times C_{process}. \quad (7)$$

I compared C_{D1} with the ATP production rate per leaf area by the dark respiration (C_{resp} (mol ATP m^{-2} s^{-1})) or an ATP production rate by the thylakoid reaction (C_{photo} (mol ATP m^{-2} s^{-1})). C_{resp} was calculated from the dark respiration rates (R_d (mol m^{-2} s^{-1})) that were actually measured and an assumption, ATP / O_2 = 29 / 6 (Noguchi *et al*. 2001b). Thus, C_{resp} is expressed as:

$$C_{resp} = R_d \times (29 / 6). \quad (8)$$

C_{photo} was calculated from the electron transfer rate (J_t (mol e^- m^{-2} s^{-1})) that was estimated fluorometrically using eqn. 1. I assumed e^- / ATP = 1.33 based on that the whole chain electron transfer with Q cycle translocates $3H^+$ / e^- (von Caemmerer 2000) and that ATP is synthesized per $4H^+$ (H^+ / ATP = 4) as measured in spinach thylakoids (Berry and Rumberg 1996). In this study, I did not take account of the cyclic electron through PSI. Thus, C_{photo} is expressed as:

$$C_{photo} = J_t / 1.33. \quad (9)$$

I also adapted e^- / ATP = 1.56 based on H^+ / ATP = 4.67 (Blankenship 2002). This number is proposed because the number of the subunit III in CF_o in spinach chloroplast is 14 and thereby $14H^+$ / 3ATP = 4.67 (Seelert *et al*. 2000). I call this ATP production rate by the thylakoid reaction, $C_{photo14}$:

$$C_{photo14} = J_t / 1.56. \quad (10)$$

I also estimated an energy cost of the repair of the photodamaged PSII core. In practice, I considered protein turnover of D1, D2, CD43 and CP47. I did not deal with the OEC because information of the repair of OEC is scarce. I also assumed that the numbers of amino acids of D2, CD43 and CP47 proteins do not change when PSII is photodamaged. The degradation rate of D2 was about one third of that of D1 in *Spirodela oligorrhiza* (Jansen *et al*. 1999). A possibility of more rapid degradation of CP43 during the assembly step of PSII in the repair cycle was indicated in *Arabidopsis thaliana* (Ma *et al*. 2007, Mulo *et al*. 2008). On the other hand, CP43 degradation rate was more or less the same as that of D1 in isolated thylakoid of *Spinacia oleracea* (Yamamoto and Akasaka 1995). From these, I assumed that CP43 turnover occurs at the same rate as the D1 turnover. The decrease in the amount of CP47 was about 75% that of CP43 (Yamamoto and Akasaka 1995) in *Spinacia oleracea*. The numbers of amino acids of the spinach D2, CP43 and CP47 proteins were assumed to be 353, 473 and 508 according to the NCBI (http://www.ncbi.nlm.nih.gov/protein/131297, http://www.ncbi.nlm.nih.gov/protein/131286 and

http://www.ncbi.nlm.nih.gov/protein/19855072), respectively. The numbers of peptide bonds of D2, CP43 and CP47 proteins are '353 − 1', '473 − 1' and '508 − 1', respectively. Processing for mature D2, CP43 or CP47 proteins has not been established but the number of peptide bonds of the mature CP43 protein is 425. I supposed that the processing for mature CP43 protein similarly occur as that for D1. Therefore total energy costs of repair of D2, CP43 and CP47 would be 3175.04, 4210.44 and 4573.14 (excluding PSII phosphorylation). From these, the rate of ATP use per leaf area for the repair of PSII, C_{PSII} (mol ATP m^{-2} s^{-1}), is expressed by $C_{PSII} = 4.08 \times C_{D1}$.

Calculation of benefits

The repair of photodamaged PSII results in recovery of the photosynthesis rate. I assessed the benefit by measuring the increase in the photosynthesis rate brought about by the repair of the photodamaged PSII. I defined gain of the photosynthesis rate (G, mol CO_2 m^{-2} s^{-1}) as the difference between the photosynthesis rate with the active repair processes and the rate of photosynthesis in the absence of the repair processes. These photosynthesis rates were determined with a portable gas exchange system (LI-6400, LI-COR). The ambient CO_2 concentration with leaf chamber was 380 ppm and the leaf temperature was around 26°C. The rate of photosynthesis (P) is expressed by the non-rectangular hyperbolic function as:

$$P = \frac{(\phi \cdot I + P_{max}) - \sqrt{(\phi \cdot I + P_{max})^2 - 4\theta \cdot \phi \cdot I \cdot P_{max}}}{2\theta} - R_d, \qquad (11)$$

where ϕ, R_d, θ and P_{max} are the initial slope, the dark respiration rate, curvature coefficient and the maximum photosynthesis rate, respectively. Thus, the gain, G, is expressed as:

G = photosynthesis rate with repairing processes (mol CO_2 m^{-2} s^{-1}) – photosynthesis rate without repairing processes (mol CO_2 m^{-2} s^{-1}). (12)

The difference in the CO_2 assimilation rate, G is, then, expressed as ATP equivalents. The latter was defined as B_{photo}. Because G of 1 mol CO_2 m^{-2} s^{-1} corresponds to 1 / 6 mol glucose m^{-2} s^{-1}, and respiration of 1 mol glucose produces 29 mol ATP; B_{photo} is expressed as:

$$B_{photo} = G \times (1 / 6) \times 29. \quad (13)$$

I also compared B_{photo} and C_{D1}.

Simulation

I applied results of the present study to consider the ecological significance of light acclimation, in particular, that of the repair activity. Photoinhibition occurs throughout the day. I estimated *a* and the repair cost throughout a day using the results obtained in the experiments described above. Daytime PPFD was expressed as a sine square curve (Hirose and Werger 1987). Assuming maximum PPFD (I_0) at noon of 1600 μmol m^{-2} s^{-1} and day length was 12 h, I expressed I at a given time of day, *t*.

$$I(t) = I_0 \times \sin^2[\ \Pi \times (t - 6) / (12)] \ (6 \leq t \leq 18). \quad (14)$$

k_{pi} and k_{rec} were expressed as quadratic functions of PPFD (= I, Fig. 5). Since *a* in the daytime always changed, I calculated the changes in *a* (Δa) using the differential form of eqn. 3. Thus, the Δa during Δt (from $t - 1$ to t) was estimated as:

$$\Delta a = [-k_{pi} \times a_{t-1} + k_{rec} \times (1 - a_{t-1})] \times \Delta t. \quad (15)$$

Then, the a_t was estimated as:

$$a_t = a_{t-1} + \Delta a. \quad (16)$$

I assume $a_0 = 1$ at 6:00 in the morning. *a* thus determined for the daytime was used to calculate C_{D1} using the eqn. 7. I also calculated the rate of photosynthesis using *a*. *a* was used with the equations in Fig. 8 to obtain parameters in eqn. 11.

Statistical analysis

The two-sided Student's *t*-test was used to test the significant difference between HL and LL plants. The symbols as *, ** and *** in the tables and figures indicate significant differences at 10%, 5% and 1%, respectively.

Results

PSII contents

PSII contents, in HL and LL leaves, determined by the repetitive single turnover method, are shown in Table 2. The PS II content on a leaf area basis was greater in HL leaves than in LL leaves by 43%. PS II content per chlorophyll did not differ significantly between HL and LL leaves.

Photoinhibition in the presence or absence of lincomycin

The fraction of active PSII, *a*, at a given time was estimated as the ratio of F_v / F_m measured after the photoinhibitory treatment for the given time and the subsequent dark treatment for 30 min relative to F_v / F_m measured before the photoinhibitory treatment. Using *a* thus obtained, I calculated k_{pi} and k_{rec}. Changes in *a* in HL and LL leaves exposed to PPFD at 400 to 3000 μmol m^{-2} s^{-1} are shown in Fig. 4. In the absence of lincomycin, the leaves exposed to 400 μmol m^{-2} s^{-1} showed only small decreases even after the photoinhibitory treatment for 120 min (Fig. 4A and B). At 800 μmol m^{-2} s^{-1}, an appreciable decrease in *a* was observed by 30 min. Then, the decrease was slowed and *a* was around 0.95 at 120 min in both HL and LL leaves. At 1600 μmol m^{-2} s^{-1}, the decrease was initially rapid and then slowed. After the photoinhibitory treatment for 120 min, *a* was above 0.9 in HL leaves whereas it was below 0.9 in LL leaves (Fig. 4E and F). By the photoinhibitory treatment at the highest PPFD of 3000 μmol m^{-2} s^{-1}, *a* continued to decrease (Fig. 4G and H). After 30 min, *a* was around 0.8 in HL leaves while it was 0.72 in LL leaves.

In the presence of lincomycin, a potent inhibitor of protein synthesis by the 70S ribosome, the decreases in *a* were more marked at any PPFD than those in the absence of lincomycin. The decrease in *a* became more marked with the increase in the photoinhibitory PPFD. Although

HL and LL leaves were exposed to the same PPFD for the same time periods, *a* values were always smaller in LL leaves than in HL leaves (Fig. 4).

Because absorptance of PPFD was similar between HL leaves (81 ± 0.72%, mean ± S.D., n = 3) than LL leaves (79 ± 2.6%, n = 3), I at first plotted k_{pi} and k_{rec} against the incident PPFD (Fig. 5A and D). k_{pi} of both HL and LL leaves apparently increased exponentially with increasing PPFD. When the data points at PPFDs below 1600 μmol m^{-2} s^{-1} for HL and LL leaves were fitted by linear functions, there were clear positive intercepts on the abscissa, 215 and 246 μmol m^{-2} s^{-1} for HL and LL, respectively. k_{pi} values in LL leaves were greater than those in HL leaves. k_{rec} of HL and LL leaves increased with PPFD up to 1600 μmol m^{-2} s^{-1}. Toward the data points obtained with the highest PPFD, however, k_{rec} decreased in both HL and LL leaves.

Fluorescence parameters in the quasi-steady state, after 25 min from the onset of the photoinhibitory treatment, are shown in Table 4. I used 'quasi' because the photoinhibition was ongoing. F_v' / F_m' decreased with the increase in PPFD and the values were marginally greater in HL leaves than in LL leaves at 400 μmol m^{-2} s^{-1}. qP decreased with the increase in the PPFD, in particular, in LL. qL showed the similar trend, although qL was considerably smaller than qP (data not shown). Φ_{PSII}' decreased with the increase in the PPFD. When compared at the same PPFD, HL leaves showed greater Φ_{PSII}' than LL leaves. NPQ increased with the increase in the PPFD. At 400 and 800 μmol m^{-2} s^{-1}, NPQ was higher in LL leaves than in HL leaves. However, at 1600 and 3000 μmol m^{-2} s^{-1}, NPQ values in HL and LL leaves were similar. Similar trends were found in Y(NPQ) (data not shown). E_Y, quantum yield of excess energy, calculated as $(F' - F_0') / F_m'$, increased with PPFD. At 400 and 800 μmol m^{-2} s^{-1}, E_Y values were greater in LL leaves than in HL leaves. However, at 1600 and 3000 μmol m^{-2} s^{-1}, values in HL and LL leaves were similar.

k_{pi} of HL and LL leaves were plotted against the rate of excess energy transfer, E_X (Fig. 5B). For the data up to E_X of 150 μmol $m^{-2} s^{-1}$, the relationship between k_{pi} and E_X for HL leaves and that for LL leaves were very similar. The regression lines almost passed through the origin. Towards the highest E_X, the increases in k_{pi} were accelerated especially in LL leaves. k_{pi} values plotted against the rate of excess energy transfer corrected for the PSII content are also shown (Fig. 5C). Because the PS II content in LL leaves was lower than that in HL leaves (Table 2), data points for LL leaves lie below those for HL leaves.

The costs of D1 protein repair

The cost of repair per unit leaf area, C_{D1}, was estimated using the parameters of $D1_{leaf}$, k_{rec}, a and $C_{process}$ as:

$$C_{D1} = D1_{leaf} \times k_{rec} \times (1 - a) \times C_{process}.$$

The HL and LL leaves were exposed to light at 400, 800 and 1600 μmol $m^{-2} s^{-1}$ for 30 – 120 min. The costs required for repairing the damaged D1 protein at 30, 60, 90 and 120 min after the onset of the photoinhibitory treatment are shown in Fig. 6. The C_{D1} of both HL and LL leaves increased with the increase in PPFD. The C_{D1} of LL leaves were always smaller than those of HL leaves.

From the dark respiration rates of HL and LL leaves, 1.4 ± 0.48 (mean ± S.D., n = 5) and 0.77 ± 0.29 (n = 5) μmol CO_2 $m^{-2} s^{-1}$, the respiratory ATP production rates (C_{resp}) were calculated as 6.0 and 3.6 μmol ATP $m^{-2} s^{-1}$, respectively. C_{D1} / C_{resp} ratios at 400 μmol $m^{-2} s^{-1}$, were from 0.74 to 1.0 and 0.69 to 1.3% for HL and LL leaves, respectively. The ratios increased with the photoinhibitory treatment. At 800 μmol $m^{-2} s^{-1}$, ratios were 2.2 to 2.9 and 2.9

to 3.8% for HL and LL leaves. At 1600 μmol $m^{-2} s^{-1}$, C_{D1} / C_{resp} ratios for the HL and LL leaves were 6.1 – 6.8% and 7.9 – 9.5%, respectively.

The ratios of C_{D1} to the photophosphorylation rate C_{photo}, C_{D1} / C_{photo}, are shown in Fig. 7. I assumed the e^- / ATP ratio of 1.33. At 400 μmol $m^{-2} s^{-1}$, C_{D1} / C_{photo} ratios for the HL and LL leaves were 0.061 – 0.085% and 0.036 – 0.066%, respectively. At 800 μmol $m^{-2} s^{-1}$, C_{D1} / C_{photo} ratios ranged from 0.12 to 0.15% and from 0.11 to 0.14% for the HL and LL leaves, respectively. At 1600 μmol $m^{-2} s^{-1}$, C_{D1} / C_{photo} ratios for the HL and LL leaves were 0.35 – 0.40% and 0.29 – 0.35%, respectively. C_{D1} / C_{photo} for the LL leaves were always somewhat smaller than those of the HL leaves. I also calculated C_{D1} / $C_{photo14}$ assuming the e^- / ATP ratio of 1.56. Besides some uncertainty of the H^+ / ATP ratio, namely from 3 to 4.67, the repair requires far less than 0.5% of ATP produced by photophosphorylation.

The calculated C_{PSII} / C_{photo}, and C_{PSII} / $C_{photo14}$ are shown in Fig. 7. The repair requires less than 2% of ATP produced by photophosphorylation even at the incident PPFD of 1600 μmol $m^{-2} s^{-1}$.

The benefits of D1 protein repair

I obtained light-photosynthesis curves after the photoinhibitory treatment in the presence of lincomycin at PPFD of 1600 μmol $m^{-2} s^{-1}$ for 30, 60, 90 and 120 min. The non-rectangular hyperbolic function was fitted to each data set by the least squares method. Parameters of the non-rectangular hyperbolic curves were plotted against *a* (Fig. 8) to see whether the changes in the light response curves can be expressed as a function of *a*. The initial slope positively related to *a* in both the HL and LL leaves. The dark respiration rate in the HL leaves was not related to *a*, whereas, in the LL leaves, the dark respiration rate somewhat increased with the photoinhibitory treatment. The degree of curvature showed positive relationships with *a* in both

HL and LL leaves. The maximum photosynthesis rate was almost independent of *a* in both the HL and LL leaves. I expressed the initial slope, the degree of curvature and the dark respiration rate in HL and LL leaves as linear functions of *a* shown in Fig. 8. The maximum photosynthesis rates in HL and LL leaves were regarded as constants and 24.8 and 17.6 μmol CO_2 m^{-2} s^{-1}, respectively. These values were P_{max} of the non-rectangular hyperbolic functions fitted to the data obtained in the absence of lincomycin. Using these linear functions and constants, I obtained the model light response curve for various *a* values. The data for light response curves actually obtained and the curves calculated based on the *a* values are shown in Fig. 9. As detailed in the legend, the determination coefficients (R^2) for the curves calculated based on the *a* values were lower than those for the curves directly fitted to the measured data. Because the differences in R^2 were small, I used light-response curves calculated from *a* values for the analyses below.

The benefits brought about by the PSII repairing (B_{photo}) were determined from the calculated light response curves for leaf photosynthesis. B_{photo} values calculated at 30, 60, 90 and 120 min from the onset of the photoinhibitory treatments at three PPFD levels are shown in Fig. 10. The B_{photo} at a given time and a PPFD denotes the difference in the photosynthesis rate in the absence of lincomycin and that the presence of lincomycin. From Fig. 4, *a* values were adapted, the corresponding light response curves and the differences in the photosynthesis rates were calculated. Then, the difference in the rate of photosynthesis was converted to that in ATP production rate. B_{photo} of both the HL and LL leaves increased with PPFD and time. B_{photo} of HL leaves were greater than those of the LL leaves at any PPFD at any time. The largest difference in B_{photo} between the HL and LL leaves was observed at 1600 μmol m^{-2} s^{-1} at 120 min, B_{photo} of the HL leaves was about 2760 μmol ATP m^{-2} min^{-1} and that of the LL leaves was about 2090 μmol ATP m^{-2} min^{-1}.

The ratios of B_{photo} to C_{D1} were also calculated (Fig. 10C and D). B_{photo} / C_{D1} of both the HL and LL leaves decreased with the increase in the incident PPFD. The ratio increased with the increase in the photoinhibitory period. At 400 μmol m^{-2} s^{-1}, B_{photo} / C_{D1} of the LL leaves were markedly larger than that of the HL leaves. At 800 and 1600 μmol m^{-2} s^{-1}, B_{photo} / C_{D1} ratios in HL leaves were slightly greater than those in LL leaves.

Simulation of daily photosynthesis

Changes in the fraction of active PSII (*a*) in the daytime in the HL and LL leaves are shown in Fig. 11A. The maximum irradiance at noon was assumed to be 1600 μmol m^{-2} s^{-1}. The lowest *a* of the HL and LL leaves occurred at noon. The LL leaves always showed lower *a* than the HL leaves. The dashed lines show the photosynthesis rates under the conditions where the repair of the photodamage did not occur. At around 14:20 and 13:20, *a* of both HL and LL leaves became 0.2.

Changes in C_{D1} in the daytime in the HL and LL leaves are shown in Fig. 11B. The highest C_{D1} of the HL and LL leaves occurred at noon. The HL leaves always showed higher C_{D1} than the LL leaves. The integrated values of C_{D1} for 12 h from 6:00 to 18:00 for the HL and LL leaves were 7940 and 6400 μmol ATP m^{-2} day^{-1}, respectively.

Changes in the photosynthesis rates are shown in Fig. 11C. When no photoinhibition was assumed, the highest photosynthesis rates at 12:00 in the HL and LL leaves were 22.2 and 16.4 μmol m^{-2} s^{-1}, respectively. When photoinhibition occurred and was repaired, the maximum photosynthesis rate of HL was 20.8 μmol m^{-2} s^{-1} at around 11:50, whereas the maximum of LL was 15.3 μmol m^{-2} s^{-1} appeared around 11:40. The integrated net photosynthesis rate for 12 h in the daytime of the HL and LL leaves under non-photoinhibited and photoinhibited (shown in parentheses) conditions were 658 (615) and 516 (479) mmol CO_2 m^{-2} day^{-1}, respectively. The

photosynthesis rates in the photodamaged with no repair activity increased towards about 9:00 but then slowly decreased to zero at around 16:15 and 15:15 in HL and LL, respectively. I used the quadratic regression curves from the zero to 3000 μmol m^{-2} s^{-1} for these calculations. However, when linear regressions of k_{pi} and k_{rec} upto 1600 μmol m^{-2} s^{-1} were used, I obtained similar results. The integrated net photosynthesis rate for 12 h in the daytime of the HL and LL leaves with photoinhibition were 615 and 466 mmol CO_2 m^{-2} day^{-1}, respectively.

Changes in the integrated photosynthesis rates in daytime as a function of k_{rec} are shown in Fig. 12. I used the quadratic regression curves from the zero to 3000 μmol m^{-2} s^{-1} for calculating k_{rec} and the obtained functions were multiplied by 0, 1/8, 1/4, 1/2, 1, 2 and 4. The integrated photosynthesis rates in HL and LL increased with the increase in k_{rec} and then virtually reached plateaux at 1 × k_{rec}. The integrated photosynthesis rates in HL and LL did not increase much with the further increase in k_{rec}.

Discussion

Photoinhibition

Leaves get photoinhibited when they are exposed to excess visible light (Kok 1956, Powles 1984). Currently, there are two hypotheses for the mechanisms of PSII photoinactivation. One is called the excess hypothesis. In this hypothesis, excess energy that is delivered to closed PSII reaction center is supposed to enhance production of reactive oxygen species (ROS), in particular, singlet oxygen, which cause damage to PSII (Ogren *et al*. 1984, Vass *et al*. 1992). Second is the two-step hypothesis. In this hypothesis, Mn in the oxygen evolution system in PSII is the first target and is released on excitation by UV or blue light and subsequently PSII reaction centre is damaged (Hakala *et al*. 2005, Ohnishi *et al*. 2005). According to the excess hypothesis, if there is no excess energy, photoinhibition will not occur. However, the two-step hypothesis suggests that photoinhibition occurs directly proportional to absorbed PPFD irrespective of the presence of the excess. The conflicting arguments have not been settled yet. Oguchi *et al*. (2011a) suggested that both mechanisms occur under physiological conditions (for a review, see Oguchi *et al*. 2011b).

The present results support the excess energy hypothesis. k_{pi} in both HL and LL leaves linearly increased with the PPFD up to 1600 μmol m^{-2} s^{-1} but showed clear intercepts at around 200 – 250 μmol m^{-2} s^{-1} (Fig. 5A). On the other hand, k_{pi} was proportional to the excess energy up to 150 μmol m^{-2} s^{-1}, although the slope increased towards 300 μmol m^{-2} s^{-1} (Fig. 5B). The further increase indicates that the photodamage does not solely depend on the excess energy. Because concentrations of ROS would be high at very high PPFD, involvement of ROS other than the singlet oxygen produced in response to the excess energy (Vass 2011) may be probable (Aro *et al*. 1993b). When blue light was used as the photoinhibitory light, PSII photodamage was observed even at very low PPFDs that hardly induced the excess in *Capsicum annuum* L.

leaves (Oguchi *et al*. 2009). From the present results together with the previous reports, the mechanisms of the photodamage may differ depending on the photoinhibitory light conditions. These conditions may be categorized into three. In low light where there is no excess energy but there is blue light, the two-step mechanism would prevail. In medium to high light, contribution of the excess energy in PSII photodamage would increase. In very high light, such as the present photoinhibitory light at 3000 μmol $m^{-2} s^{-1}$, some other effects possibly those of ROS would be superimposed.

k_{rec} plotted against PPFD increased up to 1600 μmol $m^{-2} s^{-1}$ but decreased toward the highest PPFD (Fig. 5D). This means that k_{rec} has a peak. Similar results were also obtained in the previous studies (Kato *et al*. 2002a, Chow *et al*. 2005). Importantly, it has been revealed that ROS do not accelerate the PSII photodamage but inhibits the repair process (Nishiyama *et al*. 2001, 2004, Takahashi and Badger 2011). Thus, high light energy probably decreases k_{rec} through enhancing ROS production.

There was a difference in the sensitivity to photoinhibtion between the HL and LL leaves. At 400 μmol $m^{-2} s^{-1}$, HL and LL leaves were photoinhibited similarly (Fig. 4A and B) and k_{pi} were not different (Fig. 5A). However, at or above 800 μmol $m^{-2} s^{-1}$, quantum yield of PSII were always lower (Fig. 4C – H) and k_{pi} were greater (Fig. 5A) in LL leaves than in HL leaves. In particular, at 1600 μmol $m^{-2} s^{-1}$ and 3000 μmol $m^{-2} s^{-1}$, k_{rec} of the LL leaves were smaller than these of the HL (Fig. 5D). Consequently, the LL leaves were more susceptible to the photoinhibition, despite neither the absorbed PPFD nor excess energy levels were very different between LL and HL leaves (Öquist *et al*.1992, Aro *et al*. 1993b, Park *et al*. 1996). This would be attributed to lower PSII content in LL leaves (Table 2). When k_{pi} was plotted against the rate of excess energy transfer per PSII (Fig. 5C), HL leaves showed even greater k_{pi} at any E_X / PSII.

At any photoinhibitory PPFD, k_{rec} was always greater in HL leaves than in LL leaves (Fig.

5D). In particular, k_{rec} of the HL leaves at 400 μmol $m^{-2} s^{-1}$ was much greater than that in LL leaves. These differences would be attributed to the results of acclimation to growth light. The abundance of the D1 protein repair machinery was, probably, considerably lower in LL leaves than in HL leaves.

The costs of D1 protein repair

For recovery from photodamage, leaves should spend energy. The energy source has never been apparent. However, because k_{rec} was almost zero in the dark (Chow *et al*. 2005), there would be some light-dependent process. Then, it is unlikely that ATP produced by mitochondria in the night is mainly used to repair photodamaged D1 protein. Probably, ATP produced via photosynthetic electron transport is preferentially used. C_{D1} / C_{photo} and C_{D1} / $C_{photo14}$ of both the HL and LL leaves were less than 0.5% because total ATP production due to photophosphorylation is copious compared with C_{D1}. The repair cycle does not use energy insomuch as C_{D1} affects photosynthesis as was pointed out by Raven (1989). In other words, D1 protein turnover is super-efficient in keeping photosynthetic capability because C_{D1} is extremely low compared with the total ATP production through photophosphorylation.

Although the repair costs were relatively small, effects of acclimation to growth light environment appear to be crucial. When compared at a given PPFD, k_{pi} was smaller in HL leaves than in LL leaves, due to lower E_Y (Table 4) realized by their higher photosynthetic capacity and abundant PSII per leaf area. On the other hand, k_{rec} was greater in HL leaves (Fig. 5). In the absolute sense taking account of the difference in PSII content, the repair acitivity in HL leaves was much higher. By these, HL leaves were able to keep (1 – *a*) small, which would contribute much to maintenance of the high photosynthesis rate as well as low C_{D1} (Fig. 11). On the other hand, LL leaves showed high k_{pi}. However, when dependences of k_{pi} on E_X / PSII were

compared, LL leaves tended to show lower k_{pi} (Fig. 5C). Although this cannot be fully explained at this stage, shade type chloroplasts in LL leaves with a greater PSII connectivity could play some roles.

With respect to C_{PSII}, if ATP produced via photosynthetic electron transport is preferentially used, C_{PSII} / C_{photo} and C_{PSII} / $C_{photo14}$ of both the HL and LL leaves would be less than 2%. These ratios could be still overestimated. In the repair cycle of D1 protein, I have not taken account of the processes without using ATP, such as proteolysis by Deg proteases (Haußühl *et al*. 2001, Huesgen *et al*. 2006, Itzhaki *et al*. 1998, Kapri-Pardes *et al*. 2007, Sun *et al*. 2007), because these processes are not evaluated *in vivo*. Since the one of main processes that require ATP is proteolysis, the Deg proteases would save the cost in the repair cycle. Furthermore, if the repair processes of other proteins in PSII employ similar proteases, the cost of repair of damaged PSII will be much saved as well.

The benefits of D1 protein repair

The plants should obtain a benefit when they invest energy cost in repairing the photodamaged PSII. If the benefit was smaller than the energy needed for repair, the repair of the photodamaged PSII would not occur. In this study, I determined the benefit from the difference between the photosynthesis rate with repairing processes and that in the absence of repairing processes. Then, I compared the benefit with the cost.

In the measurement of the photosynthesis rate for determining the benefits, some parameters of the photosynthetic light response curves decreased with increasing photoinhibition (Fig. 8). The similar results were obtained in *Chenopodium album* (Hikosaka *et al*. 2004).

B_{photo} of both the HL and LL leaves increased with PPFD. B_{photo} / C_{D1} values were as high as 3500 – 27000% (Fig. 10C and D). The increase in the PPFD caused the increase in the cost (Fig.

6) but it also increased the photosynthesis rate (Fig. 9) and thereby the benefit (Fig. 10A and B). By the data of C_{D1} / C_{photo} and B_{photo} / C_{D1}, I confirmed that the repair of the photodamaged PSII by the D1 protein turnover enables the photosynthesis rate to be high. There was a difference in B_{photo} and B_{photo} / C_{D1} between HL and LL leaves. B_{photo} of HL leaves were greater than those of LL leaves due to higher photosynthesis rates in HL leaves (Fig. 9). On the other hand, at 400 μmol m^{-2} s^{-1}, B_{photo} / C_{D1} of the LL leaves was greater than that of HL leaves (Fig. 10C and D). This is because k_{rec} of the HL leaves was larger than that of the LL leaves (Fig. 5D). These would suggest the possibility that HL leaves are more suited for the PSII repair in high light. However, at 800 and 1600 μmol m^{-2} s^{-1}, B_{photo} / C_{D1} in HL and LL leaves were very similar. Thus, light acclimation would result in converged B_{photo} / C_{D1}, by adjusting the concentrations of photosynthetic components including PSII, the repair activities, photosynthesis rates and E_X.

Simulation of daily photosynthesis

I simulated the changes in *a*, C_{D1} and the photosynthesis rate on a fine day using the parameters obtained in this study (Fig. 11). *a* of the LL leaves decreased with time with the increase in PPFD in the morning because LL leaves had higher sensitivity to the photoinhibition due to their higher k_{pi} and lower k_{rec} than HL leaves (Fig. 5). C_{D1} of the HL leaves increased with time in the morning because the HL leaves had higher k_{rec} (Fig. 5D) and used larger cost (Fig. 6) than LL leaves. Fig. 11C shows that the photosynthesis rates were also affected, and the maximum and integrated photosynthesis rates were decreased considerably by photoinhibition. The influences of the photoinhibition on the photosynthesis rate were large. Hence, I need to consider photoinhibition when I simulate the daily photosynthesis rate. *a* and the photosynthesis rate in the leaves without repair activity (Fig. 11A and C) showed that the photosynthetic capability of the plants was decreased after 9:00. Thus, the photodamage is a serious problem

for the plants and this is the reason why plants invest the energy for repairing. These simple simulations clearly showed how and why the plants acclimate to high light environment, and what a burden light energy forces the plants to bear.

I also calculated the integrated photosynthesis rates in daytime with various calculatd k_{rec} (Fig. 12). The integrated photosynthesis rates in HL and LL leaves increased with increasing the relative value of k_{rec}. However, the integrated photosynthesis rates in both leaves reached the plateaux with the actual k_{rec}. This result indicates that the photosynthetic activity could not be fully restored even if the plant increased k_{rec} to the extraordinarily high level. These simulation results indicated that the plants have the optimum k_{rec} for keeping the photosynthetic activity.

Table 1 The repair cycle processes and the specific energy costs

Process	Energy costs (mol ATP mol^{-1} D1)
PSII phosphorylation	1 × 3
Damaged D1 protein biodegradation	1 × 343
New D1 protein biosynthesis	
Amino acid activation	2 × 352
Error correction	0.16 × 352
Peptide bond formation and translocation	2 × 352
Tool maintenance	0.36 × 352
Amino acid turnover	3.5 × 352
Processing for mature D1 protein	1 × 1
Total	2827.04

PSII phosphorylation occurs on three proteins in the photodamaged PSII. In degradation of a damaged D1 protein, 343 peptide bonds in D1 protein are cut. *De novo* D1 protein biosynthesis requires 352 peptide bonds. In this study, I used the maximal specific energy costs proposed by Noguchi *et al*. (2001a). This includes the cost of amino acid turnover. Because I estimated for a prolonged time, the amino acid turnover should be relevant. Processing mature D1 protein occurs on 1 peptide bond. Total cost required is 2827.04 mol ATP mol^{-1} D1.

Table 2 The content of PSII in spinach leaves

	The content of PSII	
	per leaf area（μmol m^{-2}）	per 1000 Chl（mmol mol^{-1} Chl）
HL	1.67 ± 0.165	3.71 ± 0.635
LL	1.17 ± 0.0281	3.14 ± 0.452
P	0.0376 **	0.420

HL, HL leaves; LL, LLleaves. Date are means ± SD; n = 3.

Table 3 The rate constants of photodamage (k_{pi}) and repair (k_{rec})

PPFD		k_{pi} (min^{-1})	k_{rec} (min^{-1})
400	HL	$0.82 \times 10^{-3} \pm 0.022 \times 10^{-3}$ (R^2: 0.99)	$4.0 \times 10^{-2} \pm 0.31 \times 10^{-2}$ (R^2: 0.93)
	LL	$0.91 \times 10^{-3} \pm 0.025 \times 10^{-3}$ (R^2: 0.99)	$2.3 \times 10^{-2} \pm 0.26 \times 10^{-2}$ (R^2: 0.91)
	P	0.81	0.013 **
800	HL	$2.3 \times 10^{-3} \pm 0.072 \times 10^{-3}$ (R^2: 0.99)	$4.7 \times 10^{-2} \pm 0.60 \times 10^{-2}$ (R^2: 0.82)
	LL	$2.6 \times 10^{-3} \pm 0.049 \times 10^{-3}$ (R^2: 0.99)	$4.5 \times 10^{-2} \pm 0.28 \times 10^{-2}$ (R^2: 0.95)
	P	0.072 *	0.72
1600	HL	$5.7 \times 10^{-3} \pm 0.12 \times 10^{-3}$ (R^2: 0.99)	$6.7 \times 10^{-2} \pm 0.30 \times 10^{-2}$ (R^2: 0.97)
	LL	$6.9 \times 10^{-3} \pm 0.21 \times 10^{-3}$ (R^2: 0.99)	$5.3 \times 10^{-2} \pm 0.45 \times 10^{-2}$ (R^2: 0.91)
	P	0.027 **	0.17
3000	HL	$16 \times 10^{-3} \pm 0.77 \times 10^{-3}$ (R^2: 0.98)	$6.1 \times 10^{-2} \pm 0.48 \times 10^{-2}$ (R^2: 0.98)
	LL	$19 \times 10^{-3} \pm 0.93 \times 10^{-3}$ (R^2: 0.98)	$4.7 \times 10^{-2} \pm 0.86 \times 10^{-2}$ (R^2: 0.94)
	P	0.61	0.27

Each data point in Fig. 4 was obtained as the mean of the data obtained for these leaves. I randomly selected one from each data point and using five data (for 3000 μmol m^{-2} s^{-1}, from data obtained) thus selected, obtained the k_{pi} value by the least square method. Thus, for one growth light condition (HL or LL) at one PPFD, three k_{pi} values were obtained. k_{rec} were obtained with randomly selected *a* values at four or five time points and the mean k_{pi} value. *P* was calculated with mean values (n = 3) of the rate constants thus obtained for HL and LL. It had little difference with the rate constants from mean values of *a*. HL, HL leaves; LL, LL leaves. Date are means ± SE (n = 3). Determination coefficients (R^2) are also shown.

Table 4 Fluorescence parameters of spinach leaves 25 min after the onset of irradiation

PPFD		F_v' / F_m'	qP	Φ_{PSII}'	NPQ	E_Y
400	HL	0.70 ± 0.016	0.87 ± 0.031	0.61 ± 0.015	0.39 ± 0.034	0.092 ± 0.024
	LL	0.68 ± 0.033	0.84 ± 0.024	0.57 ± 0.036	0.55 ± 0.083	0.11 ± 0.015
	P	0.069 *	0.066 *	0.054	0.0023 ***	0.079 *
800	HL	0.61 ± 0.043	0.76 ± 0.041	0.46 ± 0.033	0.94 ± 0.16	0.15 ± 0.031
	LL	0.57 ± 0.056	0.66 ± 0.042	0.38 ± 0.040	1.3 ± 0.23	0.19 ± 0.035
	P	0.16	0.00013 ***	0.0070 ***	0.019 **	0.0013 ***
1600	HL	0.42 ± 0.053	0.50 ± 0.073	0.21 ± 0.052	2.3 ± 0.18	0.21 ± 0.018
	LL	0.41 ± 0.037	0.42 ± 0.075	0.17 ± 0.039	2.3 ± 0.25	0.24 ± 0.030
	P	0.71	0.17	0.15	0.90	0.14
3000	HL	0.36 ± 0.040	0.34 ± 0.026	0.12 ± 0.022	2.9 ± 0.16	0.24 ± 0.017
	LL	0.32 ± 0.0083	0.26 ± 0.016	0.084 ± 0.0077	2.9 ± 0.23	0.24 ± 0.00059
	P	0.38	0.13	0.21	0.96	0.99

HL, HL leaves; LL, LL leaves. The fluorescence parameters measured 25 min after the onset of irradiation at PPFD of 400, 800, 1600 and 3000 μmol m^{-2} s^{-1} are shown. Date are means ± SD; $n \geq 3$.

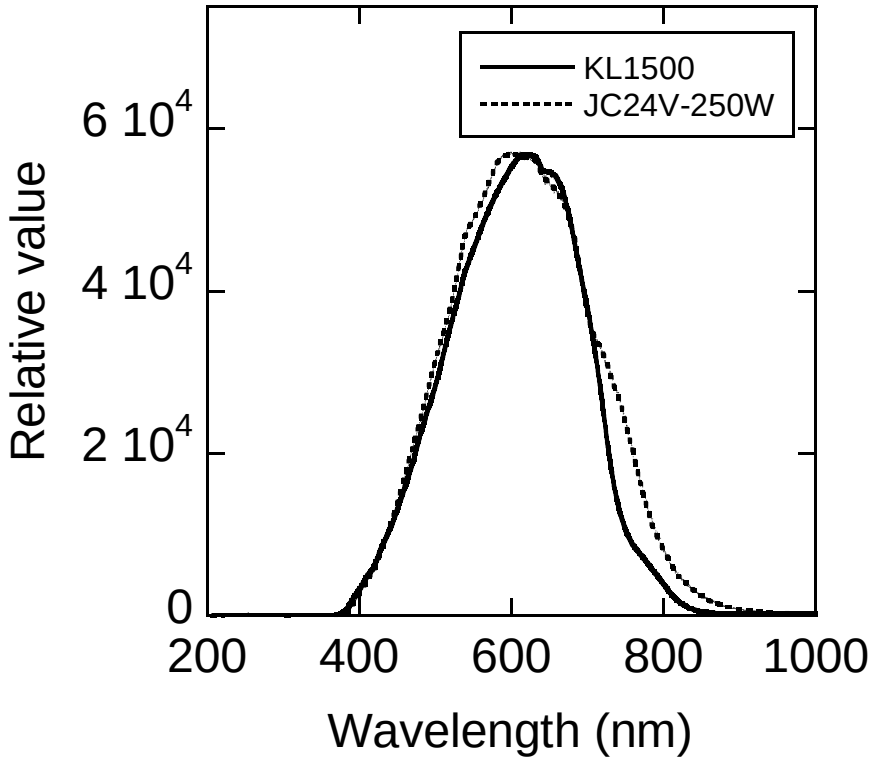

Fig. 1 Emission spectra of the two halogen lamps used in this study. The spectra were measured with a spectrophotometer (Mini-spectrometer, C10083CAH; Hamamatsu Photonics, Hamamatsu, Japan). Solid line, KL1500LCD; dotted line, JC24V-250W. Relative values are shown.

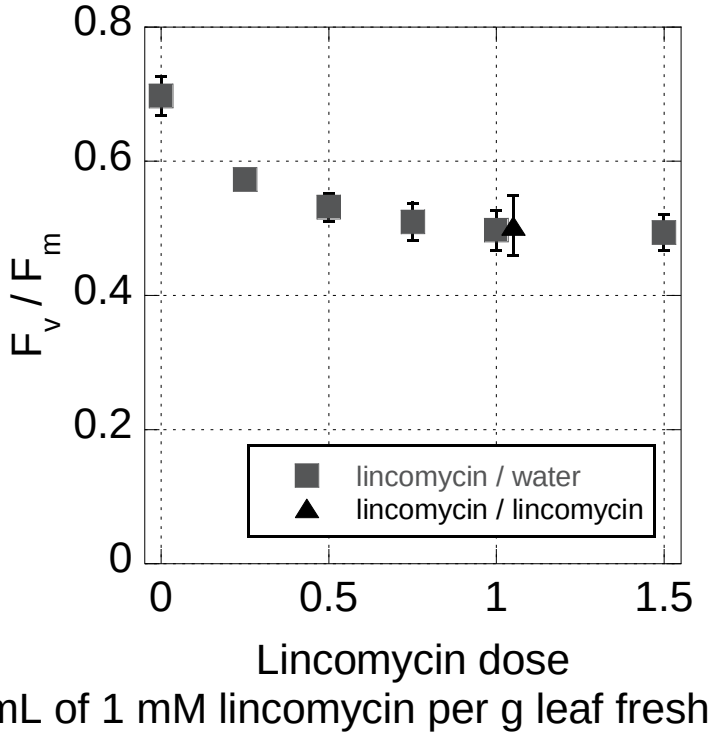

Fig. 2 Effects of lincomycin dose on PSII repair. LL spinach leaves were let absorb designated amounts of 1 mM lincomycin, and were exposed to light from a halogen lamp at PPFD of 1600 μmol m^{-2} s^{-1} for 60 min. After keeping the leaves in the dark for 30 min, F_v / F_m values were measured. Squares, the leaves were let absorb 0, 0.25, 0.5, 0.75, 1.0 or 1.5 mL of 1 mM licomycin solution per g leaf fresh weight in the dark and transferred to distilled water. After the designated amounts of the lincomycin solution were absorbed, the photoinhibition treatments were started. Triangle, leaves continued to absorb 1 mM lincomycin solution. The photoinhibition treatments were started when the leaves absorbed 1 mL of 1mM lincomycin solution per g leaf fresh weight. The means ± SD (n = 4) are shown.

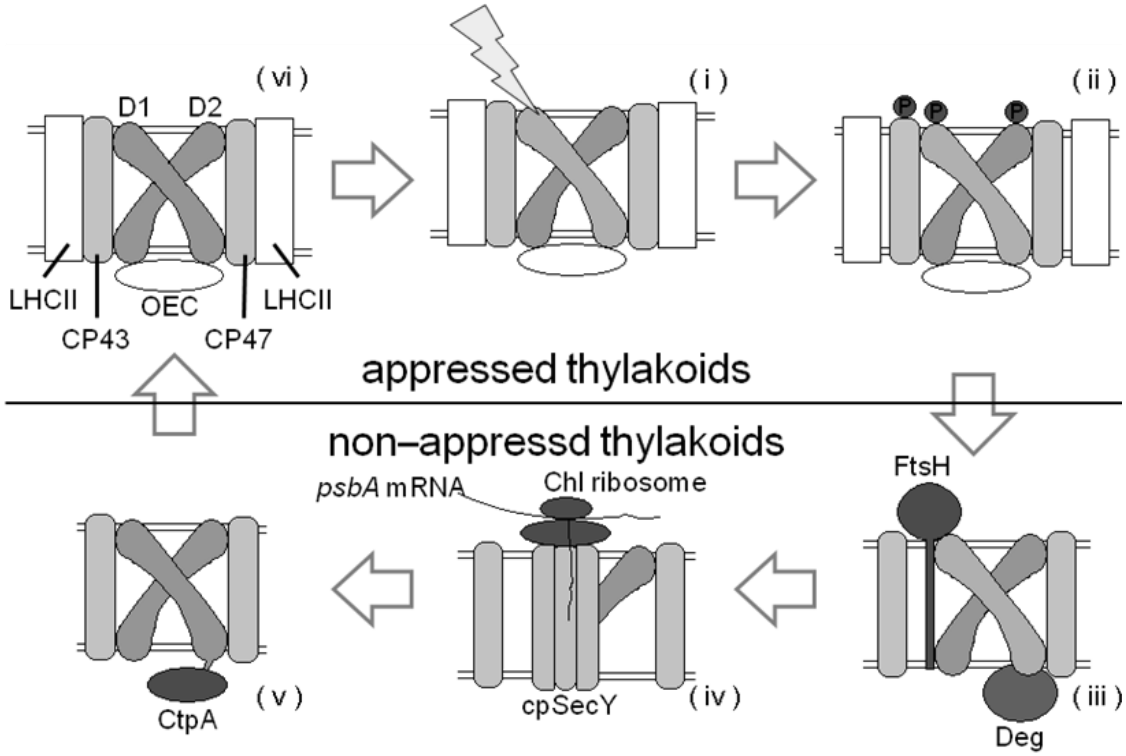

Fig. 3 A working scheme of the repair cycle of D1 protein. (i) An active PSII is inactivated by light. D1 protein in the PSII is photodamaged. (ii) The inactive PSII is phosphorylated by a phosphokinase, STN8 (Vainonen et al. 2005). (iii) The photodamaged D1 protein in the PSII is degraded by proteases, FtsH and/or Degs. (iv) Using *psb*A mRNA, a chloroplast ribosome synthesizes D1 protein *de novo*. Simultaneously, the pre-D1 protein is inserted to the position of D1 protein in the PSII by a thylakoid-transmembrane translocon, cpSecY. (v) The new D1 protein is processed by a peptidase, CtpA. This cleaves the peptide bond between 344 and 345 amino acids of a new D1 protein. (vi) The repaired PSII regains the activity. An original scheme based on Kato and Sakamoto (2009) and Mulo et al. (2008).

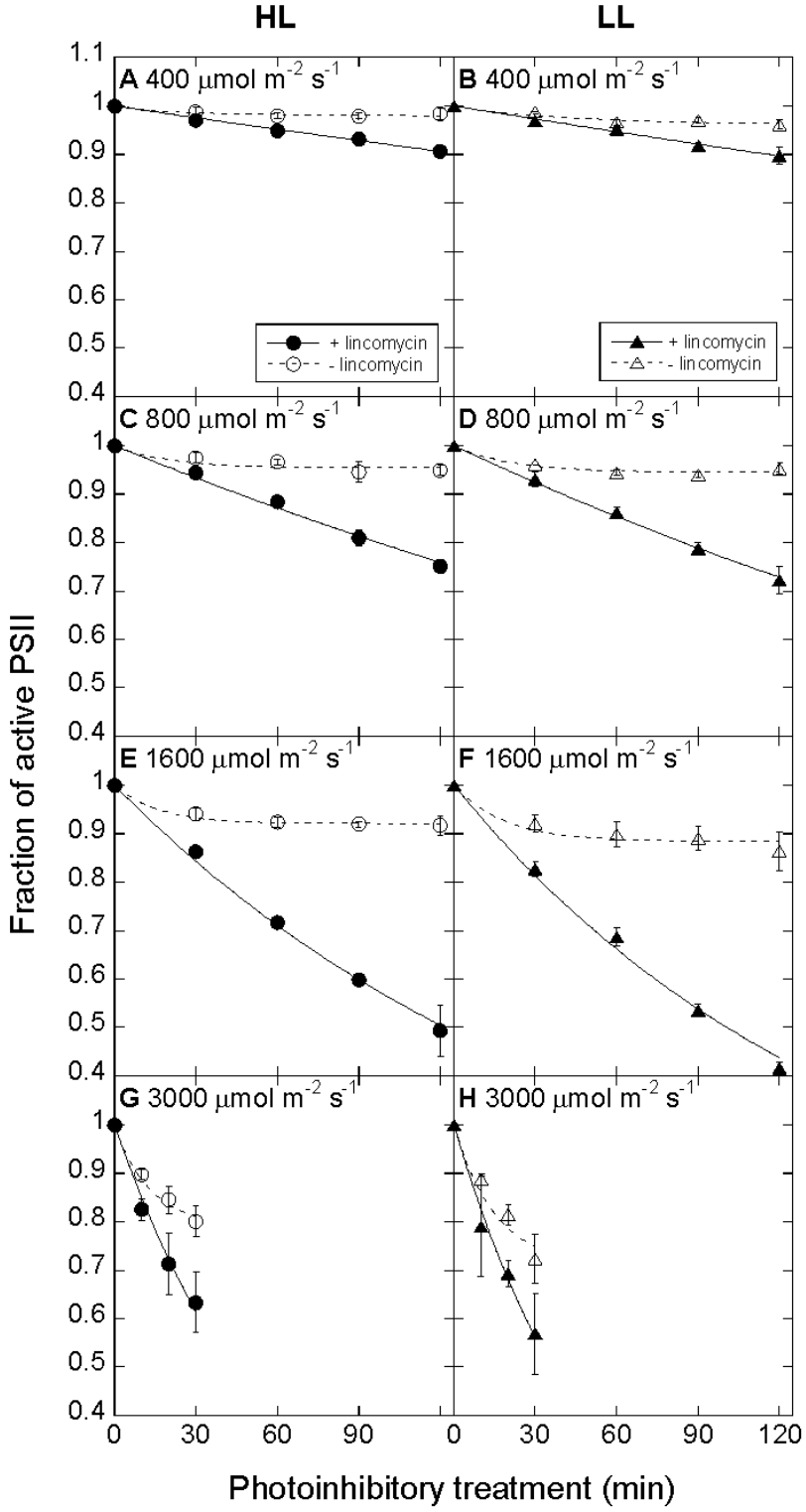

Fig. 4 Effects of photoinhibitory PPFD and duration, and lincomycin on the fraction of active PSII (*a*). Circles, HL leaves; Triangles, LL leaves. Closed symbols, leaves treated with 1 mM lincomycin; open symbols, leaves without licomycin treatment. Means ± SD (n = 3) are shown.

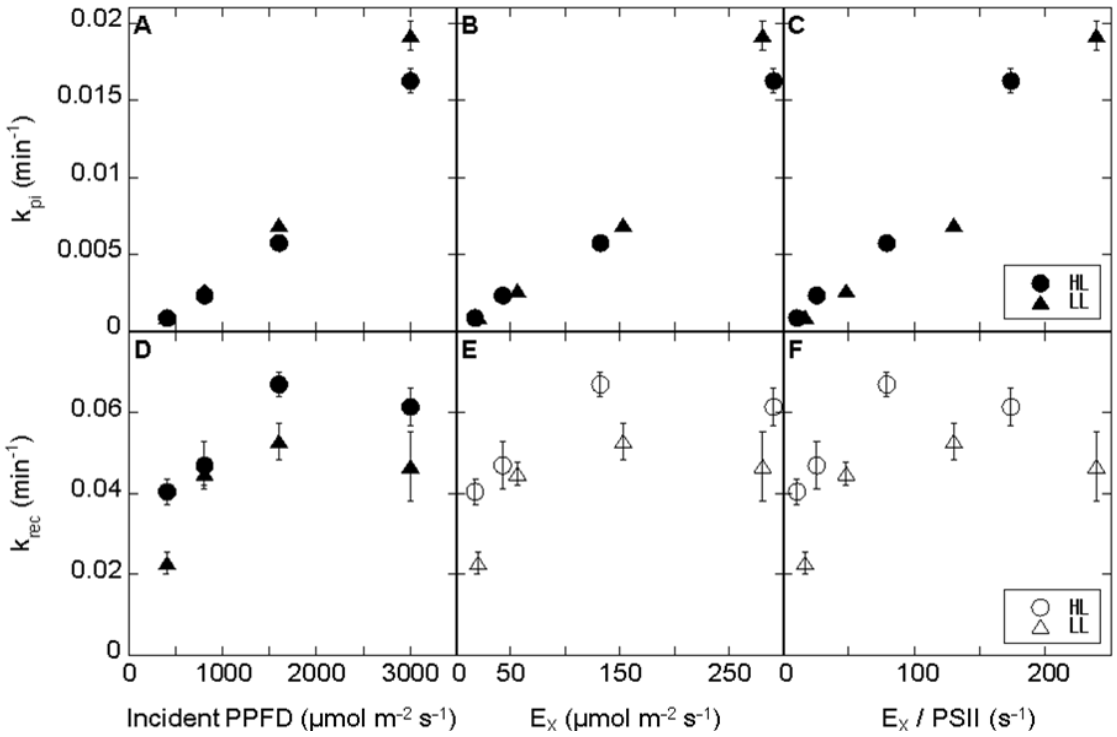

Fig. 5 k_{pi} and k_{rec} plotted against PPFD (**A**, **D**), rate of excess energy production (**B**, **E**) and rate of excess energy production per PS II (**C**, **F**). Quadratic regression equations for all the data points were: k_{pi} for HL, $y = 1.26 \times 10^{-9} x^2 + 1.63 \times 10^{-6} x$ ($R^2 = 0.999$), k_{pi} for LL, $y = 1.48 \times 10^{-9} x^2 + 1.95 \times 10^{-6} x$ ($R^2 = 0.999$); k_{rec} in HL, $y = -1.81 \times 10^{-8} x^2 + 7.44 \times 10^{-5} x$ ($R^2 = 0.521$), k_{rec} for LL, $y = -1.51 \times 10^{-8} x^2 + 6.07 \times 10^{-5} x$ ($R^2 = 0.870$). Linear regressions for the data points obtained below 1600 µmol m^{-2} s^{-1} were: k_{pi} for HL, $y = 4.09 \times 10^{-6} x - 8.80 \times 10^{-4}$ ($R^2 = 0.998$), k_{pi} for LL, $y = 5.05 \times 10^{-6} x - 12.4 \times 10^{-4}$ ($R^2 = 0.996$); k_{rec} for HL, $y = 2.25 \times 10^{-5} x + 3.04 \times 10^{-2}$ ($R^2 = 0.991$), k_{rec} for LL, $y = 2.30 \times 10^{-5} x + 1.88 \times 10^{-2}$ ($R^2 = 0.806$). Means ± SE ($n = 3$) are shown. The detailed numbers and statistical results of k_{pi} and k_{rec} for HL and LL leaves are shown in Table 3.

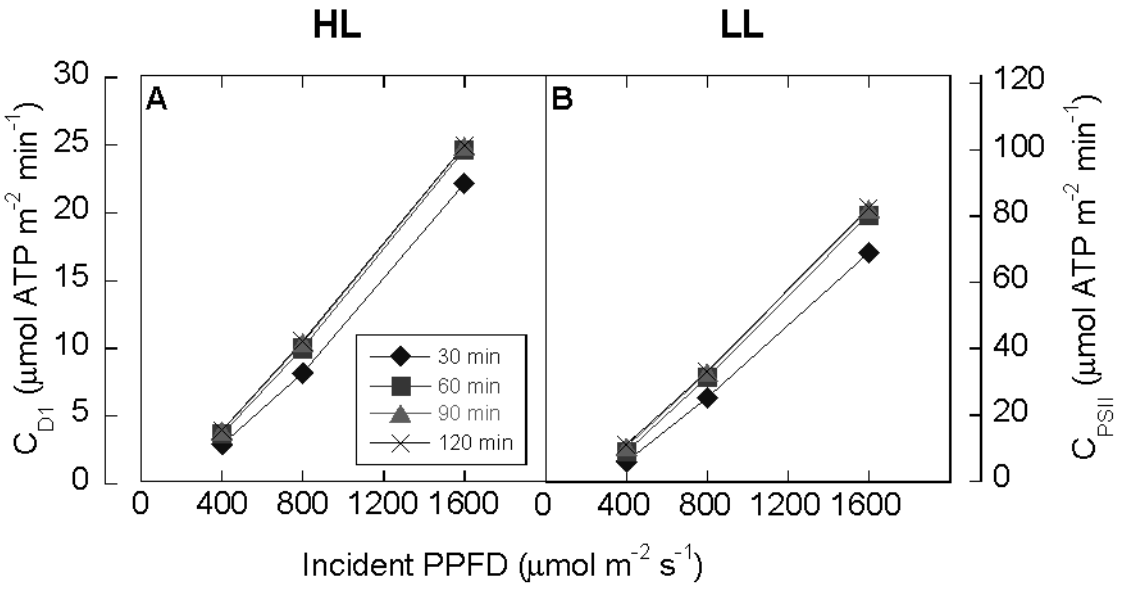

Fig. 6 Effects of the photoinhibitory PPFD and duration on the cost (C_{D1} or C_{PSII}). **A**, C_{D1} or C_{PSII} for HL leaves; **B**, C_{D1} or C_{PSII} for LL leaves. C_{D1} was calculated as $C_{D1} = D1_{leaf} \times k_{rec} \times (1 - a) \times C_{process}$. C_{PSII} was calculated as $C_{PSII} = 4.08 \times C_{D1}$.

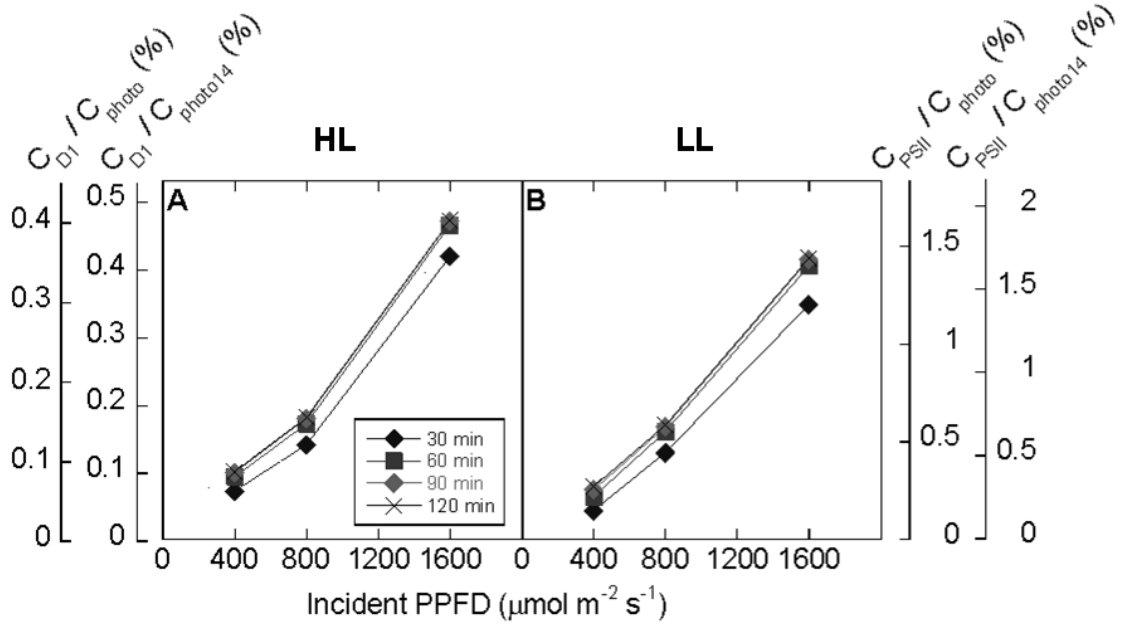

Fig. 7 Effects of the photoinhibitory PPFD and duration on the ratio of the cost (C_{D1} or C_{PSII}) to the ATP production rate by photophosphorylation (C_{photo} or $C_{photo14}$). **A**, C_{D1} / C_{photo}, C_{PSII} / C_{photo}, C_{D1} / $C_{photo14}$ or C_{PSII} / $C_{photo14}$ for HL leaves; **B**, C_{D1} / C_{photo}, C_{PSII} / C_{photo}, C_{D1} / $C_{photo14}$ or C_{PSII} / $C_{photo14}$ for LL leaves. Photosynthetic electron transport rate was estimated using the fluorescence data and absorptance values. ATP / e^- ratio is assumed to be 1.33 for C_{photo} or 1.56 for $C_{photo14}$, respectively.

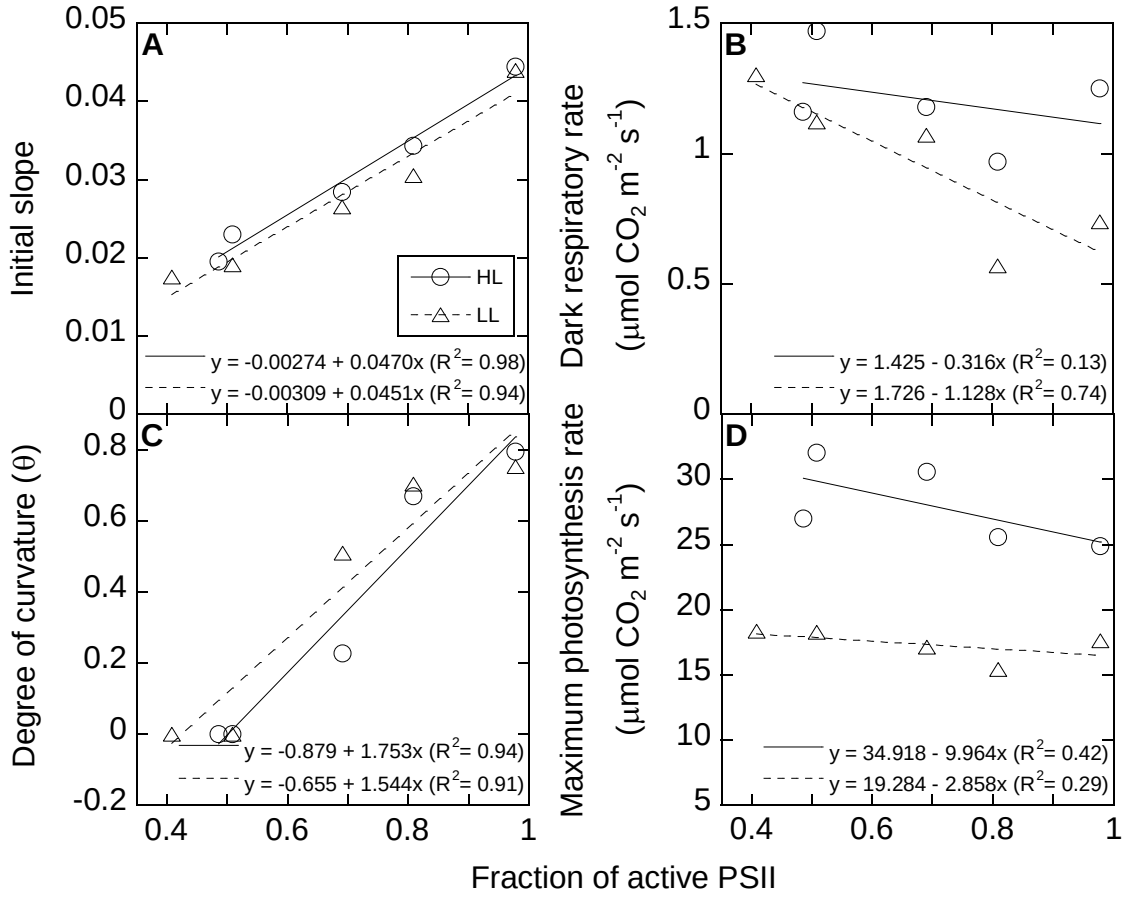

Fig. 8 Dependences of the parameters of non-rectangular hyperbolic photosynthetic light response curves on the fraction of active PSII (*a*). Non-rectangular hyperbolic curves were fitted to the rates of photosynthesis measured at seven PPFDs before the photoinhibitory treatment in the absence of lincomycin and after the photoinhibitory treatment at PPFD for various periods in the presence of lincomycin. **A**, dependence of the initial slope (ϕ); **B**, the dark respiration rate (R_d); **C**, the curvature coefficient (θ); **D**, the maximum photosynthesis rate (P_{max}) of light response curve on *a*. Circles, HL leaves; triangles, LL leaves. R^2 are determination coefficients. *F* values for the regressions were: A, $F = 0.0011$ for HL and 0.0055 for LL; B, 0.55 for HL and 0.059 for LL; C, 0.0055 for HL and 0.0012 for LL; and D, 0.23 for HL and 0.34 for LL.

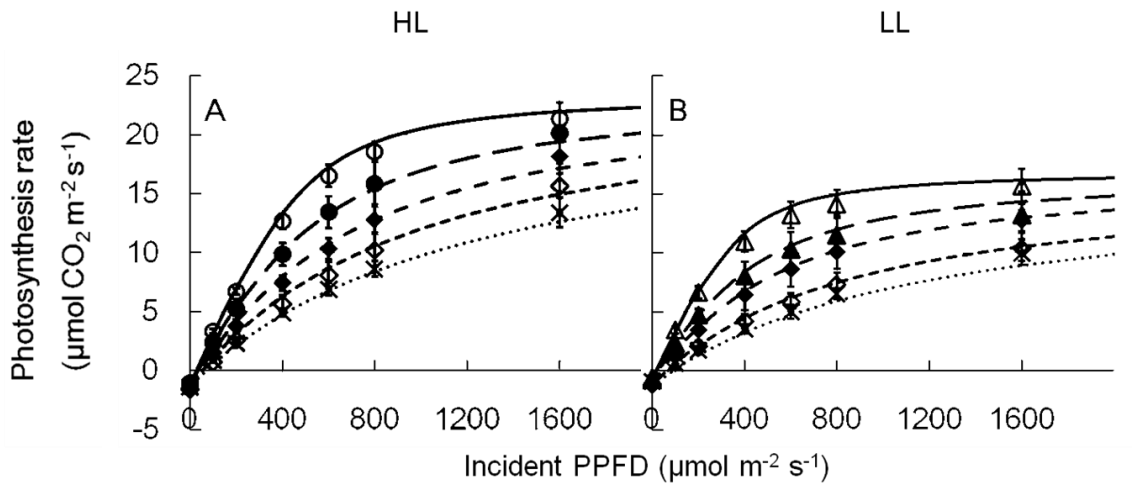

Fig. 9 Rates of photosynthesis before and after the photoinhibitory treatment in the presence of lincomycin and the model photosynthetic light response curves. The rates of photosynthesis were measured at seven PPFDs before the photoinhibitory treatment in the absence of lincomycin (open circles: HL leaves and open triangles: LLleaves) and after the photoinhibitory treatments at 1600 μmol m^{-2} s^{-1} for 30, 60, 90 and 120 min in the presence of lincomycin (closed circles and triangles: HL and LL for 30 min, closed diamonds: HL and LL for 60 min, open diamonds: HL and LL for 90 min, and crosses: HL and LL for 120 min). Using the linear functions and constants shown in Fig. 8, model photosynthetic light response curves were calculated from F_v / F_m values before and after the photoinhibitory treatment. The determination coefficients (R^2) of the model curves and those for the non-rectangular hyperbolic functions directly fitted to the data (shown in parentheses) were as follows. R^2 for the curves before photoinhibitory treatment, 0.994 (0.999) and 0.991(0.999) in the HL and LL leaves, respectively. R^2, for the calculated light-photosynthesis curves after the photoinhibitory treatment at 1600 μmol m^{-2} s^{-1} for 30 min were 0.997 (0.999) and 0.987 (0.999) in the HL and LL leaves, respectively. R^2 for 60 min were 0.993 (0.999) and 0.998 (0.999), for 90 min were 0.990 (0.999) and 0.997 (0.999), and those for 120 min were 0.994 (0.999) and 0.988 (0.999) for HL and LL leaves, respectively. The means ± SD (n = 3) are shown.

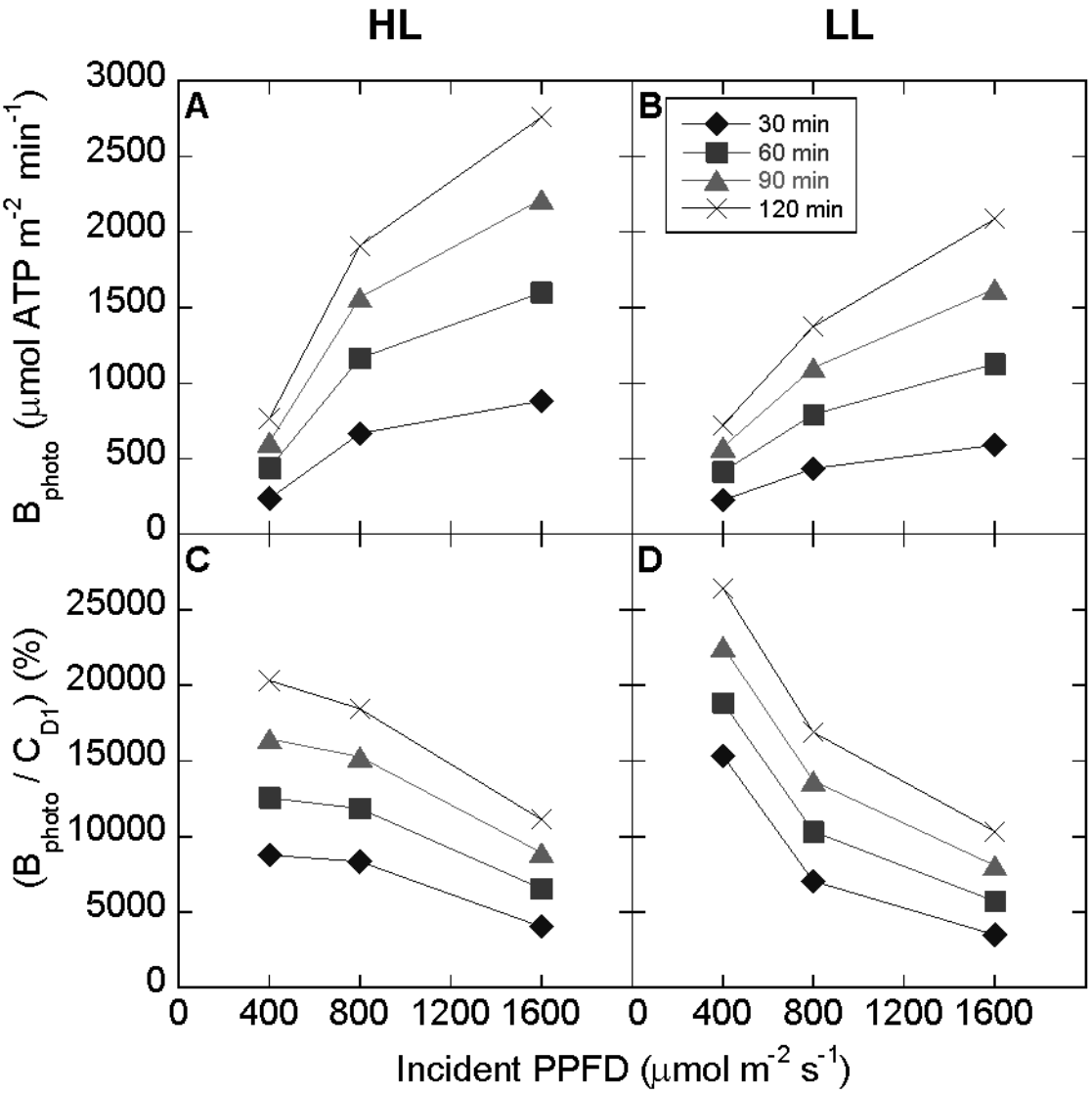

Fig. 10 The benefits of D1 protein repair (B_{photo}) and the ratio of B_{photo} to C_{D1}. **A**, B_{photo} of HL leaves; **B**, B_{photo} of LL leaves. B_{photo} was calculated as $B_{photo} = G \times (1 / 6) \times 29$. **C**, B_{photo} / C_{D1} in HL leaves; **D**, B_{photo} / C_{D1} in LL leaves. C_{D1} data used are those shown in Fig. 6.

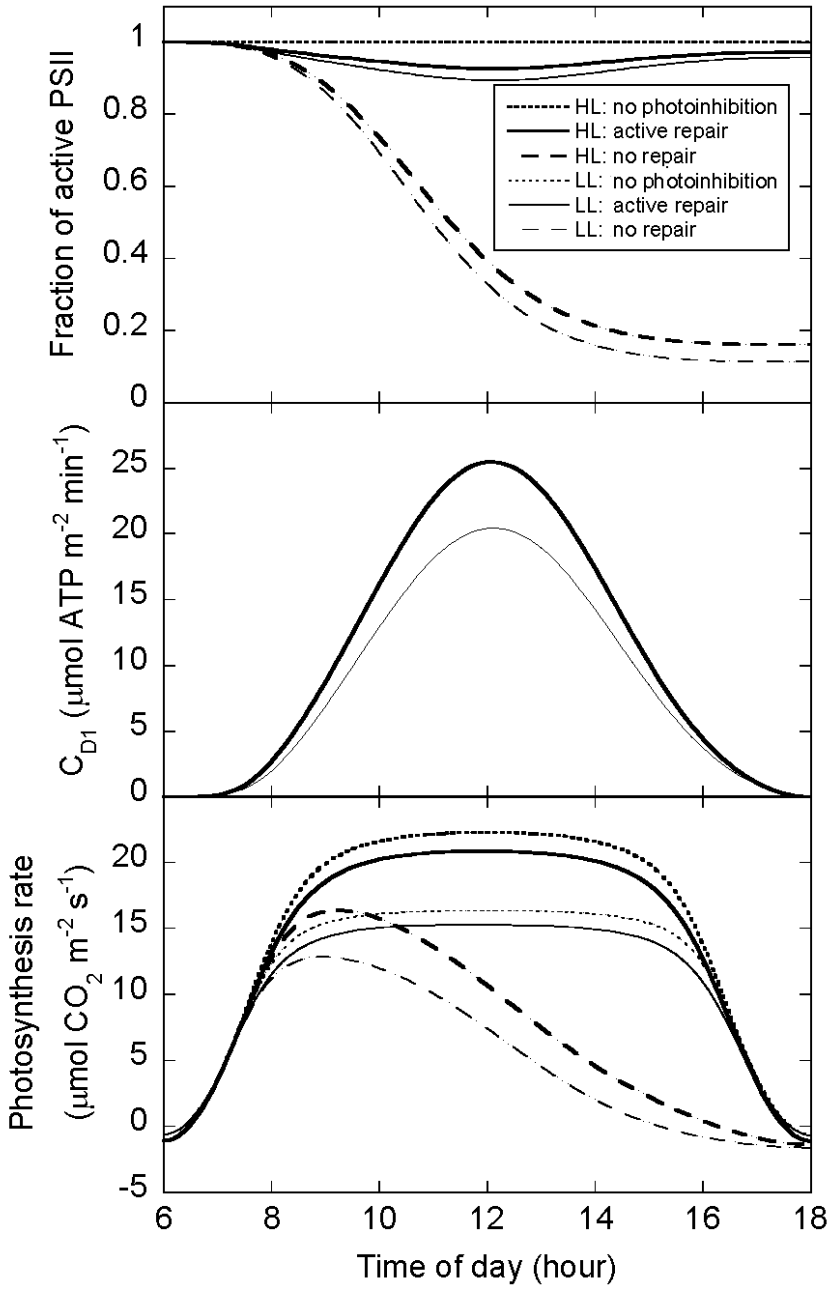

Fig. 11 Simulated changes in the fraction of active PSII (*a*), C_{D1} and photosynthesis rate in daytime.**A**, *a*; **B,** C_{D1}; **C,** photosynthesis rate. The calculations were made for daytime of 12 h (from 6:00 to 18:00) with a peak PPFD at 1600 μmol m^{-2} s^{-1} at 12:00. Changes in PPFD with time were expressed as a sine square curve. Thick lines, HL leaves; thin lines, LL leaves. Solid lines, leaves photoinhibited with active repair of photodamage; dashed lines, leaves with no photodamage repairing; dotted lines, control leaves without photoinhibition.

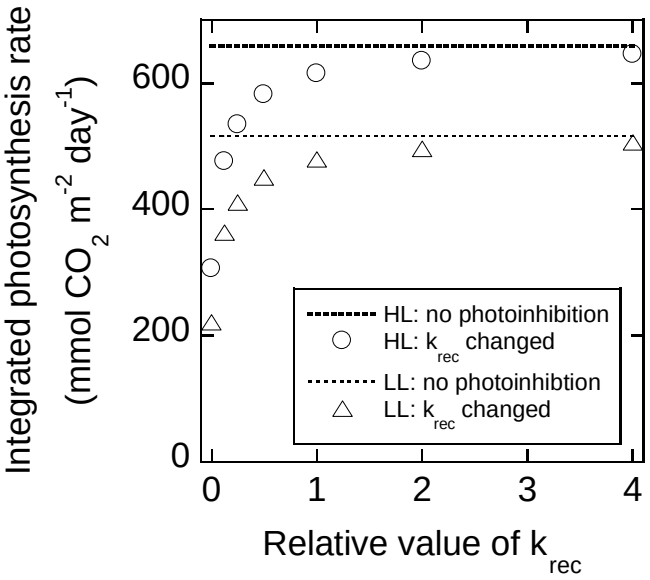

Fig. 12 Changes in the integrated photosynthesis rate in daytime with changes in k_{rec}. k_{rec} obtained by the quadratic regressions of the measured values shown in the legend from Fig. 5 were multiplied by 0, 0.125, 0.25, 0.5, 1, 2 and 4. The integrated photosynthesis rates were calculated for daytime of 12 h (from 6:00 to 18:00) with a peak PPFD at 1600 μmol m^{-2} s^{-1} at 12:00. Circles, HL leaves; triangles, LL leaves. Thick lines, HL; thin lines, LL; dotted lines, control leaves without photoinhibition.

CHAPTER 3

Analysis of the relationship of light environment, PSII photoinhibition and PSII parameters in the field plants.

Introduction

Plants produce carbohydrate by the photosynthetic processes, and light is needed as the energy source. Strong visible light, however, inhibits photosynthesis and this has been called photoinhibition (Kok 1956). The primary target of photoinhibition is PSII (Powles 1984) and the degree of the PSII photoinhibition *in vivo* is determined by the balance of two reactions, the photodamage and repair (Greer *et al*. 1986, Aro *et al*. 1993). There are two main hypotheses for the mechanisms of the photoinhibition. One is the excess energy hypothesis (Ögren *et al*. 1984, Vass *et al*. 1992). According to this hypothesis, the mechanisms of photodamage are as follows. When excitation is transferred to a closed PSII-RC, which is unable to conduct the photochemical reaction, the excited $^{1}Chl^{*}$ or $^{1}P680^{*}$ is converted into the triplet state, $^{3}Chl^{*}$ or $^{3}P680^{*}$, and leads to formation of $^{1}O_{2}$. $^{1}O_{2}$ inactivates D1 protein. This hypothesis is called acceptor side in the excess energy hypothesis (Vass *et al*. 1992). The electron transport from the Mn cluster to P680 delays when the thylakoid lumen is acidified. In this situation, when P680 and Yz change into $P680^{+}$ and Yz^{+} the portion between $P680^{+}$ and Yz^{+} is damaged. This hypothesis is the donor side hypothesis in the excess energy hypothesis (Callahan *et al*. 1986, Aro *et al*. 1993a). The other is the two-step hypothesis (Hakala *et al*. 2005, Ohnishi *et al*. 2005). This hypothesis claims that the primary photodamage occurs in the Mn cluster depending on the number of photons absorbed by the PSII Mn cluster. Subsequently, the D1 protein is damaged.

In vivo, both mechanisms would be operating in the photodamage of PSII (Oguchi *et al*. 2009).

Kok (1956) expressed the photodamage and repair of PSII as the first-order reactions. Using these equations, the rate constant for photodamege (k_{pi}) and the rate constant for repair reaction (k_{rec}) have been estimated (Kok 1956, Wünschumann and Brand 1992, Kato *et al*. 2002). k_{pi} and k_{rec} differ depending not only on the incident PPFD during the photoinhibition treatment but also on the growth irradiance (Tyystjärvi *et al*. 1992). Tyystjärvi *et al*. (1992) indicated that k_{pi} increased with the increase in growth irradiance in *Cucurbita pepo* L. In contrast, Lee *et al*. (2001) indicated that k_{pi} decreased with the increase in growth irradiance in *Capsicum annuum* L. For k_{rec}, both studies indicated that k_{rec} increased with the increase in growth irradiance. In many studies examining the effects of growth irradiance, artificial light sources such as fluorescence tubes have been used and the irradiance tends to be kept at a constant level in the daytime. Measurements of k_{pi} and k_{rec} using field plants have never been made. Would plants in the field show different k_{pi}, k_{rec} and other parameters from those in the laboratory grown plants? In this study, I used leaves of cucumber plants grown in a growth chamber at three constant irradiance levels, and those grown outdoors. Furthermore, I measured k_{pi} and k_{rec} in several plants on the university campus and in some alpine plants in the Himalayas. I examined relationships between the growth light environment and the rate constants of PSII photoinhibition by comparing the data obtained with the field plants and those obtained with the

plants grown in the growth chamber.

I also examined the major fluorescence parameters including the qP, NPQ and excess energy. Using the field-grown plants such as *Vinca minor* L., Demmig-Adams *et al*. (1996) examined that the relationships between the fluorescence parameters like qP, NPQ and fraction of excess energy (Excess = $(F_v' / F_m') \times (1 - qP)$, same parameter with E_Y) and growth irradiance. qP and NPQ increased with the increase in growth irradiance, whereas E_Y decreased with the increase in growth irradiance. In *Vicia faba* L. 'Minpo' plants grown in a growth chamber, Stefanov and Terashima (2008) showed that qP and NPQ increased with the increase in growth irradiance and excess energy parameter ($\Phi_{ExC} = F / F_m' - (F_v / F_m + F_o / F_m')$) decreased with the increase in growth irradiance. With chamber-grown spinach plants (*Spinacia oleracea* L. 'Torai'), I showed that (CHAPTER 2), at a given irradiance, NPQ and the yield of excess energy ($E_Y = (F_v' / F_m') \times (1 - qP)$) were smaller in high-light plants than in low-light plants, although the differences become obscure at high irradiance.

NPQ was identified as a fluorescence parameter determining both the rate of photodamage and that of repair from the photodamage (Li *et al*. 2002, Takahashi *et al*. 2009). According to the excess hypothesis, NPQ decreases the rate of photodamage, whereas, according to the two-step hypothesis, NPQ increases the rate of repair by suppressing ROS generation (Takahashi *et al*. 2009). Tu *et al*. (2012) grew *Berteroa incana* (L.) DC. in the field and in a growth chamber.

NPQ was greater in the field plants. However, in their study, the rate constants of PSII photoinhibition or those for the repair were not compared.

In the field, irradiance incident on a leaf fluctuates dynamically with time due to clouds and other structures including the leaf canopy above the leaf under consideration. The fluctuating light induces PSI photoinhibition (Tikkanen *et al*. 2010, Kono *et al*. 2014). On the other hand, it has been shown that the high irradiance components of the fluctuating light enhances NPQ capacity (Alter *et al*. 2012). In this study, through measuring the rate constants of PSII photoinhibition and repair, and various fluorescence parameters, I examined the influence of growth light environment in the field on the photosynthetic reactions.

Kato *et al*. (2002) showed that conditions inducing stomatal closure or occlusion, and/or thickening the leaf boundary layer accelerate the photoinhibition even at low PPFD levels. In this study, I carefully avoided these effects (see Materials and methods).

Materials and methods

Plant materials on the University of Tokyo campus

Plants occurring in clusters of more than 50 cm × 50 cm on the campus of the University of Tokyo (35° 42' N, 139° 45' E, 23 m ASL) were used. Samplings were made from 7 September to 12 November 2013 and from 16 to 23 July 2014 (average air temperatures and total precipitations for September, October and November in 2013 were 25.2°C and 231.5 mm, 19.8°C and 440.0 mm, 13.5°C and 26.0 mm, respectively, and those of July 2014 were 26.8°C and 105.5 mm). The plants used were *Erigeron philadelphicus* L. (Asteraceae), *Fagopyrum dibotrys* H. Hara (Polygonaceae), *Houttuynia cordata* Thunb. (Saururaceae), *Persicaria chinensis* H. Gross (Polygonaceae), *Plantagoa siatica* L. (Plantaginaceae) and *Polygonum longisetum* Bruijin (Polygonaceae). The leaves that were expanded most recently were collected. All plants have amphistomatous leaves.

Cucumis sativus L. 'Nanshin' (Cucurbitaceae), purchased from Takii & Co., Kyoto, Japan, were grown at either of the three photosynthetically active photon flux density (PPFD) levels in a growth chamber with a 14 h light / 10 h dark cycle at an air temperature of 23°C for about 20 days. Light was provided by a bank of white fluorescent lamps (FPR96EX-N/A: Toshiba, Tokyo, Japan). PPFDs were adjusted with black screen cloths. PPFDs measured just above these plants were 35, 170 and 500 μmol m^{-2} s^{-1} and these are called LL, ML and HL, respectively. Seeds

were sown in vermiculite in 200 mL cups and supplied with deionized water. After germination, the plants were supplied with the 1 / 500 strength of a commercial nutrient solution, Hyponex 6-10-5 (Hyponex Japan, Osaka, Japan), containing 6.00% total nitrogen (2.90% ammonia-nitrogen and 1.05% nitrate-nitrogen), 10.0% water-soluble phosphate, 5.0% water-soluble potassium, 0.05% water-soluble magnesium, 0.001% water-soluble manganese and 0.005% water-soluble boron. First true leaves before unfolding of the second true leaves were used in this study. The first true leaf of *C. sativus* is amphistomatous.

Cucumis sativus L. 'Nanshin' (Cucurbitaceae) were also grown outdoors on the campus of the University of Tokyo. The cucumber plants, germinated in vermiculite at 500 μmol m^{-2} s^{-1} in the growth chamber mentioned above, were moved outdoors on the campus and supplied with the 1 / 500 strength of Hyponex 6-10-5 every other days. Samplings were made from 23 April to 21 May and 8 to 30 July 2014 (average air temperatures and total precipitations for April and May in 2014 were 15.0°C and 155.0 mm, and 20.3°C and 135.5 mm, respectively). First true leaves before unfolding of the second true leaves were used in this study. First true leaves in April to May fully unfolded in two weeks but those in July unfolded in one week from the germination.

Plant materials in the Jaljale Himal

Leaves of *Bergenia purpurascens* Engl. (amphistomatous leaves, Saxifragaceae, Collecting

No. 1227019, East of Nepal: Jaljale Himal, August 2012) and *Rheum acuminatum* Hook. f. & Thomson ex Hook. (hypostomatous leaves, Polygonaceae, Collecting No. 1227020, E. Nepal: Jaljale Himal, August 2012) were collected from the plants occurring in clusters greater than 50 cm × 50 cm. Leaves of *Bistorta milletioides* H. Ohba & S. Akiyama (hypostomatous leaves, Polygonaceae, Collecting No. 1221079, E. Nepal: Jaljale Himal, August 2012), were collected evenly from the distribution area along a cliff ridge. These sampling sites were located in the Jaljale Himal (27° 27' N, 87° 27' E, 4126 m ASL). Leaves of these plants were sampled from 14 to 20 August 2012. The average air temperature in daytime from 6:00 to 18:00 during this period was 10.9°C, and max / min temperatures in the daytime were 17.2 / 7.4°C.

Leaves of *Cremanthodium oblongatum* C. B. Clarke (amphistomatous leaves, Asteraceae, Collecting No. 1221136, E. Nepal: Jaljale Himal - Tin Pokhari, August 2012), *Cremanthodium pinnatifidum* Benth. (hypostomatous leaves, Asteraceae, Collecting No. 1221135, E. Nepal: Jaljale Himal - Tin Pokhari, August 2012) and *Cremanthodium reniforme* Benth. (hypostomatous leaves, Asteraceae, Collecting No. 1227024, E. Nepal: Jaljale Himal - Tin Pokhari, August 2012) were collected from plants in monospecific clusters in the Jaljale Himal - Tin Pokhari (27° 29' N, 87° 27' E 4310 m ASL). These plants were sampled from 22 to 26 August 2012. The average air temperature in daytime from 6:00 to 18:00 was 7.9°C, max / min temperatures in the daytime were 11.5 / 5.5°C. For Himalayan plants as well, the most recently

fully expanded leaves were collected.

Light environments in the fields

Light environment was evaluated as the open sky ratio (OSR) for each of the sampling sites using hemispherical photographs taken with a camera and a lens (COOLPIX 4500 and LC-ER1, NIKON, Tokyo, Japan). To obtain OSRs we analyzed these photos with software CanopOn 2 (http://takenaka-akio.org/etc/canopon2/). For the field plants on the Hongo campus of the University of the Tokyo, the daily PPFD was calculated for each of the hemispherical photos taken at the sampling sites using software (LIA32, http://www.agr.nagoya-u.ac.jp/~shinkan/LIA32/) and the data of the daily total shortwave radiation (TSR) in Tokyo provided by the Japan Meteorological Agency (http://www.jma.go.jp/jma/index.html).

LIA32 gives maximal PPFD values for the site where the hemispherical photograph was taken at every 5 min on a given calendar day as well as maximal PPFD values of the imaginary completely open site at the same location. The daily TSR data were obtained for the preceding 14 days before the sampling of the leaves. Photosynthetically active radiation (PAR) is assumed to be 43% of the TSR (Bassham 1977). The average photon energy of PAR (E_{photon}) was assumed to be 2.17×10^5 J mol^{-1} (Campbell and Norman 1998). Thus, the daily PPFD at the

sampling site was calculated as:

daily PPFD = (maximal PPFD at the site / maximal PPFD at the completely open site at the same location) × 0.43 × daily TSR / E_{photon}.

Daily PPFD was calculated for each of the preceding 14 days before the sampling and averaged.

Light environment of the site where cucumber plants were grown outdoors was measured with a quantum sensor (LI-190A, LI-COR, Lincoln, NE, USA). PPFD of the site was measured at every 1 min everyday from 22 April to 20 May 2014. Daily PPFD was averaged for successive 14 days preceding the day of sampling. For the cucumber plants grown in July 2014, PPFD of the site was measured at every 5 min everyday from 8 to 30 July 2014. Daily PPFD was averaged for successive 7 days preceding the day of sampling. We also estimated the daily PPFD with the above-mentioned method using the hemispherical photo. The ratio of the measured PPFD to the estimated PPFD was 95.6%, indicating very high accuracy of the estimations using the hemispherical photos.

The daily PPFD in the Himalayas was calculated based on the data obtained in the field sites. We measured the PPFDs at 9:00, 12:00 and 15:00 everyday from 14 to 20 August at the Jaljale Himal campsite and from 22 to 26 August at the campsite between Jaljale Himal and Tin Pokhari. The PPFD of the campsite ($PPFD_{cs}$) was converted to PPFD at the completely open site ($PPFD_{os}$) using the ratio of the maximum PPFD for the imaginary completely open site at the

same geographical location ($PPFD_{LIAos}$) to maximum PPFD at the campsite ($PPFD_{LIAcs}$), both estimated with LIA32 at every 5 min for a given calendar day. Namely,

$PPFD_{os} = PPFD_{cs} \times (PPFD_{LIAos} / PPFD_{LIAcs})$.

PPFD of the sampling site at a given time ($PPFD_{sample}$) was calculated from the $PPFD_{os}$, PPFD at the imaginary completely open site at the same location of the sampling site ($PPFD_{LIAos\text{-}sample}$), and PPFD at the sampling site ($PPFD_{LIAsample}$) estimated with LIA32 as:

$PPFD_{sample} = PPFD_{os} \times (PPFD_{LIAsample} / PPFD_{LIAos\text{-}sample})$.

For $PPFD_{sample}$ values from 6:00 to 9:55, from 10:00 to 14:55, and from 15:00 to 18:00 $PPFD_{os}$ values that were estimated based on $PPFD_{cs}$ values measured at 9:00, 12:00 and 15:00, respectively, were used to take account of weather changes on each day. Note that LIA32 ver. 0.3781 does not take account of the time zone. We corrected the time difference of 3:15 between Japan and Nepal.

Photoinhibtion treatments

The sample leaves were exposed to PPFD at 400 or 1200 μmol m^{-2} s^{-1} to induce PSII photoinhibition. During the exposure to light, the leaves were kept at air temperature (25℃ for the plants on the University of Tokyo campus or air temperature in the Jaljale Himal) using a fan. The light was provided by white light emitting diodes (LED) (NSPW70CS-K1 RAIJIN: Nichia,

Tokushima, Japan).

To inhibit the repair process of D1 protein in PSII, we used lincomycin, an inhibitor of the chloroplast-encoded protein synthesis by the 70S ribosome (CHAPTER 2). In the experiments conducted in the laboratory, the leaves were fed with more than 1 mL of the 1 mM lincomycin solution / g leaf fresh weight via their petioles in the dark at 25°C. The leaves were kept on the air in the presence and absence of lincomycin solution during the photoinhibition treatment at 25°C. The petioles were soaked in the 1 mM lincomycin solution or deionized water during the photoinhibition treatment. The laminae were kept in air. The fan minimized the leaf boundary layer. The leaves in the Jaljale Himal were fed with 1 mM lincomycin solution via their petioles in the dark and dry air until they absorbed more than 1 mL of the 1 mM lincomycin solution / g leaf fresh weight. The petioles were soaked in the 1 mM lincomycin solution or deionized water during the photoinhibition treatment. The laminae were kept in air. The leaf temperature was stabilized, and the leaf boundary layer was minimized with a fan.

Chlorophyll (Chl) fluorescence parameters

We measured the maximum quantum yield of PSII, F_v / F_m where $F_v = F_m - F_o$ (Kitajima and Butler 1975, Krause and Weis 1991), in the leaf with a fluorometer (PAM-2500, Walz, Effeltrich, Germany). The saturating pulse at PPFD of 6250 μmol m^{-2} s^{-1} was given for 0.8 s to obtain F_m.

Before the measurements of fluorescence, the leaves were kept in the dark for at least 30 min. These measurements were conducted at room temperature.

Quantum yield of PSII photochemistry, Φ_{PSII} or $Y(II) = (F_m' - F) / F_m'$, (Genty *et al*. 1989), non-photochemical quenching, $NPQ = F_m / F_m' - 1$, (Bilger and Björkman 1990), photochemical quenching coefficients, $qP = (F_m' - F) / (F_m' - F_o')$, (Schreiber *et al*. 1994) and the yield of excess energy, $E_Y = (F_v' / F_m') \times (1 - qP)$, (Demmig-Adams *et al*. 1996, Stefanov and Terashima 2008) were calculated according to the puddle model. The yields of non-photochemical energy dissipation, $Y(NPQ) = F / F_m' - F / F_m$, $Y(NO) = F / F_m$, and the quenching coefficient, $qL = qP \times F_o' / F$, according to the lake model (Kramer *et al*. 2004), were also calculated. The actinic light was white LEDs at 400 or 1200 μmol m^{-2} s^{-1}. These white LEDs were the same ones that were used for the photoinhibitory treatments. The Chl fluorescence parameters were measured 10 min after the onset of the actinic light. For measurements of the Chl fluorescence parameters, the petioles of the plant leaves were kept in deionized water and the laminae were kept in air at 25°C. The leaf boundary layer was minimized with a fan.

Calculation of the rate constants of photodamage (k_{pi}) and repair (k_{rec}) was according to CHAPTER 2.

Statistical analysis

The two-sided Welch's *t*-test was used to test the significant difference between the chamber-grown cucumber and, the outdoor cucumber leaves or the field plants. Asterisks, *, in the figures indicate significant differences at 5% between the outdoor cucumber leaves or the field plants, and the regression lines for the chamber grown cucumber leaves.

Results

Relationships between k_{pi}, k_{rec} and PSII fluorescence parameters, and the daily PPFD in cucumber leaves

Data for the leaves from the cucumber plants grown in the growth chamber or outdoors, photoinhibited at 400 μmol m^{-2} s^{-1}, are shown in Figure 13. k_{pi}, k_{rec} and various fluorescence parameters calculated according to both the puddle model and lake model are plotted against mean daily PPFD. For the leaves grown outdoors, the data are plotted against the mean daily PPFD for 7 days before the sampling. Fluorescence parameters were obtained with the PAM–2500 after the onset of illumination with the white LEDs at 400 μmol m^{-2} s^{-1} for 10 min. These white LEDs were the same ones used for the photoinhibitory treatments. Regression lines are drawn for the data obtained with the three groups of cucumber plants grown in the continuous light at 35, 170 and 500 μmol m^{-2} s^{-1} for 14 h per day.

k_{pi} decreased with the increase in daily PPFD (Fig. 13A). k_{rec} increased with daily PPFD (Fig. 13B). k_{pi} and k_{rec} in the plants grown outdoors lay somewhat below the regression lines, although, neither of these differences was significant (Figs. 13A and B). Φ_{PSII} by the puddle model, which is identical to Y(II) by the lake model, in cucumber leaves at 400 μmol m^{-2} s^{-1} increased with daily PPFD, and Φ_{PSII} of the outdoor leaves showed no significant difference (Fig. 13C). PSII fluorescence parameters analyzed by the puddle model are NPQ, qP and E_Y. NPQ

decreased with the increase in daily PPFD, and NPQ of the outdoor leaves showed no significant difference (Fig. 13D). qP increased with daily PPFD, and qP of the outdoor leaves lay near the regression line (Fig. 13E). E_Y decreased with daily PPFD. E_Y of the outdoor leaves was close to the regression line (Fig. 13F). Y(NPQ) by the lake model showed a pattern similar to that of NPQ (Fig. 13G). For qL by the lake model corresponds to qP of the puddle model, the trend of qL was similar to that of qP (Fig. 13H). Y(NO) that contains the fraction corresponding to E_Y showed only small differences depending on the daily PPFD (Fig. 13I).

Data for the leaves of the cucumber plants grown in the growth chamber or outdoors, treated at 1200 μmol m^{-2} s^{-1}, are shown in Figure 14. For the leaves grown outdoors, the data are plotted against the mean daily PPFD for 7 days before the sampling. Regression lines are drawn for the data obtained with the cucumber leaves from the plants grown in the growth chamber. k_{pi} decreased with daily PPFD (Fig. 14A). k_{rec} increased with daily PPFD (Fig. 14B). k_{pi} and k_{rec} of the outdoor leaves lay near the regression lines (Figs. 14A and B). Φ_{PSII} increased with daily PPFD. Φ_{PSII} of the outdoor plants was close to the regression line (Fig. 14C). NPQ increased slightly with daily PPFD. NPQ of the leaves from the outdoor plants lay above the regression line, although the difference was not statistically significant (Fig. 14D). qP increased with daily PPFD and those of the outdoor leaves lay near the regression line (Fig. 14E). E_Y decreased with daily PPFD. E_Y of the outdoor leaves lay on the regression line (Fig. 14F). Y(NPQ) decreased

slightly with daily PPFD and Y(NPQ) of the outdoor leaves lay near the regression line (Fig. 14G). The trend for qL was similar to that for qP (Fig. 14H). Y(NO) value of the outdoor leaves was significantly lower than the regression line (Fig. 14I).

The rate constants of photodamage and repair in Erigeron philadelphicus, Fagopyrum dibotrys, Hottuynia cordata, Persicaria chinensis, Plantago asiatica *and* Polygonum longisetum *sampled on the University of Tokyo campus*

When the photoinhibitory treatment was conducted at 400 μmol m^{-2} s^{-1}, the k_{pi} values of the field plants somewhat decreased with OSR (Fig. 15A). When the treatment was conducted at 1200 μmol m^{-2} s^{-1}, k_{pi} increased in all the plants particularly in the plants from high OSR sites and the all plants gave similar the k_{pi} values. The relationship between k_{pi} and OSR was, thus, weaker for the photoinhibition treatment at 1200 μmol m^{-2} s^{-1} than that at 400 μmol m^{-2} s^{-1} (Figs. 15A and B). k_{rec} obtained at 400 μmol m^{-2} s^{-1} and 1200 μmol m^{-2} s^{-1} were both positively related to OSR. Moreover, the absolute values were not markedly different between the photoinhibitory PPFD levels (Figs. 15C and D). There were some data that did not conform to these trends. For example, k_{rec} in *Po. longisetum* obtained at 400 μmol m^{-2} s^{-1} was much lower than the regression line and that of *Pl. asiatica* from 52.7% OSR obtained at 400 μmol m^{-2} s^{-1} was higher than the regression line (Figs. 15C).

The field plants collected in October 2013, November 2013 and July 2014 were photoinhibited at 400 μmol m^{-2} s^{-1} and those collected in September 2013, October 2013 and July 2014 were photoinhibited at 1200 μmol m^{-2} s^{-1} (Fig. 16). The daily PPFDs for the field plants are mean values for 14 days before the respective sampling days. Regression lines are drawn for the data obtained with the chamber-grown cucumber leaves. k_{pi} and k_{rec} in November 2013 obtained at 400 μmol m^{-2} s^{-1} are plotted against daily PPFD (Fig. 16A and G). k_{pi} of the field plants were considerably lower than the regression line (Fig. 16A). k_{rec} of the field plants were near the regression line (Fig. 16G).

k_{pi} and k_{rec} in September 2013, photoinhibited at 1200 μmol m^{-2} s^{-1}, are plotted against daily PPFD (Figs. 16D and J). k_{pi} in *Pe. chinensis* was considerably lower than the regression line (Fig. 16D) indicating that *Pe. chinensis* was more resistant to photoinhibition than cucumber. The k_{rec} values for the plants from the field almost followed the regression line (Fig. 16J).

k_{pi} and k_{rec} in October 2013, photoinhibited at both 400 and 1200 μmol m^{-2} s^{-1}, are plotted against daily PPFD (Figs. 16B, E, H and K). k_{pi} of the field plants were significantly lower than the regression lines, except for *Pl. asiatica* at the daily PPFD of 4.4 mol m^{-2} day^{-1} photoinhibited at 1200 μmol m^{-2} s^{-1} (Figs. 16B and E). k_{rec} of the field plants lay near the regression lines, except for *Pl. asiatica* at 4.4 mol m^{-2} day^{-1} photoinhibited at 1200 μmol m^{-2} s^{-1} (Figs. 16B and K).

Relationships between k_{pi}, k_{rec} and PSII fluorescence parameters, and the daily PPFD in the plants sampled on the University of Tokyo campus

The field plants collected in July 2014 were photoinhibited at 400 or 1200 μmol m^{-2} s^{-1}. The daily PPFDs for the field plants are mean values for 14 days before the respective sampling days. k_{pi}, k_{rec} and various fluorescence parameters are plotted against daily PPFD (Figs. 17 and 18). The same regression lines that are shown in Figs. 13 and 14 are drawn. k_{pi} of the field plants were significantly lower than the regression lines, except for *Pl. asiatica* (Figs. 17A and 18A). k_{rec} of the field plants lay below the regression lines, except for *Pl. asiatica* at 28.3 mol m^{-2} day^{-1} daily PPFD (Figs. 17B and 18B). Φ_{PSII} of the field plants were mostly lower than the regression line (Figs. 17C and 18C). However, Φ_{PSII} in *Pl. asiatica* at the daily PPFD of 28.3 mol m^{-2} day^{-1} were around the regression lines. NPQ of the field plants were significantly above the regression line (Figs. 17D and 18D), except for *Pl. asiatica* at 28.3 mol m^{-2} day^{-1} daily PPFD. qP of the field plants were significantly lower than the regression lines, except for *Pl. asiatica* 28.3 mol m^{-2} day^{-1} daily PPFD (Fig. 17E and 18E). Except for qP in *Fa. dibotrys* at 400 μmol m^{-2} s^{-1} and *Pl. asiatica* at the daily PPFD of 22.0 mol m^{-2} day^{-1} at 1200 μmol m^{-2} s^{-1}, neither of the qL values of the filed plants significantly remote from the regression line (Fig. 17E and 18E). The E_Y values of the field plants were mostly around the regression lines (Figs.

17F and 18F). Y(NPQ) showed a pattern similar to that of NPQ (Figs. 17G and 18G). For qL measured at 400 μmol m^{-2} s^{-1}, the trend was similar to that of qP (Fig. 17H), although qL of *Ho. cordata* was not statistically remote from the regression line. For qL measured at 1200 μmol m^{-2} s^{-1}, the trend was similar to that of qP (Fig. 18H). However, mean values of qL for the field plants showed no significant differences with the regression line except for *Pl. asiatica* at the daily PPFD of 22.0 mol m^{-2} day^{-1} photoinhibited at 1200 μmol m^{-2} s^{-1}, the qL value of which was significantly lower than the regression line. Y(NO) showed a trend considerably different from those of E_Y (Figs. 17I and 18I). Y(NO) of *Pl. asiatica* at 28.3 mol m^{-2} day^{-1} was not significantly below the regression line. However, mean values of Y(NO) for the other three field plants were all significantly below the regression lines.

Relationships between k_{pi} and k_{rec}, and the daily PPFD and between k_{pi} and k_{rec} and the incident PPFD and excess energy during the photoinhibitory treatment

For k_{pi} and k_{rec}, all the data for the field plants photoinhibited at 400 or 1200 μmol m^{-2} s^{-1} were plotted against daily PPFD. These were also plotted against the incident PPFD and excess energy during the photoinhibitory treatments (Fig. 19). The excess energy (μmol m^{-2} s^{-1}) was calculated as E_Y × the incident PPFD (μmol m^{-2} s^{-1}). E_Y was measured with the PAM–2500 using the white LEDs as the actinic light at 400 or 1200 μmol m^{-2} s^{-1}. The data points shown in

Figure 19C and F consist of cucumber plants grown in the chamber, those grown outdoors in July 2014, and the field plants sampled in July 2014.

Strong negative relationships were obtained between the k_{pi} values of cucumber plants and the daily PPFD, whereas the relationship between the field plants and the daily PPFD were weak (Fig. 19A). When the k_{pi} values were plotted against the incident PPFD and the excess energy, not only cucumber plants but also the all field plants showed high relationships (Figs. 19B and C). The k_{pi} values of all the field plants showed high relationship with the incident PPFD however those of all the field plants showed a weak relationship with the excess energy (Figs. 19B and C). The k_{rec} values of cucumber plants and other field plants increased with the increase in the daily PPFD (Fig. 19D). However, k_{rec} of all of the field plants and the all plants showed very weak relationships with the incident PPFD and the excess energy (Figs. 19E and F). Only cucumber plants grown in the chamber, k_{rec} decreased with the increase in the incident PPFD and markedly decreased with the increase in excess energy (Figs. 19E and F).

The rate constants of photodamage and repair in relation to light environments in the plants in the Jaljale Himal

When the photoinhibitory treatment was conducted at 1200 μmol m^{-2} s^{-1}, the k_{pi} and k_{rec} values of the field plants showed weak relationships with OSR (Fig. 20). However, k_{pi} and k_{rec}

showed much stronger relationships with daily PPFD. With the increase in daily PPFD, not only k_{rec} but also k_{pi} increased (Fig. 21).

Discussion

Relationships between k_{pi} and k_{rec}, and the daily PPFD in cucumber leaves

Several studies have shown that the increase in the growth irradiance induces the decrease in k_{pi} and the increase in k_{rec} (Tyystjärvi *et al*. 1992 for *Cucurbita pepo* L., Aro *et al*. 1993 for *Pisum sativum* L. 'Greenfeast', Kato *et al*. 2002 for *Chenopodium album* L., and CHAPTER 2 for *Spinacia oleracea* L. 'Torai'). In cucumber plants grown at three PPFD levels in the growth chamber, k_{pi} decreased and k_{rec} increased with the increase in growth irradiance irrespective of the photoinhibitory PPFDs (Figs. 13A, 13B, 14A and 14B). The k_{pi} and k_{rec} values plotted against daily PPFD in the cucumber plants grown outdoors were around the regression lines for the growth-chamber grown plants (Figs. 13A, 13B, 14A and 14B). In addition, the k_{rec} values at 1200 μmol m^{-2} s^{-1} were lower than those at 400 μmol m^{-2} s^{-1} in the cucumber plants grown outdoors (Figs. 13B, 14B and 19E). The slope of the regression line of k_{rec} for the growth-chamber grown plants was minus (Fig. 19E). This trend is consistent with the previous study showing that k_{rec} has a peak against the incident PPFD probably due to inhibition of the repair system by an enhanced ROS production (CHAPTER 2).

Relationships between k_{pi} and k_{rec}, and light environments in the field plants

When plotted against OSR, the field plants on the University of Tokyo campus showed trends

similar to those for cucumber only for k_{rec} (Fig. 15). When k_{pi} and k_{rec} were plotted against daily PPFD separately for the two photoinhibitory treatments at 400 μmol m^{-2} s^{-1} and 1200 μmol m^{-2} s^{-1}, the field plants on the campus showed weaker relationships (Figs. 19A and D, Regression lines not shown). The equations for the regression lines and determination coefficients were as follows: k_{pi} at 400 μmol m^{-2} s^{-1} vs. daily PPFD, $y = 1.88 \times 10^{-5} x + 1.23 \times 10^{-3}$ ($R^2 = 0.20$); k_{pi} at 1200 μmol m^{-2} s^{-1} vs. daily PPFD, $y = -2.74 \times 10^{-5} x + 5.69 \times 10^{-3}$ ($R^2 = 0.029$); k_{rec} at 1200 μmol m^{-2} s^{-1} vs. daily PPFD, $y = 2.92 \times 10^{-3} x + 3.20 \times 10^{-2}$ ($R^2 = 0.37$). However, k_{rec} at 400 μmol m^{-2} s^{-1} markedly increased with the increase in the daily PPFD, $y = 6.15 \times 10^{-3} x + 1.40 \times 10^{-2}$ ($R^2 = 0.64$). These weak relationships may be attributed to several exceptionally high or low values: k_{pi} of *Pe*. *chinensis* in September 2013 and that of *Fa*. *dibotrys* July 2014 photoinhibited at 1200 μmol m^{-2} s^{-1}, were low (Figs. 16D and E), and k_{rec} of *Pl*. *asiatica* in October 2013 photoinhibited at 1200 μmol m^{-2} s^{-1} was especially high (Fig. 16K). However, when plotted against the daily PPFD, not only the chamber grown cucumber plants but also the field plants on the campus showed strong relationships (Fig. 19D).

For the plants in the Jaljale Himal, the relationship between these rate constants, k_{pi} and k_{rec}, and OSR did not show the trends similar to the field plants on the campus in Tokyo, especially in k_{rec} (Fig. 20). However, with the daily PPFD, the rate constants of the Jaljale Himal plants showed stronger relationships (Fig. 21). Relationships between the OSR and the daily PPFD

might be influenced by topography. The *Rheum acuminatum* occurred on the site having 1.5-fold OSR of the site of *Bistorta milletioides* while the daily PPFD differed by 2.2-fold. *Bistorta milletioides* sampled in this study hung on a cliff surface where direct sunlight was cut by the cliff in the whole morning. The seasonal factor was also important. The *Cremanthodium* spp. occurred in the site of high OSR but the daily PPFD was low because they were exposed to more rainy and cloudy days. I stayed in these campsites in August 2012 and this area would be wetter in July (Terashima *et al*. 1993). Although I used the data of PPFD actually measured at the campsite, the durations were rather short. Interspecific differences would be also very important. *Cremanthodium* spp. used in this study occurred in the similar sites but their k_{rec} were different. (Figs. 20 and 21). Indeed, the differences in the k_{pi} depending on species were also large for the field plants on the campus (Figs. 16 and 21).

Lee *et al*. (2001) reported that the increase in the growth irradiance induced the increases in k_{pi} and the increases in k_{rec} in *Capsicum annuum* L. They argued that photoinactivated PSII in the shade-type thylakoids dissipate excess energy more efficiently than sun-type thylakoids (Anderson and Aro 1994). In contrast to the controversial views for k_{pi} vs. growth irradiance, k_{rec} increased with the daily PPFD in the plants both from the university campus and the Jaljale Himal (Figs. 16G, H, I, J, L and 21B), excepting for the high k_{rec} of *Pl. asiatica* in October 2013 by the photoinhibition treatment at 1200 μmol m^{-2} s^{-1} (Fig. 16K). This would be due to species

characteristic of *Pl. asiatica* because the k_{rec} of *Pl. asiatica* in September 2013 by the photoinhibition treatment at 1200 μmol m^{-2} s^{-1} showed a similar value (Fig. 16J). In the Jaljale Himal plants as well, k_{rec} increased with the daily PPFD as mentioned above (Fig. 21). In Jaljale Himal, the measurements were conducted at temperatures much lower than 25°C. Because a fan was used to deliver the ambient air, the temperature might be roughly at 10°C. k_{pi} at 10°C was greater than that at 25°C by 1.5 folds while k_{rec} was about 20% of that at 25°C (Tsonev and Hikosaka 2003). If k_{rec} in the plants in the Jaljale Himal had been measured at 25°C, the k_{rec} obtained would be very high. Presumably, even when PSII is damaged because k_{pi} is enhanced by low temperatures, considerable k_{rec} values at low temperatures will recover the damage.

Relationships between k_{pi}, k_{rec} and PSII fluorescence parameters, and the daily PPFD in the plants

The NPQ values of the cucumber leaves grown outdoors, were near the regression line for the cucumber leaves grown at three PPFD levels in the growth chamber (Figs. 13D and 14D). However, NPQ of the first true leaves of cucumber plants grown outdoors for one more week after the full expansion was significantly above the regression line for the chamber-grown cucumber leaves (1.22 ± 0.32 at 400 μmol m^{-2} s^{-1} and 2.14 ± 0.10 at 1200 μmol m^{-2} s^{-1}). It has been shown that, in *Arabidopsis thaliana* (L.) Heynh. plants grown with artificial sunflecks for

one week, NPQ was enhanced (Alter *et al*. 2012). In *Berteroa incana* (L.) DC., field-grown plants showed higher NPQ than the growth-chamber plants (Tu *et al*. 2012). However, Tu *et al*. (2012) grew *B. incana* plants at PPFDs of 100 and 600 μmol m^{-2} s^{-1} in the growth chambers. The higher PPFD would be needed to be comparable to the light environment in the open field site. By comparing the data with the regression line for cucumber plants grown in the growth chamber, I clearly showed that NPQ of the field plants on the university campus were markedly higher than those of the chamber-grown cucumber leaves, except for *Pl. asiatica* at 28.3 mol m^{-2} day^{-1} daily PPFD (Figs. 17D and 18D). These *Pl. asiatica* plants were from an open site that showed the high OSR and the high daily PPFD (Figs. 15 and 16). Judging from OSR and daily PPFD, these *Pl. asiatica* plants might not experience many sunflecks.

NPQ of the field plants were higher than those of the chamber-grown cucumber leaves. This trend would be probably attributed to the light fluctuation in natural light environment. NPQ capacity would be acclimated to the highest light intensity in the fluctuating light (Alter *et al*. 2012, Kono and Terashima 2014). In the field, plants are often exposed to direct solar radiation. The chamber-grown cucumber plants were exposed to high light at 1200 μmol m^{-2} s^{-1} in this experiment for the first time, whereas the field plants experienced greater PPFDs many times.

NPQ were higher and qP were lower in the field plants on the university campus than those in cucumber, except for *Pl. asiatica* at 28.3 mol m^{-2} day^{-1} daily PPFD (Figs. 17E and 18E).

Reflecting these trends, E_Y in the field plants were similar to those in the chamber-grown cucumber (Figs. 17F and 18F). However, k_{pi} in the field plants on the campus were tended to be lower than those of cucumber leaves, (Figs. 17A and 18A). In particular, *Fa. dibotrys* with high NPQ showed low k_{pi} (Figs. 17 and 18).

When k_{pi} was plotted against E_Y, k_{pi} of the field plants were lower than those of cucumber leaves, especially, for the k_{pi} values at 1200 μmol m^{-2} s^{-1} (figure not shown). There are some reports showing that k_{pi} relates with E_Y (Kato *et al*. 2003, CHAPTER 2). I calculated the excess energy and plotted the all k_{pi} against the excess energy (Fig. 19C). The k_{pi} values increased with the excess energy and the k_{pi} values of the wild plants were lower than those of the chamber grown cucumbers (Fig. 19C). The strong relationships between k_{pi} and excess energy have been shown in the previous studies (Kato *et al*. 2003, CHAPTER 2). On the other hand, the k_{pi} values were strongly related to the incident PPFD as well (Fig. 19B). The strong relationships between the k_{pi} values and incident PPFD have been also reported (Tyystjärvi and Aro 1996). However, the k_{pi} vs. incident PPFD of all of the plants and that for the field plants had positive intercepts on the incident PPFD (Fig. 19B). The cucumber plants grown in the lowest PPFD showed the smallest intercept on the incident PPFD, and with the increase in the growth PPFD, the intercept increased. For the field plants with higher NPQ, the intercept was greater (Fig. 19C). For the present data, the values were more proportional to the incident PPFDs than the excess energy

levels. However, the k_{pi}-regression line against the excess energy for all plants including the chamber-grown plants as well as the field plants showed a strong relationship. There are some reports showing that k_{pi} is independent of E_Y (for a review, see Takahashi and Badger 2011). Takahashi *et al*. (2009) indicated that NPQ is not effective in protecting PSII reaction centers. Indeed, in *Pl*. *asiatica* at the daily PPFD of 22.0 mol m^{-2} day^{-1}, the k_{pi} values similar to those of cucumber when treated at 400 or 1200 μmol m^{-2} s^{-1} although NPQ was higher and E_Y was not lower than in cucumber (Figs. 17 and 18). In some plants (*Ho*. *cordata* and *Fa*. *dibotrys*), the NPQ values were higher and k_{pi} was lower than, but E_Y was similar to those of cucumber plants (Figs. 17 and 18). Low Y(NO) rather than low E_Y might be more related to the low k_{pi} values (Figs. 17I and 18I).

What effect does NPQ have on photoinhibition? A recent theory indicates that NPQ accelerates k_{rec} through suppressing ROS production (Murata *et al*. 2012). Is NPQ the main factor to determine k_{rec}? When I plotted k_{rec} against NPQ for all the plants, there was no relationship (figure not shown). By contrast, k_{rec} had a relationship with the daily PPFD (Fig. 19D). It has been well known that the k_{rec} values are greater in high-light grown plants than in low-light grown plants (Tyystjärvi *et al*. 1992, Kato *et al*. 2002, CHAPTER 2). In addition, plants have their optimum k_{rec} for keeping the photosynthesis (CHAPTER 2). However, it has never been shown what factor influences k_{rec}. In this study, I propose that the k_{rec} value was

determined depending mainly on daily PPFD.

If NPQ affects not only k_{pi} but also k_{rec}, plants can increase Φ_{PSII} and qP keeping k_{pi} and k_{rec} through decreasing of E_Y. However, the data of the field plants did not show such the tendency. When NPQ of the field plants were greater than those of the chamber-grown cucumber, Φ_{PSII} and qP were lower. k_{pi} and k_{rec} were also lower than the regression lines for the chamber-grown cucumber (Figs. 17 and 18). In contrast, the E_Y values of the field plants were similar to those on the regression line (Figs. 17F and 18F). What mechanisms affect such the k_{pi} and E_Y values of the field plants? Excess energy would lead to production of ROS. However, ROS would be scavenged by various scavengers. Probably, the plants grown in the field have higher dissipation ability of excess energy. For example, β-carotene quenches $^1O_2$ generated via $^3P680^*$ (Asada 2006). H_2O_2 that is produced in PSI and known to inhibit the repair of photodamaged PSII, is removed via the water-water cycle (Asada 1999, Nishiyama *et al*. 2001).

Plants acclimate light environments

In the fields, plants would acclimate their NPQ capacity to the highest light intensity. The high NPQ decreases Φ_{PSII}. Therefore, the decreased electron flow to PSI suppresses production of H_2O_2. Additionally, the high dissipation capacity of excess energy can decrease k_{pi}. The leaves with low k_{pi} values can save energy for k_{rec}. However, when incident light is enough high,

plants would not need to enhance NPQ nor cut down Φ_{PSII} to decrease k_{pi}, because the plants can use light energy to make enough chemical energy to get sufficient k_{rec} for their growth light environments.

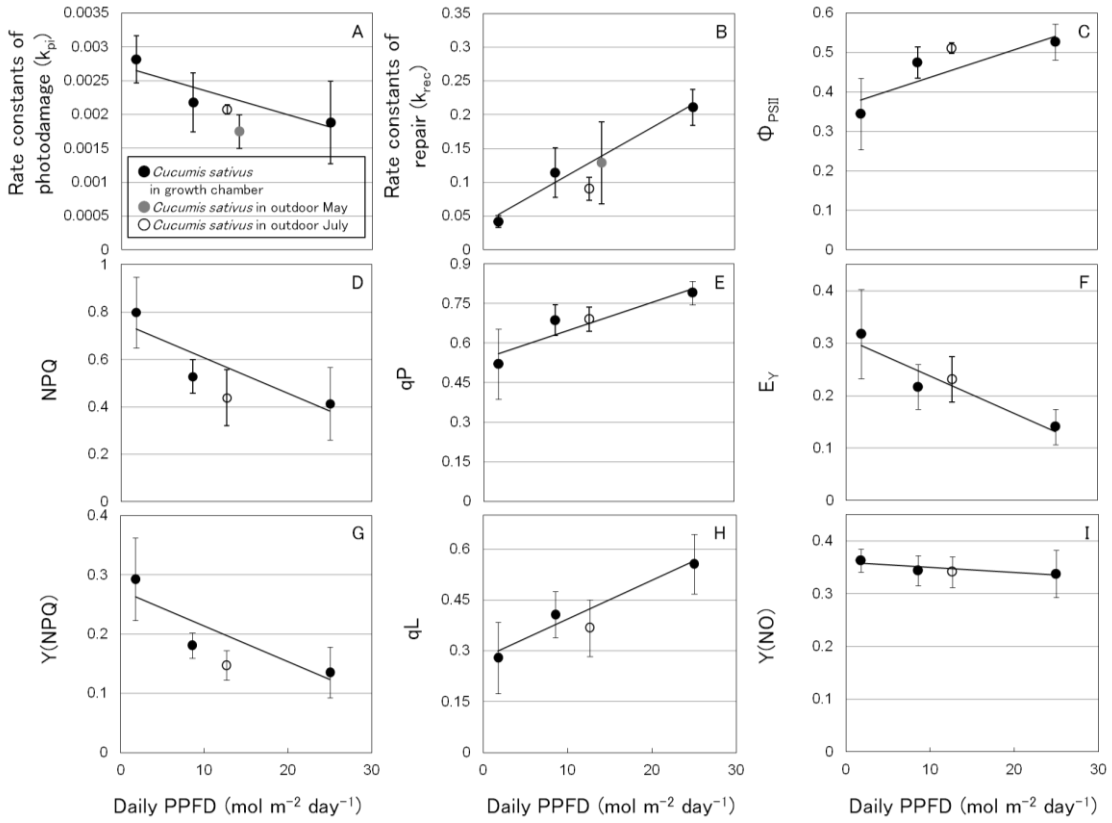

Fig. 13 Relationships between the rate constants for photodamage (k_{pi}) and repair (k_{rec}) and PSII fluorescence parameters of cucumber leaves treated at 400 µmol m^{-2} s^{-1}.

k_{pi} and k_{rec} were obtained for the cucumber leaves grown outdoors in May and July 2014 and for the chamber at three different PPFDs. The leaves were photoinihibited at 400 µmol m^{-2} s^{-1} (A and B). The Φ_{PSII}, NPQ, qP, E, Y(NPQ), qL and Y(NO) were measured at 400 µmol m^{-2} s^{-1} (C – I). ●, *Cucumis sativus* grown in the growth chamber and, ● and ○, *Cucumis sativus* grown outdoors on the campus in May and July 2014. Regression lines are drawn for the data obtained with cucumber leaves that were grown in continuous light at 35, 170 and 500 µmol m^{-2} s^{-1} for 14 h per day. The regression lines were: k_{pi} at 400 µmol m^{-2} s^{-1}, $y = -3.59 \times 10^{-5} x + 2.71 \times 10^{-3}$

(R^2 = 0.81) (A), k_{rec} at 400 µmol m^{-2} s^{-1}, y = 7.03 × 10^{-3} x + 3.95 × 10^{-2} (R^2 = 0.97) (B), Φ_{PSII} at 400 µmol m^{-2} s^{-1}, y = 6.99 × 10^{-3} x + 3.66 × 10^{-1} (R^2 = 0.78) (C), NPQ at 400 µmol m^{-2} s^{-1}, y = –1.48 × 10^{-2} x + 7.55 × 10^{-1} (R^2 = 0.80) (D), qP at 400 µmol m^{-2} s^{-1}, y = 1.06 × 10^{-2} x + 5.40 × 10^{-1} (R^2 = 0.86) (E), E_Y at 400 µmol m^{-2} s^{-1}, y = –7.05 × 10^{-3} x + 3.08 × 10^{-1} (R^2 = 0.90) (F), Y(NPQ) at 400 µmol m^{-2} s^{-1}, y = –6.02 × 10^{-3} x + 2.74 × 10^{-1} (R^2 = 0.79) (G), qL at 400 µmol m^{-2} s^{-1}, y = 1.14 × 10^{-2} x + 2.79 × 10^{-1} (R^2 = 0.96) (H) and Y(NO) at 400 µmol m^{-2} s^{-1}, y = –9.60 × 10^{-4} x + 3.59 × 10^{-1} (R^2 = 0.75) (I). Means ± SD are shown for the leaves from the plants grown in the growth chamber ($n \geq 5$) and those from the plants grown outdoors ($n \geq 3$), respectively.

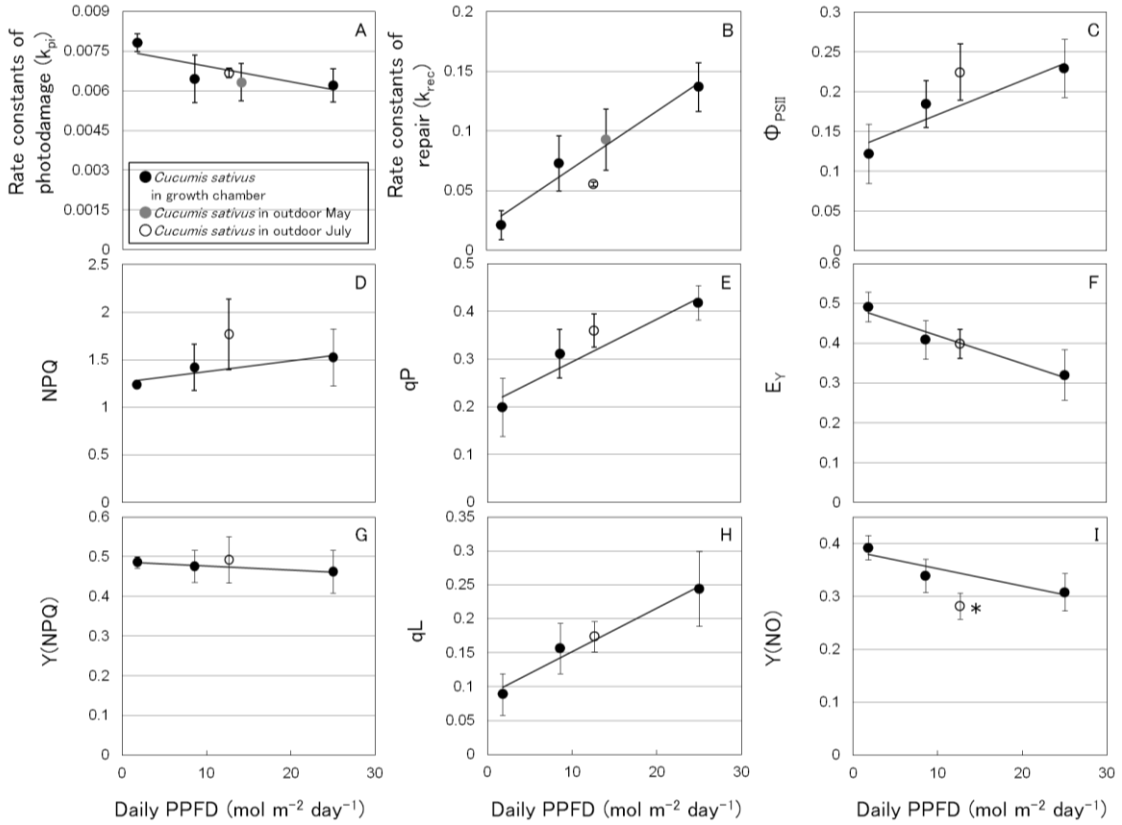

Fig. 14 Relationships between the rate constants for photodamage (k_{pi}) and repair (k_{rec}) and PSII fluorescence parameters of cucumber leaves treated at 1200 µmol m^{-2} s^{-1}.

k_{pi} and k_{rec} were obtained for the cucumber leaves grown outdoors in May and July 2014 and for the chamber at three different PPFDs. The leaves were photoinihibited at 1200 µmol m^{-2} s^{-1} (A and B). The Φ_{PSII}, NPQ, qP, E, Y(NPQ), qL and Y(NO) were measured at 1200 µmol m^{-2} s^{-1} (C – I). ●, *Cucumis sativus* grown in the growth chamber and, ● and ○, *Cucumis sativus* grown outdoors on the campus in May and July 2014. Regression lines are drawn for the data obtained with cucumber leaves that were grown continuous light at 35, 170 and 500 µmol m^{-2} s^{-1} for 14 h per day. The regression lines were: k_{pi} at 1200 µmol m^{-2} s^{-1}, $y = -5.92 \times 10^{-5} x + 7.52 \times 10^{-3}$ (R^2

= 0.66) (A), k_{rec} at 1200 µmol m^{-2} s^{-1}, y = 4.78 × 10^{-3} x + 2.04 × 10^{-2} (R^2 = 0.96) (B), Φ_{PSII} at 1200 µmol m^{-2} s^{-1}, y = 4.27 × 10^{-3} x + 1.28 × 10^{-1} (R^2 = 0.89) (C), NPQ at 1200 µmol m^{-2} s^{-1}, y = 1.12 × 10^{-2} x + 1.26 (R^2 = 0.86) (D), qP at 1200 µmol m^{-2} s^{-1}, y = 8.90 × 10^{-3} x + 2.05 × 10^{-1} (R^2 = 0.93) (E), E_Y at 1200 µmol m^{-2} s^{-1}, y = –6.98 × 10^{-3} x + 4.89 × 10^{-1} (R^2 = 0.95) (F), Y(NPQ) at 1200 µmol m^{-2} s^{-1}, y = –9.86 × 10^{-4} x + 4.86 × 10^{-1} (R^2 = 0.98) (G), qL at 1200 µmol m^{-2} s^{-1}, y = 6.43 × 10^{-3} x + 8.72 × 10^{-2} (R^2 = 0.97) (H) and Y(NO) at 1200 µmol m^{-2} s^{-1}, y = –3.30 × 10^{-3} x + 3.85 × 10^{-1} (R^2 = 0.86) (I). Means ± SD are shown for the leaves from the plants grown in the growth chamber ($n \geq 5$) and those from the plants grown outdoors ($n \geq 3$), respectively.

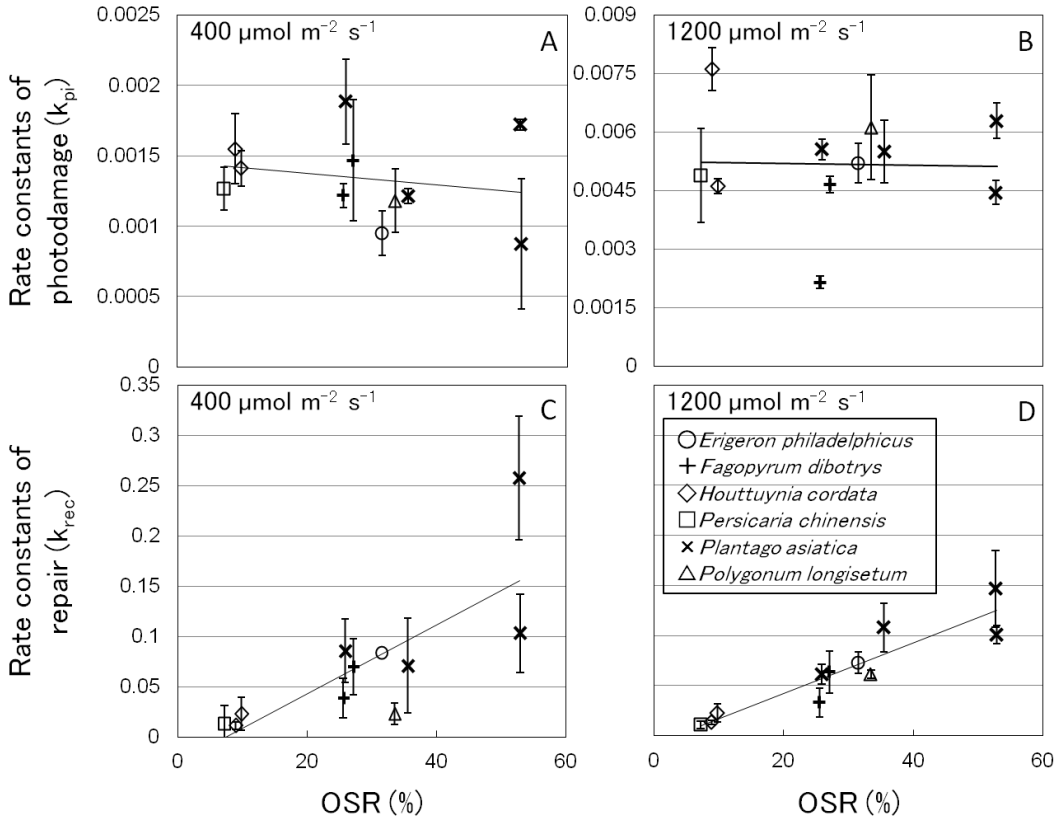

Fig. 15 Dependences of the rate constants for photodamage (k_{pi}) and repair (k_{rec}) on OSR.

Rate constants of photodamage (k_{pi}) in the field plants treated at 400 μmol m^{-2} s^{-1} (A) or 1200 μmol m^{-2} s^{-1} (B) and rate constants of repair (k_{rec}) in the field plants treated at 400 μmol m^{-2} s^{-1} (C) or 1200 μmol m^{-2} s^{-1} (D) are shown. ○, *Erigeron philadelphicus*; ＋, *Fagopyrum dibotrys*; ◇, *Hottuynia cordata*; □, *Persicaria chinensis*; ×, *Plantago asiatica* and △, *Polygonum longisetum*. Regression lines were: k_{pi} at 400 μmol m^{-2} s^{-1}, $y = -4.10 \times 10^{-6} x + 1.46 \times 10^{-3}$ ($R^2 = 0.044$), k_{pi} at 1200 μmol m^{-2} s^{-1}, $y = -2.30 \times 10^{-6} x + 5.25 \times 10^{-3}$ ($R^2 = 0.00069$), k_{rec} at 400 μmol m^{-2} s^{-1}, $y = 3.42 \times 10^{-3} x - 2.57 \times 10^{-2}$ ($R^2 = 0.59$) and k_{rec} at 1200 μmol m^{-2} s^{-1}, $y = 2.52 \times 10^{-3} x - 8.07 \times 10^{-3}$ ($R^2 = 0.85$). Means ± SD ($n \geq 3$) are shown.

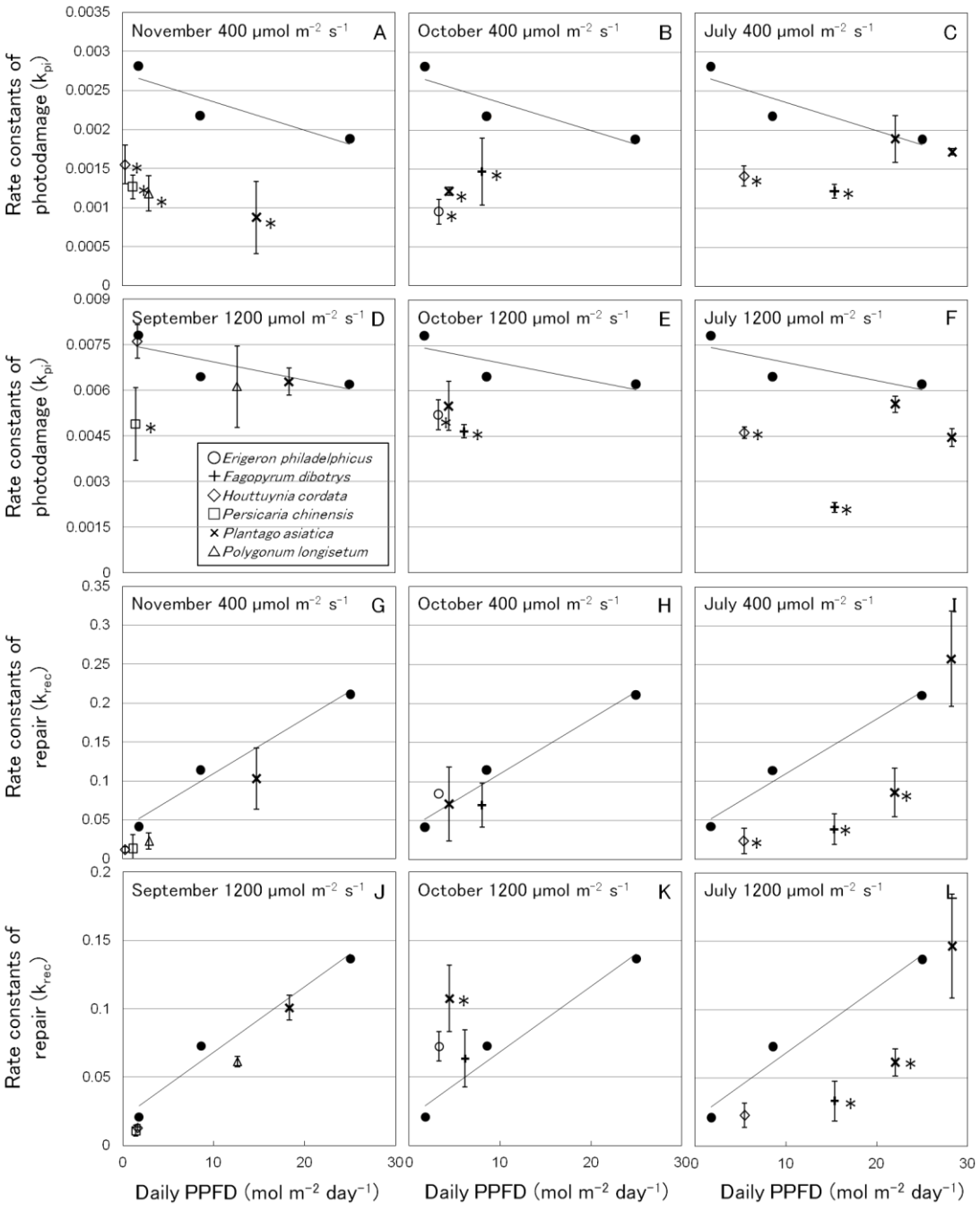

Fig. 16 Dependence of the rate constants for photodamage (k_{pi}) and repair (k_{rec}) on the daily PPFD.

The k_{pi} and k_{rec} were obtained for the leaves of the field plants collected on the campus and for cucumber leaves grown at three different PPFD in the growth chamber. The leaves sampled

in November 2013 were photoinihibited at 400 μmol m^{-2} s^{-1} (A and G). The leaves sampled in October 2013 were photoinihibited at 400 (B and H) or 1200 μmol m^{-2} s^{-1} (E and K). The leaves sampled in July 2014 were photoinihibited at 400 (C and I) or 1200 μmol m^{-2} s^{-1} (F and L). The leaves sampled in September 2013 were photoinihibited at 1200 μmol m^{-2} s^{-1} (D and J). ○, *Erigeron philadelphicus*; ＋, *Fagopyrum dibotrys*; ◇, *Hottuynia cordata*; □, *Persicaria chinensis*; ×, *Plantago asiatica* and △, *Polygonum longisetum*. The regression lines and the equations of cucumber leaves are the same as those in Figs. 13 and 14.

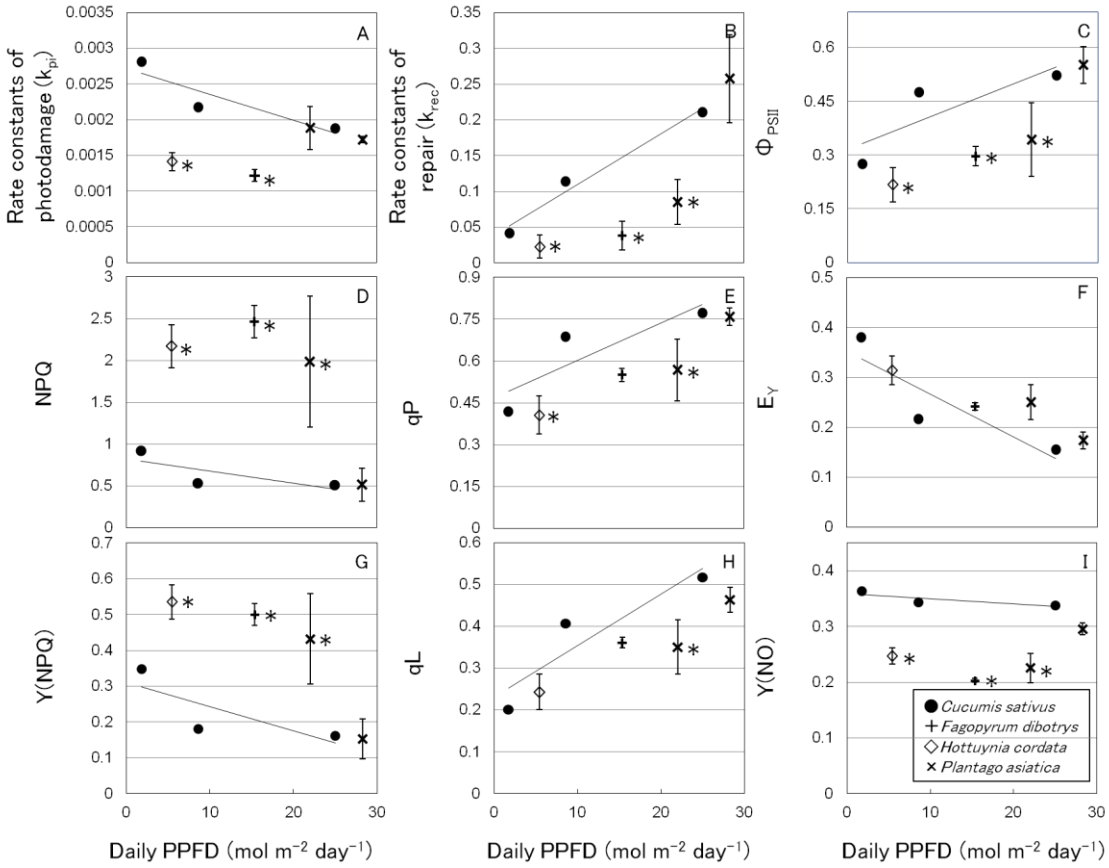

Fig. 17 Relationships between the rate constants for photodamage (k_{pi}) and repair (k_{rec}), and PSII fluorescence parameters, and daily PPFD.

The k_{pi} and k_{rec} were obtained for the leaves of the field plants collected in July 2014 and the cucumber leaves grown at three different PPFD in the growth chamber. The leaves were photoinihibited at 400 μmol m^{-2} s^{-1} (A and B). The Φ_{PSII}, NPQ, qP, E_Y, Y(NPQ), qL and Y(NO) were measured at 400 μmol m^{-2} s^{-1} (C – I). The symbols of plants leaves are ●, *Cucumis sativus*; ＋, *Fagopyrum dibotrys*; ◇, *Hottuynia cordata* and ×, *Plantago asiatica*. Means ± SD (n ≥ 3) are shown. Regression lines are drawn for the data obtained with cucumber leaves that were grown continuous light at 35, 170 and 500 μmol m^{-2} s^{-1} for 14 h per day. Means ± SD (n ≥

5) are shown. The regression lines are the same as those in Fig. 13.

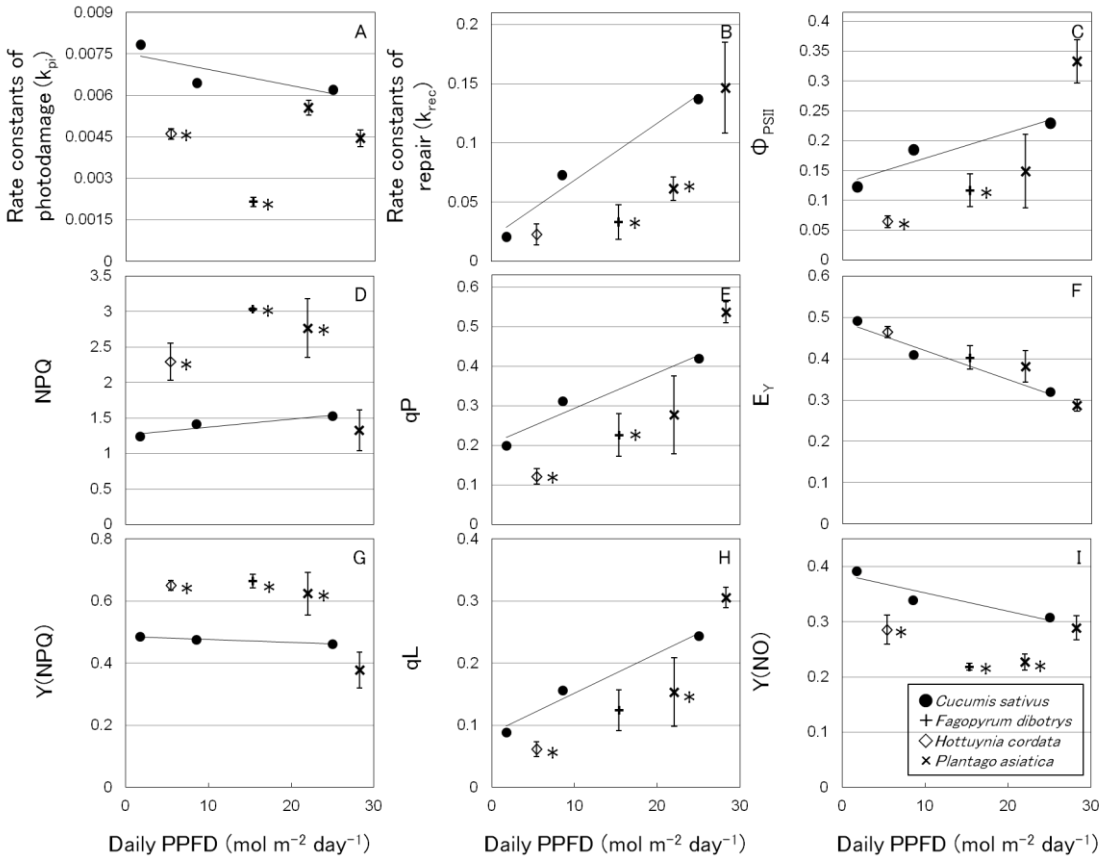

Fig. 18 Relationships between the rate constants for photodamage (k_{pi}) and repair (k_{rec}), and PSII fluorescence parameters, and daily PPFD.

The k_{pi} and k_{rec} were obtained for the leaves of the field plants collected in July 2014 and the cucumber leaves grown at three different PPFD in the growth chamber. The leaves were photoinihibited at 1200 μmol m^{-2} s^{-1} (A and B). The Φ_{PSII}, NPQ, qP, E_Y, Y(NPQ), qL and Y(NO) were measured at 1200 μmol m^{-2} s^{-1} (C – I). The symbols of plants leaves are ●, *Cucumis sativus*; ＋, *Fagopyrum dibotrys*; ◇, *Hottuynia cordata* and ×, *Plantago asiatica*. Means ± SD ($n \geq 3$) are shown. Regression lines are drawn for the data obtained with cucumber leaves that were grown continuous light at 35, 170 and 500 μmol m^{-2} s^{-1} for 14 h per day.

Means ± SD ($n \geq 5$) are shown. The regression lines are the same as those in Fig. 14.

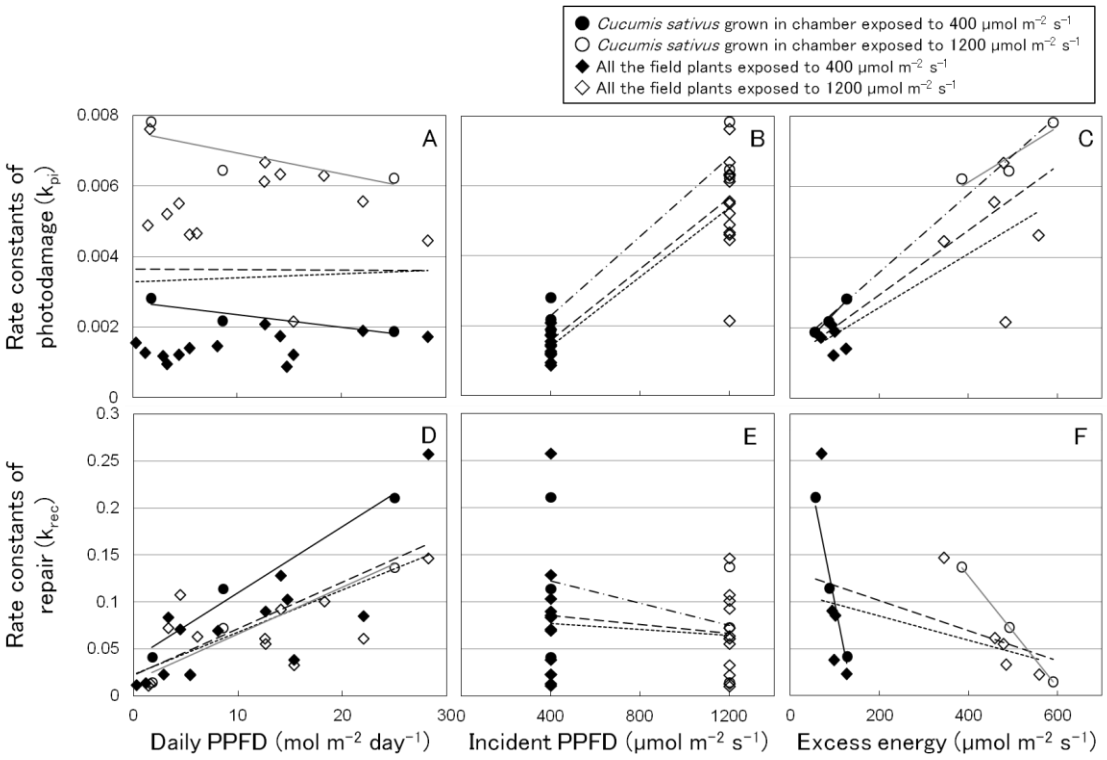

Fig. 19 Rate constants of photodamage (k_{pi}) and repair (k_{rec}) plotted against daily PPFD, incident PPFD and excess energy during the photoinhibitory treatments.

Rate constants of photodamage (k_{pi}: A and B) and repair (k_{rec}: C and D) in the chamber-grown cucumber and the field plants treated at 400 or 1200 µmol m^{-2} s^{-1}. Excess energy (µmol m^{-2} s^{-1}) was calculated as E_Y × the incident PPFD. ● and black solid-lines, *Cucumis sativus* grown in the chamber exposed to 400 µmol m^{-2} s^{-1}; ○ and gray solid-lines, *Cucumis sativus* grown in the chamber exposed to 1200 µmol m^{-2} s^{-1}; dash-dot-lines, the all *Cucumis sativus* grown in the chamber; ◆, all the field plants including *Cucumis sativus* grown in the field exposed to 400 µmol m^{-2} s^{-1}; ◇, all the field plants including *Cucumis sativus* grown in the field exposed to 1200 µmol m^{-2} s^{-1}; dot-lines, all the field plants including *Cucumis sativus* grown in the field

and dash-lines, the all plants. The equations of regression lines were: k_{pi} and k_{rec} on daily PPFD of chamber-grown cucumber leaves exposed to 400 or 1200 μmol m^{-2} s^{-1} were same with Figs. 13 and 14, k_{pi} on daily PPFD of all of the field plants, $y = 1.09 \times 10^{-5} x + 3.29 \times 10^{-3}$ (R^2 = 0.0016); k_{pi} on daily PPFD of the all plants, $y = -9.45 \times 10^{-7} x + 3.63 \times 10^{-3}$ (R^2 = 0.0000125); k_{pi} on incident PPFD of the all chamber-grown cucumber plants, $y = 5.67 \times 10^{-6} x + 2.15 \times 10^{-5}$ (R^2 = 0.94); k_{pi} on incident PPFD of all the field plants, $y = 4.95 \times 10^{-6} x - 5.52 \times 10^{-4}$ (R^2 = 0.81); k_{pi} on incident PPFD of the all plants, $y = 5.08 \times 10^{-6} x - 4.45 \times 10^{-4}$ (R^2 = 0.80); k_{pi} on excess energy of cucumber leaves, $y = 1.33 \times 10^{-5} x + 1.09 \times 10^{-3}$ (R^2 = 0.98) at 400 μmol m^{-2} s^{-1} and $y = 7.78 \times 10^{-6} x + 3.02 \times 10^{-3}$ (R^2 = 0.84) at 1200 μmol m^{-2} s^{-1}; k_{pi} on excess energy of the all chamber-grown cucumber plants, $y = 1.11 \times 10^{-5} x + 1.34 \times 10^{-3}$ (R^2 = 0.98); k_{pi} on excess energy of all the field plants, $y = 7.62 \times 10^{-6} x + 1.03 \times 10^{-3}$ (R^2 = 0.60); k_{pi} on excess energy of the all plants, $y = 9.15 \times 10^{-6} x + 1.09 \times 10^{-3}$ (R^2 = 0.70); k_{rec} on daily PPFD of all the field plants, $y = 4.50 \times 10^{-3} x + 2.25 \times 10^{-2}$ (R^2 = 0.48); k_{rec} on daily PPFD of the all plants, $y = 4.93 \times 10^{-3} x + 2.22 \times 10^{-2}$ (R^2 = 0.55); k_{rec} on incident PPFD of the all chamber-grown cucumber plants, $y = -5.92 \times 10^{-5} x + 1.46 \times 10^{-1}$ (R^2 = 0.13); k_{rec} on incident PPFD of all the field plants, $y = -1.51 \times 10^{-5} x + 8.29 \times 10^{-2}$ (R^2 = 0.013); k_{rec} on incident PPFD of the all plants, $y = -2.34 \times 10^{-5} x + 9.47 \times 10^{-2}$ (R^2 = 0.027); k_{rec} on excess energy of cucumber leaves, $y = -2.36 \times 10^{-3} x + 3.35 \times 10^{-1}$ (R^2 = 0.97) at 400 μmol m^{-2} s^{-1} and $y = -5.94 \times 10^{-4} x + 3.65 \times$

10^{-1} (R^2 = 0.99) at 1200 µmol m^{-2} s^{-1}; k_{rec} on excess energy of all the field plants, y = –1.28 × 10^{-4} x + 1.10 × 10^{-1} (R^2 = 0.12); and k_{rec} on excess energy of the all plants, y = –1.59 × 10^{-4} x + 1.33 × 10^{-1} (R^2 = 0.21).

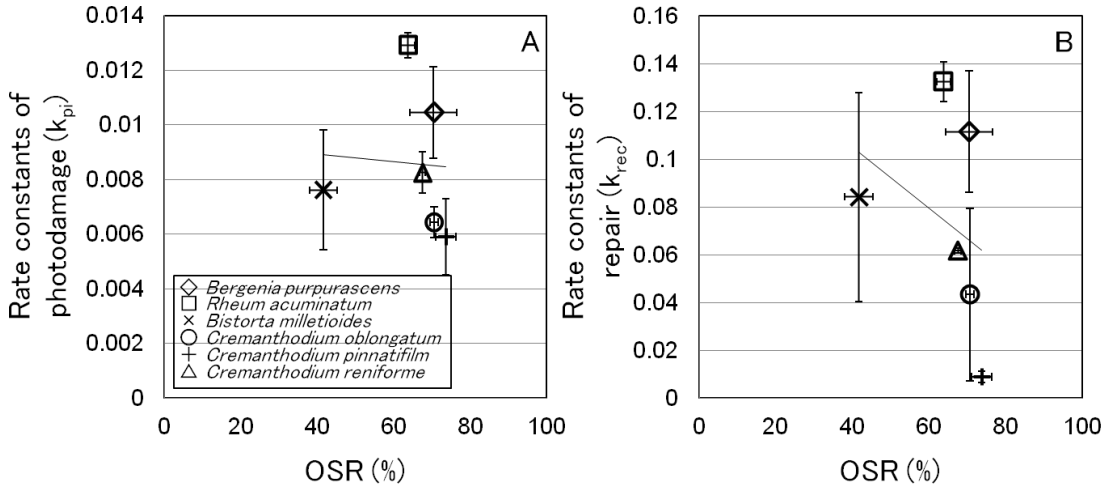

Fig. 20 OSR dependence of the rate constants for photodamage (k_{pi}) and repair (k_{rec}) on the field plants in the Jaljale Himal.

Rate constants of photodamage (k_{pi}: A) and repair (k_{rec}: B) were the photoinhibition-treated field plants at 1200 μmol m^{-2} s^{-1}. ◇, *Bergenia purpurascens*; □, *Rheum acuminatum*; ×, *Bistorta milletioides*; ○, *Cremanthodium oblongatum*; ＋, *Cremanthodium pinnatifilm*; and △, *Cremanthodium reniforme*. Regression lines are drawn for the data obtained with the all field plants in the Jaljale Himal. Regression lines were: k_{pi}, $y = -1.29 \times 10^{-5} x + 9.44 \times 10^{-3}$ (R^2 = 0.0033) and k_{rec}, $y = -1.27 \times 10^{-3} x + 1.56 \times 10^{-1}$ (R^2 = 0.11). Means ± SD (n = 3) are shown.

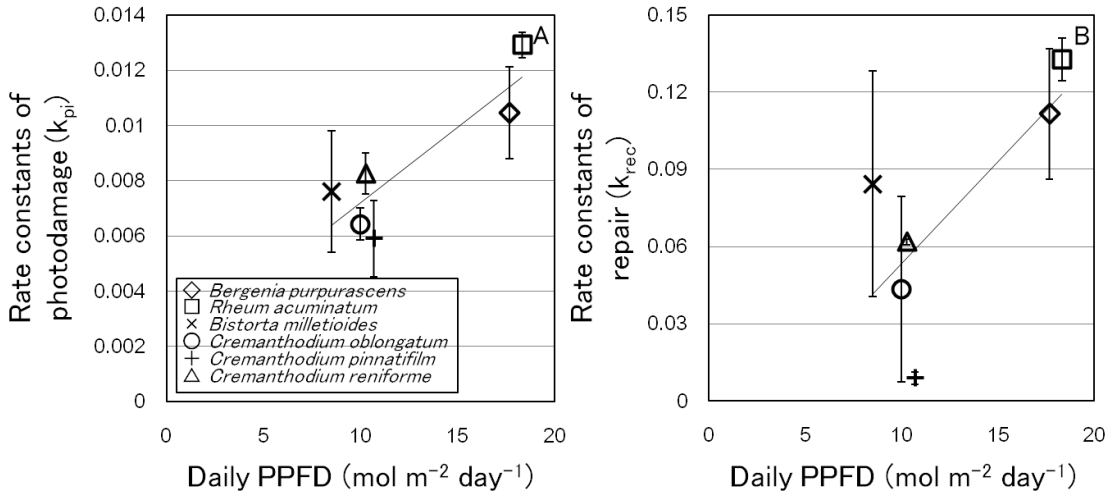

Fig. 21 Dependence of the rate constants for photodamage (k_{pi}) and repair (k_{rec}) on the daily PPFD.

The k_{pi} and k_{rec} were obtained for the leaves of the field plants collected in Jaljale Himal. The leaves were photoinihibited at 1200 μmol m^{-2} s^{-1} (A and B). ◇, *Bergenia purpurascens*; □, *Rheum acuminatum*; ×, *Bistorta milletioides*; ○, *Cremanthodium oblongatum*; ＋, *Cremanthodium pinnatifilm*; and △, *Cremanthodium reniforme*. Regression lines are drawn for the data obtained with all the field plants in the Jaljale Himal. Regression lines were: k_{pi}, $y = 5.46 \times 10^{-4} x + 1.74 \times 10^{-3}$ ($R^2 = 0.77$) and k_{rec}, $y = 7.86 \times 10^{-3} x - 2.45 \times 10^{-2}$ ($R^2 = 0.55$). Means ± SD (n = 3) are shown.

CHAPTER 4

Photoreactivation of the chilling-inactivated Mn cluster in *Cucumis sativus* L. leaves.

Introduction

Photosynthesis is a series of biochemical reactions that eventually produces oxygen and carbohydrates using light energy. The oxygen-evolution is the result of water oxidation by the manganese (Mn) cluster in the oxygen-evolving complex (OEC). The Mn cluster driven by a single turnover flash transfers an electron to the photosystem II reaction center (PSII-RC) via Yz, tyrosine residue of the D1 protein (for a review, see Ono 2001). Four flashes are needed to produce one O_2 through oxidation of two H_2O molecules (Joliot *et al*. 1969, Ono *et al*. 1992).

The Mn cluster loses Mn ions by the treatment with Tris or NH_2OH in vitro. The inactivated Mn cluster requires three factors for its reactivation (Ono 2001). Mn ion and Ca ion are needed (Tamura and Cheniae 1987). These are important constituents of the Mn cluster formulated as Mn_4CaO_5 (Umena *et al*. 2011). Another important factor is visible light. In the dark, reactivation of the inactivated Mn cluster does not occur (Ono and Inoue 1982). The light triggers an electron transfer in the PSII core complex. This electron transfer oxidizes the PSII-RC. Then, a loosely associated Mn ion provides an electron to the PSII-RC and simultaneously the Mn ion is incorporated to the OEC (Tamura *et al*. 1991). For activation of the OEC, at least two light dependent processes and one or more slow rate limiting dark processes are involved (Radmer and Cheniae 1971, Ono 2001).

The photosynthetic apparatus in *Cucumis sativus* L. is sensitive to chilling both in the light

and in the dark (Kaniuga *et al*. 1978, Terashima *et al*. 1991). When cucumber leaves are treated at 0˚C in the dark for 48 h, the Mn cluster is almost-totally inactivated due to two to three Mn ions are released from the Mn cluster (Shen *et al*. 1990). Two of the extrinsic OEC proteins are also disassembled (Shen *et al*. 1990). The chilling-inactivated Mn cluster in cucumber leaves is in the over-reduced state (Higuchi *et al*. 2003). These processes are reversible. The inactivated OEC can be reactivated by a low light treatment for 20 min (Shen *et al*. 1990, Higuchi *et al*. 2003).

There have been arguments concerning the mechanisms of the photoinhibition. In particular, the two-step hypothesis of the photoinhibition (Hakala *et al*. 2005, Ohnishi *et al*. 2005) urged us to re-address the photoactivation problems. The two-step hypothesis alleges that the first step of the photoinhibition is the release of Mn ion from the Mn cluster induced by the light absorbed by a Mn(III) in the Mn cluster. The Mn(III) shows high absorption in ultra-violet (UV) and blue region. The second step is the damage to the D1 protein in the PSII-RC by photosynthetically active light. Not only blue but also red is effective because chlorophyll well absorbs light at these wavelengths. The second process corroborates the excess energy hypothesis, the other hypothesis for the photoinhibition mechanism (Ögren *et al*. 1984, Vass *et al*. 1992). I need to re-examine photoreactivation processes of the Mn cluster in the repair cycle of PSII in the context of the two-step hypothesis. In this study, I clarified that the most effective photon flux

density for the photoreactivation and that the wavelength dependence of the photoreactivation in the chilled-cucumber leaf.

Materials and methods

Plant materials

Cucumber plants (*Cucumis sativus* L. 'Nanshin'), purchased from Takii & Co., Kyoto, Japan, were grown in a growth chamber, 14 h light / 10 h dark cycle at an air temperature of 23°C for about 20 days. Light was supplied by a bank of cool white fluorescent lamps (FPR96EX-N/A: Toshiba, Tokyo, Japan), and the photosynthetically active photon flux density (PPFD) just above the plants was 200 μmol m^{-2} s^{-1}. Seeds were sown in vermiculite in 200 mL cups and supplied with deionized water. After germination, the plants were supplied with a 1000-fold diluted Hyponex 6-10-5 (Hyponex Japan, Osaka, Japan), the undiluted solution of which contained 6.00% total nitrogen (2.90% ammoniac-nitrogen and 1.05% nitrate-nitrogen), 10.0% water-soluble phosphate, 5.0% water-soluble potassium, 0.05% water-soluble magnesium, 0.001% water-soluble manganese and 0.005% water-soluble boron. Only the first true leaves harvested from the plants and were used in this study.

Chilling pretreatments

The first true leaf was cut at the base of the petiole, and the petiole was cut in deionized water again to avoid embolism in the xylem. When leaves were treated in the dark, the leaves were floated on iced water at 0°C in a glass container placed on ice in a dark box for 48 h.

Photoreactivation treatments

The dark-chilled leaves were exposed to PPFD at 5, 10, 25, 100, 500 or 1000 μmol m^{-2} s^{-1} at 25℃ to induce photoreactivation. The leaves were floated on the water at 25°C and exposed to the light for 30 min. Air temperature around the leaves was kept at 25℃ using a fan. Because cucumber leaves are amphistomatous, the adaxial stomata were active. A boundary layer was thin because of the use of the fan. The light was provided by white, blue, green or red LEDs. Emission spectra of these LEDs are shown in Fig. 22. The white, blue, green and red LEDs were NSPW70CS-K1 RAIJIN (Nichia, Tokushima, Japan), NSPB500AS (Nichia, Tokushima, Japan), LP-508U70GC (PEACE CORPORATION, Saitama, Japan) and LP-B5R250-3A (PEACE CORPORATION, Saitama, Japan), respectively.

To inhibit repair process of D1 protein in PSII, we used lincomycin, an inhibitor of the chloroplast-encoded protein synthesis by the 70S ribosome, according to CHAPTER 2. The leaves were fed with more than 1 mL of the 1 mM lincomycin solution / g leaf fresh weight via their petioles in the dark at 25°C. The leaves were floated on the 1 mM lincomycin solution during the chilling pretreatments and the photoreactivation treatments.

Chlorophyll (Chl) fluorescence parameters

We measured the maximum quantum yield of PSII, F_v / F_m where $F_v = F_m – F_o$ (Kitajima and Butler 1975, Krause and Weis 1991), in the leaf with a fluorometer (PAM-2500, Walz, Effeltrich, Germany). Fluorescence parameters, incipient fluorescence (F_o), maximum fluorescence (F_m) and variable fluorescence ($F_v = F_m – F_o$), were measured with the fluorometer. The saturating pulse at PPFD of 6250 μmol m^{-2} s^{-1} was given for 0.8 s to obtain F_m. Before the measurement of fluorescence, the leaves were kept in the dark for at least 30 min. These measurements were conducted at room temperature.

Isolation of thylakoids

Thylakoids were isolated according to Terashima *et al*. (1991). Leaf segments were homogenized in an isolation medium containing 0.3 M sorbitol, 10 mM NaCl, 5 mM $MgCl_2$, 0.1% (w/v) bovine serum albumin and 40 mM Hepes-KOH (pH 7.0), with a Polytron PT-2000 homogeniser (Kinematica, Luzern, Switzerland) at a line voltage of 3. The homogenate was filtered through 26 μm nylon mesh and the filtrate was centrifuged at 3500 × g for 4 min. The precipitate was re-suspended carefully in a medium that contained 0.3 M sorbitol, 10 mM NaCl, 5 mM $MgCl_2$ and 40 mM Hepes-KOH (pH 7.5). All these isolation procedures were made keeping the sample temperature at 4°C. Chlorophylls were extracted with 80% acetone and determined according to Porra *et al*. (1989).

Measurement of thylakoid activities

Electron transport rates through PSII was assayed as the electron transport to dichlorophenol indophenol (DCIP) in a reaction medium containing 100 μM DCIP, 20 mM methylamine, 0.3 M sorbitol, 10 mM NaCl, 5 mM $MgCl_2$ and 40 mM Hepes-KOH (pH 7.5) with or without 1 mM diphenylcarbazide (DPC). DPC is an electron donor that directly delivers electrons to PSII-RC. Red light at PPFD of 11000 μmol m^{-2} s^{-1} was provided by KL2500 LCD and KL1500 LCD (Schott, Mainz, Germany) to the suspension is a cuvette though a red cut off filter V-R65 (Toshiba, Tokyo, Japan) and the absorbance change at 540 nm was monitored with a spectrophotometer (Hitachi 356, Hitachi High-Tech Fielding, Tokyo, Japan). All measurements were made at room temperature of ca. 25°C.

Results

Photoreactivation efficiency showed clear peaks at very low PPFD levels

Cucumber leaves were treated with the dark-chilling for 48 h and then exposed to the white light at various PPFDs for 30 min. The photoreactivation of the Mn cluster in PSII peaked at low PPFD range (5–25 μmol m^{-2} s^{-1}) (Figs. 23 and 24). When the leaves were exposed to the white LED, the maximum value of F_v / F_m of 0.65 and those of the DCIP photoreduction rates with and without DPC of 160–170 mmol DCIP mol^{-1} Chl s^{-1} were attained at 10 μmol m^{-2} s^{-1} (Figs. 23A and 24A). At the greater PPFD, the F_v / F_m and DCIP photoreduction rate without DPC gradually decreased to 0.14 and 17 mmol DCIP mol^{-1} Chl s^{-1} at 1000 μmol m^{-2} s^{-1}. The rate in the presence of DPC decreased to 41 mmol DCIP mol^{-1} Chl s^{-1} at 1000 μmol m^{-2} s^{-1} (Figs. 23A and 24A).

Light was differently effective in the photoreactivation depending on its waveband

Cucumber leaves were treated with the dark-chilling for 48 h and then exposed to the lights of different colors at various PPFDs for 30 min. When the leaves were exposed to red, the maximum value of F_v / F_m of 0.60 at 5 μmol m^{-2} s^{-1} and those of DCIP photoreduction rates with and without DPC of 100–120 mmol DCIP mol^{-1} Chl s^{-1} were attained at 5–10 μmol m^{-2} s^{-1} (Figs. 23B and 24B). At greater PPFD, the F_v / F_m and DCIP photoreduction rate without DPC

gradually decreased to 0.14 and 9 mmol DCIP mol^{-1} Chl s^{-1} at 1000 μmol m^{-2} s^{-1}, while the rates with DPC remained to be 55–75 mmol DCIP mol^{-1} Chl s^{-1} at 25–1000 μmol m^{-2} s^{-1} (Figs. 23B and 24B). When the leaves irradiated by the green LEDs, the maximum F_v / F_m of 0.64 at 10 μmol m^{-2} s^{-1} and those of DCIP photoreduction rates with and without DPC of 160–180 mmol DCIP mol^{-1} Chl s^{-1} were attained at 5–10 μmol m^{-2} s^{-1} (Figs. 23C and 24C). At greater PPFD, the F_v / F_m and DCIP photoreduction rate without DPC gradually decreased to 0.20 and 32 mmol DCIP mol^{-1} Chl s^{-1} at 1000 μmol m^{-2} s^{-1}, while the rates with DPC remained to be 65 mmol DCIP mol^{-1} Chl s^{-1} (Figs. 23C and 24C). When the leaves were illuminated with blue light, the DCIP photoreduction rate without DPC could never reach the rate with DPC (Fig. 24D). The maximum F_v / F_m value was 0.57 and DCIP photoreduction rate with DPC was 100 mmol DCIP mol^{-1} Chl s^{-1} but without DPC was 67 mmol DCIP mol^{-1} Chl s^{-1} at 10 μmol m^{-2} s^{-1} (Figs. 23D and 24D). As PPFD increased, the F_v / F_m gradually decreased to 0.22 at 1000 μmol m^{-2} s^{-1} (Fig. 23D). The DCIP photoreduction rates with DPC were more than 50 mmol DCIP mol^{-1} Chl s^{-1} even at 1000 μmol m^{-2} s^{-1} but those without DPC decreased steeply to 16 mmol DCIP mol^{-1} Chl s^{-1} at 100 μmol m^{-2} s^{-1} and then reached to 6 mmol DCIP mol^{-1} Chl s^{-1} at 1000 μmol m^{-2} s^{-1} (Fig. 24D).

Photosynthetic capability after photoreactivation

After the dark-chilling for 48 h and the reactivation treatment with white light at 10 μmol m^{-2} s^{-1} for 30 min, the cucumber leaf was irradiated at 500 μmol m^{-2} s^{-1} for various period up to 1 h. F_v / F_m decreased from 0.64 to 0.46 with irradiation time (Fig. 25A). DCIP photoreduction rates in the absence and presence of DPC increased to 170–180 mmol DCIP mol^{-1} Chl s^{-1} for 15 min and then decreased to 120 mmol DCIP mol^{-1} Chl s^{-1} with irradiation time (Fig. 25B). The effect of DPC on the DCIP photoreduction rates was not obsereved (Fig. 25B).

Discussion

Reactivation of the PSII activity, through the re-incorporation of Mn ions to the OEC to form the Mn cluster, clearly requires light (Ono and Inoue 1987, Tamura and Cheniae 1987). However, the most efficient reactivation was observed at very low PPFDs (Figs. 23 and 24). Stronger light inhibited not only the reactivation of the Mn cluster but also the photochemistry of PSII-RC (Fig. 24). PSII that were not reactivated would be more susceptible to photoinhibition of PSII-RC, which explains the decline in the DCIP photoreduction rate by DPC with the increase in PPFD (Fig. 24). In some PSII, the reactivation of the Mn cluster and the damage to the Mn cluster would occur subsequently. In such reaction centers, PSII-RC would be eventually damaged.

Before this experiment, I hypothesized that red light would most efficiently reactivate the Mn cluster and green light would be least effective. This was because, the reactivation of the Mn cluster requires electron transfers by PSII-RC (Ono 2001), and the Chl molecules in PSII-RC preferentially absorb red and blue light. Blue light would reactivate the Mn cluster as efficiently as red light. However, the Mn cluster must be more susceptible to blue light, because the Mn cluster absorbs blue light much more than red light (Hakala *et al*. 2005). However, the result was inconsistent with my hypothesis.

When the photoreactivation treatment was conducted with the blue LED, the DCIP

photoreduction rates without DPC were considerably lower than those with DPC even at low PPFDs of 5–10 μmol photon m^{-2} s^{-1} (Fig. 24D). This indicates that the reactivation was most strongly inhibited in blue light. In the blue light, the DCIP photoreduction rate without DPC decreased drastically with the increase in PPFD and attained 16 mmol DCIP mol^{-1} Chl s^{-1} even at 100 μmol photon m^{-2} s^{-1} (Fig. 24D). This would be due to the fact that the blue light is most effectively absorbed by the Mn ions. These facts were good agreement with the previous studies showing that blue light induces photoinihibition most strongly (Ohnishi *et al*. 2005, Oguchi *et al*. 2009). In contrast, the photoreactivation occurred most efficiently in green light (Fig. 24C). Because the green light is less absorbed by the Mn ions and PSII-RC (Hakala et al. 2005), while it is delivered to more evenly throughout the leaf (Terashima *et al*. 2009). The Mn cluster photoreactivation requires the electron flow (Tamura and Cheniae 1987, Ono 2001). The red light would be less absorbed by the Mn ions (Hakala *et al*. 2005). However, the red light inhibited the reactivation of the Mn cluster at relatively low PPFDs (Fig. 24B). Because the red light is less absorbed by the Mn ions as compared with the blue light but considerably absorbed by PSII-RC (Ohnishi *et al*. 2005), PSII would be damaged in PSII-RC irrespective of the states of the Mn cluster, whether the cluster is active or inactive. These results indicate that the green light facilitates the photoreactivation of the inactivated Mn cluster most efficiently in the leaf. Furthermore, the DCIP photoreduction rates at 500 μmol photon m^{-2} s^{-1} without DPC were

different depending on the light color, whereas the DCIP photoreduction rate with DPC were not different as such (Fig. 24). These results suggest that the Mn cluster is more sensitive to light color than PSII-RC.

Probably, the green light is delivered to evenly across the leaf and reactivates the Mn cluster of most of the mesophyll cells in the leaf. In contrast, the blue and red lights are absorbed preferentially in the adaxial part of the mesophyll and, more strongly inactivate PSII-RC than reactivate the Mn cluster. It is necessary to conduct similar experiments using optically thin suspensions of chloroplasts to clarify wavelength and irradiance dependences of reactivation.

After the reactivation treatment with white light at 10 μmol m^{-2} s^{-1} for 30 min of the leaves chilled in the dark for 48 h, the leaves were irradiated at 500 μmol photon m^{-2} s^{-1} (Fig. 25). F_v / F_m decreased with irradiation time (Fig. 25A). The DCIP photoreduction rates in the absence and presence of DPC increased for 15 min and decreased with irradiation time (Fig. 25B). Probably, the photoreactivation activity of the Mn cluster or somewhere in PSII was damaged by the chilling-treatment. If the damage to the reactivation processes is the case, the activity of photoreactivation of the Mn cluster assessed in the present study will be underestimated.

This study showed that the chilled-cucumber leaves were photoreactivated most effectively at low light. However, in strong light, in particular, in strong blue light, the reactivation of the Mn cluster was inhibited. Moreover, the PSII photochemistry was inhibited. If the two-step

hypothesis is the only mechanism for photoinbition, and if the reactivation of the Mn cluster in the PSII repair cycle is the similar process of photoreactivation, the reactivation of the Mn cluster would not occur in the strong light. Then, such the situation further induces photoinhibition of PSII-RC. However, cucumber leaves, which had not been chilled and treated with high white light at 1000 μmol m^{-2} s^{-1} for 30 min showed high F_v / F_m (0.74) and thylakoids isolated from these leaves showed high DCIP photoreduction rates (300 mmol DCIP mol^{-1} Chl s^{-1} in the absence and 260 mmol DCIP mol^{-1} Chl s^{-1} in the presence of DPC). This means that the repair cycle proceeded well in very high light. However, the very high DCIP photoreduction rates are probably affected by not only PSII but by also PSI. I need to examine the all of activated and inactivated DCIP photoreduction rates with the use of isolated PSII particle to exclude the PSI effect. More importantly, the PSII particle will show that behavior of PSII including Mn cluster at the photoinhibition.

Photoreactivation of the Mn cluster in the PSII repair process should be studied, if the two-step mechanism is the main mechanism of photoinhibition.

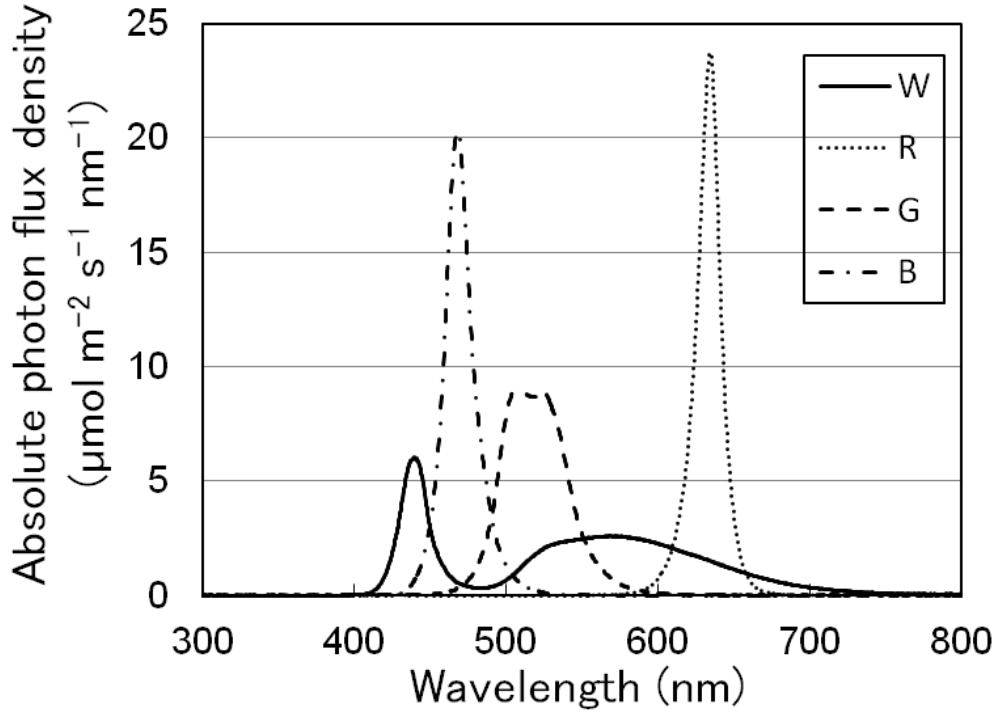

Fig. 22 Emission spectra of the LEDs at PPFD of 500 μmol m^{-2} s^{-1}.

Emission spectra of the four LEDs used in this study are shown. The spectra were measured with a spectrophotometer (USB2000+; Ocean Optics, FL, USA). W, white LED; R, red LED; G, green LED and, B, blue LED.

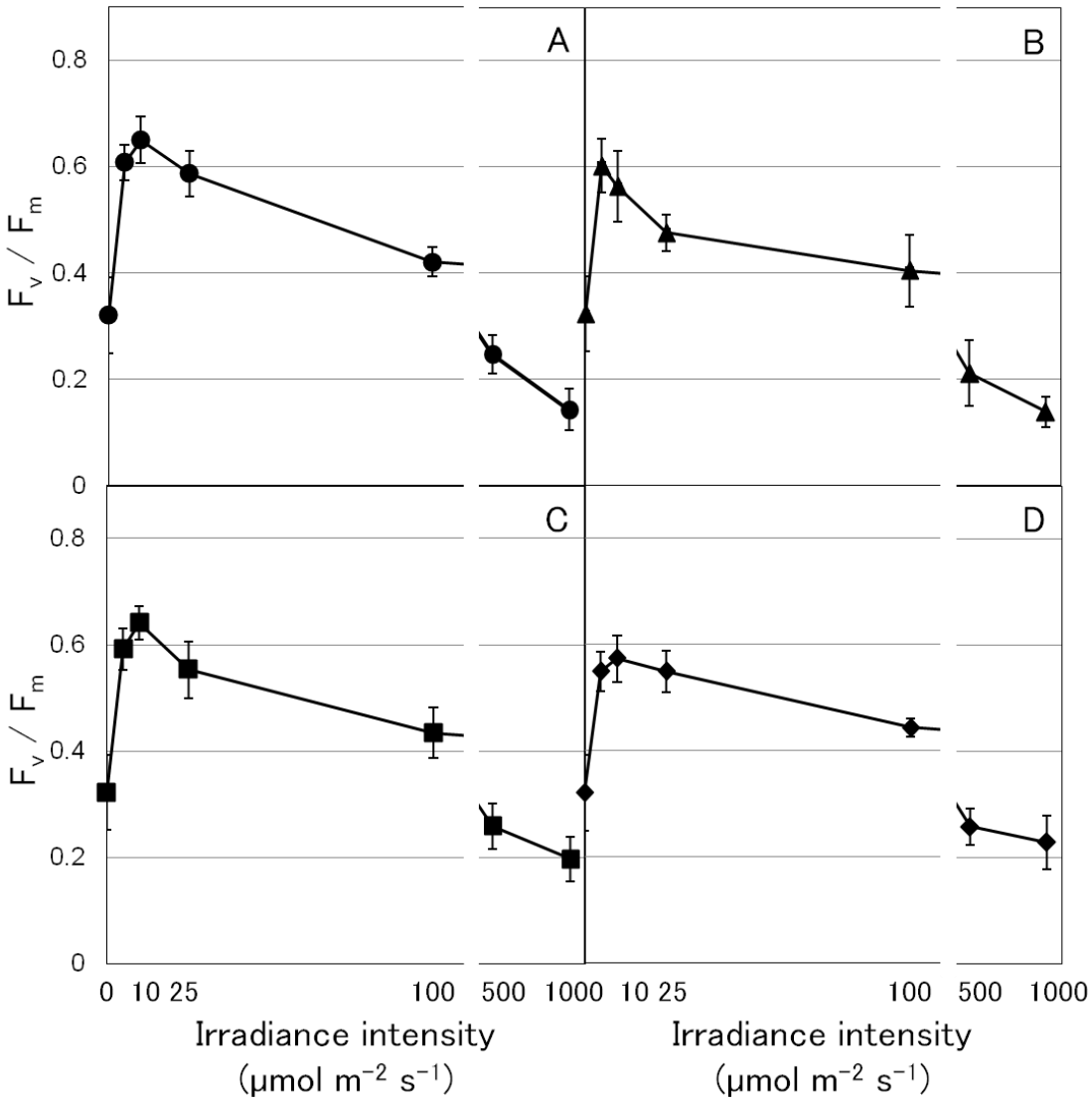

Fig. 23 F_v / F_m of cucumber leaves reactivated at various irradiance for 30 min after the dark-chilling treatment.

Cucumber leaves were treated in the dark at 0°C for 48 h and were irradiated at PPFD of 0, 5, 10, 25, 100, 500 or 1000 μmol m^{-2} s^{-1} for 30 min. Photoreactivation was conducted with white LED (A), red LED (B), green LED (C) or blue LED (D). The means ± SD ($n \geq 3$) are shown.

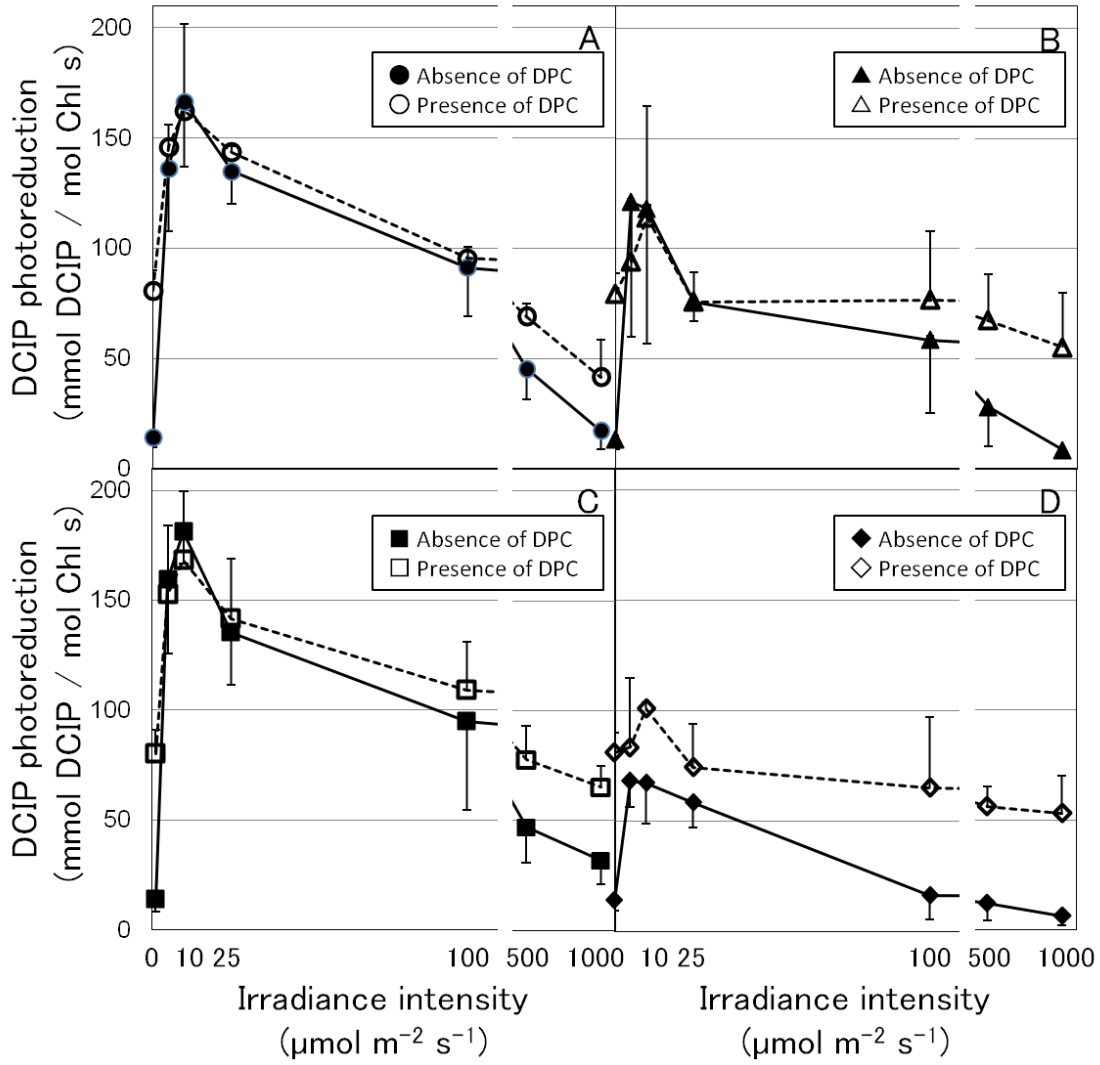

Fig. 24 DCIP photoreduction rates in the absence and presence of DPC of the thylakoid membranes after reactivation treatment.

DCIP photoreduction rates in the absence and presence of DPC of the thylakoid membranes isolated from cucumber leaves that were dark chilled and then reactivated at PPFD of 0, 5, 10, 25, 100, 500 or 1000 μmol m^{-2} s^{-1} for 30 min. The filled and open symbols denote absence and presence of DPC, respectively. The leaves were photoreactivated with white LED (A), red LED (B), green LED (C) or blue LED (D). The means ± SD ($n \geq 3$) are shown.

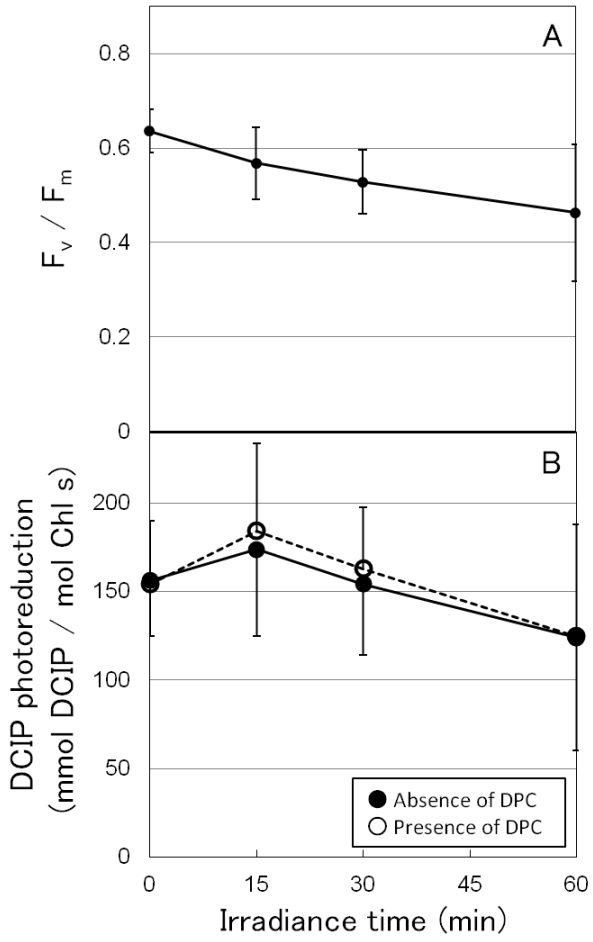

Fig. 25 F_v / F_m and DCIP photoreduction rates in the absence and presence of DPC in the leaves irradiated at 500 μmol m^{-2} s^{-1} after the dark-chilling and photoreactivation treatment with white light at 10 μmol m^{-2} s^{-1} for 30 min.

Cucumber leaves that were dark chilled for 48 h and then photoreactivation with white LED at 10 μmol m^{-2} s^{-1} for 30 min were irradiated at 500 μmol m^{-2} s^{-1} for indicated time. After the measurement of F_v / F_m (A), thylakoids were isolated and DCIP photoreduction rates were measured in the absence or presence of DPC (B). Filled and open symbols denote absence and presence of DPC. The means ± SD ($n \geq 3$) are shown.

General discussion

The cost of D1protein turnover and the determinant factor of k_{rec}

Plants overcome photoinhibition through a costly and complicated repair process. I estimated the amount of ATP for repairing D1 protein and other components in CHAPTER 2. The amount of ATP needed corresponded to 0.1-2% of ATP produced by the photophosphorylation. This is an amount that can be covered well in the chloroplast. I showed with a simulation using this result and various k_{rec} values that the repair activity (k_{rec}) *in vivo* is kept at the proper level. The daily photosynthesis rate was not influenced by the higher k_{rec} values whereas decreased markedly when the lower k_{rec} values were assumed. What is a factor responsible for the adjustment of k_{rec}? k_{pi} is influenced by the incident PPFD (Tyystjärvi and Aro 1996) or excess energy (Kato *et al*. 2003, CHAPTER 2). In CHAPTER 3, the k_{pi} values were more proportional to the incident PPFDs than the excess energy levels. However, the k_{pi}-regression line against the excess energy for all the plants including the chamber-grown plants as well as the field plants showed a strong relationship. k_{rec} is known to be influenced by incident PPFD and to show a broad peak against incident PPFD (Chow *et al*. 2005, Kato *et al*. 2002a, CHAPTER 2). Further, the present study revealed the fact that the k_{rec} values had a strong relationship against OSR and daily PPFD. This indicates that growth light environment affects k_{rec}. Because plants should pay a cost of the repair the photodamage to maintain high rates of photosynthesis, it is necessary to have an appropriate repair activity. It appears that the plants are able to adjust the repair activity depending on the growth light environments. Moreover, these results indicate the existence of a rate-determining factor of k_{rec}. Nishiyama *et al*. (2011) claimed that the elongation factor, EF-G, would be a rate-limiting factor in a cyanobacterium. They showed that EF-G is regulated by ROS and thioredoxin. There may be a similar regulation mechanism in the plants.

Photoreactivation of inactivated Mn cluster

The researchers supporting the two-step hypothesis have not paid attention to the problem that the inactivated Mn cluster should be reactivated without damage to the D1 protein and turnover of the D1 protein (Hakala *et al*. 2005). I showed that the photoreactivation of the inactivated Mn cluster using cucumber leaves that had been chilled in the dark to give damage to the Mn cluster in CHAPTER 4. The photoreactivation showed a strong dependence on wavelength. The blue light was most effective in inactivation of OEC while the green light most effectively reactivate OEC. This would be explained by the wavelength dependence of the Mn cluster and the chlorophyll in PSII. The blue light is most absorbed by the Mn cluster and the chlorophyll. The red light is well absorbed by the chlorophyll. The green light cannot be very well absorbed by the Mn cluster or by the chlorophyll. However, the green light that can be delivered more evenly to all the chloroplasts throughout the leaf is useful in the photosynthesis (Terashima *et al*. 2009). The green light has beneficial effects on the photosynthesis by driving and keeping photosynthesis efficiently in the whole leaf. If I use optically thin suspensions of PSII particles with inactivated Mn cluster, the Mn clusters will be reactivated by the red light. Probably, the blue light will similarly reactivate the PSII particles. However, it is probable that the inactivation by the blue light occurs faster than the reactivation. Such kinetics studies are needed.

New paradigm of the repair of PSII photoinhibition

Oguchi *et al*. (2009, 2011) suggested that both of the excess energy and the two-step mechanisms are operational in the photoinhibition *in vivo*. In addition, I suggest that at least some fraction of the Mn cluster inactivated by light will be reactivated without damaging the D1 protein. When the PSII photoinhibition occurs by the excess energy hypothesis, the inactivated

PSII will be repaired by the D1 protein turnover. On the other hand, when the PSII photoinhibition occurs by the two-step hypothesis, the inactivated PSII will be repaired by the reactivation of the Mn cluster keeping the PSII-RC activity or by the D1 protein turnover including activation of the Mn cluster. In the latter case, degradation of the D1 protein is necessary before the reactivation of the Mn cluster (Nishiyama *et al*. 2006). Also during the turnover of the D1 protein, Psb27 is associated with the PSII core complex at the site near the OEC being site (Nowaczyk *et al*. 2006). In addition, the Psb27 inactivates the PSII core complex (Grasse *et al*. 2011). Actually, in the Psb27 deficient mutant, the repair activity of the photoinhibition decreases drastically (Chen *et al*. 2006). After Psb27 dissociates from the PSII core complex, the Mn ions should be bound to the D1 protein by a PratA-like protein, LPA1, before OEC combines with the PSII core complex (Stengel *et al*. 2012, Peng *et al*. 2006). PratA was reported from a cyanobacterium and transports a Mn ion to a newly-developed PSII core complex (Stengel *et al*. 2012). Plants do not have a homolog of PratA. However, LPA1 in the plants and REP27 in green alga are envisaged to have a similar function (Peng *et al*. 2006, Park *et al*. 2007, Dewez *et al*. 2009, Nickelsen and Rengstl 2013). Because the Psb27 works in not only the repair process of PSII but also the newly-developing process of the PSII core complex, LPA1 probably works also in both processes (Becker *et al*. 2011). The PSII core complex combines the Mn ions, and the Mn cluster is photoactivated. Then, OEC binds to the PSII core complex. Taking account of these studies, the repair process of the PSII photoinhibition on the ground of the two-step hypothesis would be as follows.

When Mn in the Mn cluster absorbs light energy, the exited Mn is released from the Mn cluster. The PSII core complex in PSII having this inactivated OEC is inactivated by excess energy. PSII having the photodamaged D1 protein is phosphorylated and then released from the appressed thylakoids. Psb27 binds to PSII-RC that has lost its OEC. The inactivated PSII is

dephosphorylated and the photodameged D1 protein is degraded in the stroma thylakoid. The photodamaged PSII is degraded by the ATP-dependent protease FtsH and the ATP-independent protease Deg. The photodamaged D1 protein is cleaved to 10 kD and 23 kD by Deg2. Then, the 23 kD fragment is degraded by FtsH and the 10 kD fragment is degraded by Deg1, Clp etc. After the photodamaged D1 protein is removed from PSII, PSII requires a newly-synthesized D1 protein. The D1 protein, coded by the chloroplast gene, *psbA*, is sythesized by the chloroplast ribosome from the *psbA* mRNA. The newly-synthesized D1 protein is inserted into PSII during the *de novo* D1 protein synthesis by the chloroplast gene coded translocon cpSecY. The newly-synthesized D1 protein is matured by CtpA with processing on the C-terminal part of the newly-synthesized D1 protein. In this situation, Psb27 is released from the PSII core complex having matured D1 protein. LPA1 transports the Mn ion to the matured D1 protein. The transported Mn ion precariously binds to residues of the D1 protein. When electron transport occurs in PSII by light energy, the D1protein plucks out the electron from Mn(II) to compensate for the losing electron. The Mn(II) lost electron stably binds to the D1 protein via change to Mn(III). Thus, the Mn ion binds to the D1 protein by light energy and the Mn cluster is reactivated. Then, the OEC-proteins bind to PSII. The repaired PSII forms the PSII-LHCII complex and joins the electron transport in the grana thylakoid.

In the future

A new paradigm of the photoinhibition was proposed by the two-step hypothesis. However, the repair process premised on the two-step hypothesis is still unclear because the complete scenario of the repair process of the photoinhibition and, above all, the dynamic state of the repaired PSII and the Mn cluster remain undefined. How do the Mn ions bind to the repaired PSII? Does the Mn cluster entirely dissociate from the PSII core complex during the D1 protein

turnover? Is there the additional cost on the repair process of the Mn cluster? In the present knowledge, even if I add the Mn cluster activation to the cost of D1 protein turnover as above, the cost will not increase much. This is because the Mn cluster activation does not require ATP and thereby tool maintenance of the Mn cluster consumes little energy cost. Also, I would like clarify the actual state of the Mn cluster during the repair process in the photoinhibition. Probably, the process is as outlined above. The Mn cluster will not be reactivated before the degradation of the damaged D1 protein, and the reactivation process of PSII would be kept in the plants.

References

Adam Z, Clarke AK (2002) Cutting edge of chloroplast proteolysis. Trends Plant Sci 7:451-456. doi:10.1016/S1360-1385(02)02326-9

Alter P, Dreissen A, Luo FL, Matsubara S (2012) Acclimatory responses of *Arabidopsis* to fluctuating light environment: comparison of different sunfleck regimes and accessions. Photosyn Res 113:221-237. doi:10.1007/s11120-012-9757-2

Anderson JM, Aro EM (1994) Grana stacking and protection of Photosystem II in thylakoid membranes of higher plant leaves under sustained high irradiance: an hypothesis. Photosynth Res 41:315-326. doi:10.1007/BF00019409

Aro EM, Kettunen R, Tyystjarvi E (1992) ATP and light regulate D1 protein modification and degradation Role of D1* in photoinhibition. FEBS Lett 297:29-33. doi:10.1016/0014-5793(92)80320-G

Aro EM, Virgin I, Andersson B (1993a) Photoinhibition of photosystem II. Inactivation, protein damage and turnover. Biochim Biophys Acta 1143:113-134. doi:10.1016/0005-2728(93)90134-2

Aro EM, McCaffery S, Anderson JM (1993b) Photoinhibition and D1 protein degradation in peas acclimated to different growth irradiances. Plant Physiol 103:835-843. doi:10.1104/pp.103.3.835

Asada K (1999) The water-water cycle in chloroplasts: scavenging of active oxygens and dissipation of excess photons. Annu Rev Plant Physiol Plant Mol Biol 50:601-639. doi:10.1146/annurev.arplant.50.1.601

Asada K (2006) Production and scavenging of reactive oxygen species in chloroplasts and their functions. Plant Physiol 141:391-396. doi:10.1104/pp.106.082040

Baena-González E, Aro EM (2002) Biogenesis, assembly and turnover of photosystem II units. Phil Trans R Soc Lond B 357:1451-1460. doi:10.1098/rstb.2002.1141

Bassham JA (1977) Increasing crop production through more controlled photosynthesis. Science

197:630-638. doi:10.1126/science.197.4304.630

Becker K, Cormann KU, Nowaczyk MM (2011) Assembly of the water-oxidizing complex in photosystem II. J Photochem Photobiol B 104:204-211. doi:10.1016/j.jphotobiol.2011.02.005

Bilger W, Björkman O (1990) Role of the xanthophyll cycle in photoprotection elucidated by measurements of light-induced absorbency changes, fluorescence and photosynthesis in leaves of *Hedera canariensis*. Photosynth Res 25:173-185. doi:10.1007/BF00033159

Blankenship RE (2002) Molecular Mechanisms of Photosynthesis, Wiley-Blackwell, Blackwell Science, Oxford

Callahan FE, Becker DW, Cheniae GM (1986) Studies on the photoactivation of the water-oxidizing enzyme: II. Characterization of weak light photoinhibition of PSII and its light-induced recovery. Plant Physiol 82:261-269. doi:10.1104/pp.82.1.261

Campbell GS, Norman JM (1998) Radiation basics 10. In: Campbell GS, Norman JM (eds) An Introduction to Environmental Biophysics 2nd ed. Springer, Berlin, pp 147-165

Chen H, Zhang D, Guo J, Wu H, Jin M, Lu Q, Lu C, Zhang L (2006) A Psb27 homologue in *Arabidopsis thaliana* is required for efficient repair of photodamaged photosystem II. Plant Mol Biol 61:567-575. doi:10.1007/s11103-006-0031-x

Chow WS (1994) Photoprotection and photoinhibitory damage. Adv Mol Cell Biol 10: 151-196. doi:10.1016/S1569-2558(08)60397-5

Chow WS, Hope AB, Anderson JM (1989) Oxygen per flash from leaf disks quantifies Photosystem II. Biochim Biophys Acta 973:105-108. doi:10.1016/S0005-2728(89)80408-6

Chow WS, Lee HY, He J, Hendrickson L, Hong YN, Matsubara S (2005) Photoinactivation of photosystem II in leaves. Photosynth Res 84:35-41. doi:10.1007/s11120-005-0410-1

Chow WS, Jiang C, Wang X, Gao H, Shi L (2011) Systemic regulation of leaf anatomical structure, photosynthetic performance, and high-light tolerance in sorghum. Plant Physiol 155:1416-1424. doi:10.1104/pp.111.172213

Debus RJ (2001) Amino acid residues that modulate the properties of tyrosine Y_Z and the manganese cluster in the water oxidizing complex of photosystem II. Biochim Biophys Acta 1503:164-186. doi:10.1016/S0005-2728(00)00221-8

Demmig B, Björkman O (1987) Comparison of the effect of excessive light on chlorophyll fluorescence (77K) and photon yield of O_2 evolution in leaves of higher plants. Planta 171:171-184. doi:10.1007/BF00391092

Demmig-Adams B, Adams III WW (1992) Photoprotection and other responses of plants to high light stress. Annu Rev Plant Physiol Plant Mol Biol 43:599-626. doi:10.1146/annurev.pp.43.060192.003123

Demmig-Adams B, Adams III WW, Barker DH, Logan BA, Bowling DR, Verhoeven AS (1996) Using chlorophyll fluorescence to assess the fraction of excess excitation. Physiol Plant 98:253-264. doi:10.1034/j.1399-3054.1996.980206.x

Dewez D, Park S, García-Cerdán JG, Lindberg P, Melis A (2009) Mechanism of REP27 protein action in the D1 protein turnover and photosystem II repair from photodamage. Plant Physiol 151:88-99. doi:10.1104/pp.109.140798

Diner BA (2001) Amino acid residues involved in the coordination and assembly of the manganese cluster of photosystem II. Proton-coupled electron transport of the redox-active tyrosines and its relationship to water oxidation. Biochim Biophys Acta 1503:147-163. doi:10.1016/S0005-2728(00)00220-6

Diner BA, Ries DF, Cohen BN, Metz JG (1988) COOH-terminal processing of polypeptide D1 of the photosystem II reaction center of Scenedesmus obliquus is necessary for the assembly of the oxygen-evolving complex. J Biol Chem 263:8972-8980.

Epstein E (1994) The anomaly of silicon in plant biology. Proc Natl Acad Sci USA 91:11-17. doi:10.1073/pnas.91.1.11

Genty B, Briantais JM, Baker NR (1989) The relationship between the quantum yield of photosynthetic electron transport and quenching of chlorophyll fluorescence. Biochim Biophys Acta 990:87-92. doi:10.1016/S0304-4165(89)80016-9

Grasse N, Mamedov F, Becker K, Styring S, Rögner M, Nowaczyk MM (2011) Role of novel dimeric photosystem II (PSII)-Psb27 protein complex in PSII repair. J Biol Chem 286:29548-29555. doi:10.1074/jbc.M111.238394

Greenberg BM, Gaba V, Mattoo AK, Edelman M (1987) Identification of a primary in vivo degradation product of the rapidly-turning-over 32 kd protein of photosystem II. EMBO J 6:2865-2869.

Greer DH, Berry JA, Björkman O (1986) Photoinhibtion of photosynthesis in intact been leaves. Role of light and temperature, requirement for chloroplast-protein synthesis during recovery. Planta 168:253-260. doi:10.1007/BF00402971

Hakala M, Tuominen I, Keränen M, Tyystjärvi T, Tyystjärvi E (2005) Evidence for the role of the oxygen-evolving manganese complex in photoinhibition of Photosystem II. Biochim Biophys Acta 1706:68-80**.** doi:10.1016/j.bbabio.2004.09.001

Haußühl K, Andersson B, Adamska I (2001) A chloroplast DegP2 protease performs the primary cleavage of the photodamaged D1 protein in plant photosystem II. EMBO J 20:713-722. doi:10.1093/emboj/20.4.713

Higuchi M, Noguchi T, Sonoike K (2003) Over-reduced states of the Mn-cluster in cucumber leaves induced by dark-chilling treatment. Biochim Biophys Acta 1604:151-158. doi:10.1016/S0005-2728(03)00044-6

Hirose T, Werger MJA (1987) Nitrogen use efficiency in instantaneous and daily photosynthesis of leaves in the canopy of a *Solidage altissima* stand. Physiol Plant 70:215-222. doi:10.1111/j.1399-3054.1987.tb06134.x

Huesgen PF, Schuhmann H, Adamska I (2006) Photodamaged D1 protein is degraded in *Arabidopsis* mutants lacking the Deg2 protease. FEBS Lett 580:6929-6932. doi:10.1016/j.febslet.2006.11.058

Inagaki N, Maitra R, Satoh K, Pakrasi HB (2001) Amino acid residues that are critical for in vivo catalytic activity of CtpA, the carboxyl-terminal processing protease for the D1 protein of photosystem II. J Biol Chem 276:30099-30105.doi:10.1074/jbc.M102600200

Ishikawa Y, Yamamoto Y, Otsubo M, Theg SM, Tamura N (2002) Chemical modification of amine groups on PS II protein(s) retards photoassembly of the photosynthetic water-oxidizing complex. Biochemistry 41:1972-1980. doi:10.1021/bi0102499

Jegerschold C, Styring S (1991) Fast oxygen-independent degradation of the D1 reaction center protein in photosystem II. FEBS Lett 280:87-90. doi:10.1016/0014-5793(91)80210-T

Joliot P, Barbieri G, Chabaud R (1969) Un nouveau modele des centres photochimiques du systeme II. Photochem Photobiol 10:309-329. doi:10.1111/j.1751-1097.1969.tb05696.x

Kaniuga Z, Sochanowicz B, Ząbek J, Krystyniak K (1978) Photosynthetic apparatus in chilling-sensitive plants : I. Reactivation of hill reaction activity inhibited on the cold and dark storage of detached leaves and intact plants. Planta 140:121-128. doi:10.1007/BF00384910

Kato MC, Hikosaka K, Hirose T (2002a) Photoinactivation and recovery of photosystem II in *Chenopodium aibum* leaves grown at different levels of irradiance and nitrogen availability. Func Plant Biol 29:787-795. doi:10.1071/PP01162

Kato MC, Hikosaka K, Hirose T (2002b) Leaf discs floated on water are different from intact leaves in photosynthesis and photoinhibition. Photosyn Res 72:65-70. doi:10.1023/A:1016097312036

Kato MC, Hikosaka K, Hirotsu N, Makino A, Hirose T (2003) The excess light energy that is neither utilized in photosynthesis nor dissipated by photoprotective mechanisms determines the rate of photoinactivation in photosystem II. Plant Cell Physiol 44:318-325. doi:10.1093/pcp/pcg045

Kato Y, Sakamoto W (2009) Protein quality control in chloroplasts: a current model of D1 protein degradation in the photosystem II repair cycle. J Biochem 146:463-469. doi:10.1093/jb/mvp073

Kato Y, Sun X, Zhang L, Sakamoto W (2012) Cooperative D1 degradation in the photosystem II repair mediated by chloroplastic proteases in *Arabidopsis*. Plant Physiol 159:1428-1439. doi:10.1104/pp.112.199042

Kettunen R, Pursiheimo S, Rintamäki E, van Wijk KJ, Aro EM (1997) Transcriptional and

translational adjustments of *psbA* gene expression in mature chloroplasts during photoinhibition and subsequent repair of photosystem II. Eur J Biochem 247:441-448. doi:10.1111/j.1432-1033.1997.00441.x

Kimura Y, Ono T (2006) Structural and functional studies of photosynthetic oxygen evolving Mn cluster by means of FTIR spectroscopy. Biophysics 46:124-129.

Kitajima M, Butler WL (1975) Quenching of chlorophyll fluorescence and primary photochemistry in chloroplasts by dibromothymoquinone. Biochim Biophys Acta 376:105-115. doi:10.1016/0005-2728(75)90209-1

Kok B (1956) On the inhibition of photosynthesis by intense light. Biochim Biophys Acta 21:234-244. doi:10.1016/0006-3002(56)90003-8

Kok B, Forbush B, McGloin M (1970) Cooperation of charges in photosynthetic O_2 evolution. I. A linear four step mechanism. Photochem Photobiol 11:467-475. doi:10.1111/j.1751-1097.1970.tb06017.x

Kono M, Noguchi K, Terashima I (2014) Roles of the cyclic electron flow around PSI (CEF-PSI) and O_2-dependent alternative pathways in regulation of the photosynthetic electron flow in short-term fluctuating light in *Arabidopsis thaliana*. Plant Cell Physiol 55:990-1004. doi:10.1093/pcp/pcu033

Kono M, Terashima I (2014) Long-term and short-term responses of the photosynthetic electron transport to fluctuating light. J Photochem Photobiol B. in press. doi:10.1016/j.jphotobiol.2014.02.016

Kramer DM, Johnson G, Kiirats O, Edwards GE (2004) New fluorescence parameters for determination of Q_A redox state and excitation energy fluxes. Photosynth Res 79:209-218. doi:10.1023/B:PRES.0000015391.99477.0d

Krause GH, Weis E (1991) Chlorophyll fluorescence and photosynthesis: the basic. Annu Rev Plant Physiol Plant Mol Biol 42:313-349. doi:10.1146/annurev.pp.42.060191.001525

Lee HY, Hong YN, Chow WS (2001) Photoinactivation of photosystem II complexes and photoprotection by non-functional neighbours in *Capsicum annuum* L. leaves. Planta

212:332-342. doi:10.1007/s004250000398

Li XP, Müller-Moulé P, Gilmore AM, Niyogi KK (2002) PsbS-dependent enhancement of feedback de-excitation protects photosystem II from photoinhibition. Proc Natl Acad Sci USA 99:15222-15227. doi:10.1073/pnas.232447699

Lindahl M, Spetea C, Hundal T, Oppenheim AB, Adam Z, Andersson B (2000) The thylakoid FtsH protease plays a role in the light-induced turnover of the photosystem II D1 protein. Plant Cell 12:419-431. doi:10.1105/tpc.12.3.419

Long SP, Humphries S, Falkowski PG (1994) Photoinhibition of photosynthesis in nature. Annu Rev Plant Physiol Plant Mol Biol 45:633-662. doi:10.1146/annurev.pp.45.060194.003221

Mulo P, Sirpiö S, Suorsa M Aro EM (2008) Auxiliary proteins involved in the assembly and sustenance of photosystem II. Photosynth Res 98:489-501. doi: 10.1007/s11120-008-9320-3

Murata N, Allakhverdiev SI, Nishiyama Y (2012) The mechanism of photoinhibition in vivo: re-evaluation of the roles of catalase, α-tocopherol, non-photochemical quenching, and electron transport. Biochim Biophys Acta 1817:1127-1133. doi:10.1016/j.bbabio.2012.02.020

Nickelsen J, Rengstl B (2013) Photosystem II assembly: from cyanobacteria to plants. Annu Rev Plant Biol 64:609-635. doi:10.1146/annurev-arplant-050312-120124

Nishiyama Y, Allakhverdiev SI, Murata N (2006) A new paradigm for the action of reactive oxygen species in the photoinhibition of photosystem II. Biochim Biophys Acta 1757:742-749. doi:10.1016/j.bbabio.2006.05.013

Nishiyama Y, Allakhverdiev SI, Murata N (2011) Protein synthesis is the primary target of reactive oxygen species in the photoinhibition of photosystem II. Physiol Plant 142:35-46. doi:10.1111/j.1399-3054.2011.01457.x

Nishiyama Y, Yamamoto H, Allakhverdiev SI, Inaba M, Yokota A, Murata N (2001) Oxidative stress inhibits the repair of photodamage to the photosynthetic machinery. EMBO J 20:5587-5594. doi:10.1093/emboj/20.20.5587

Nishiyama Y, Allakhverdiev SI, Yamamoto H, Hayashi H, Murata N (2004) Singlet oxygen

inhibits the repair of photosystem II by suppressing the translation elongation of the D1 protein in *Synechocystis* sp. PCC 6803. Biochemistry 43*:* 11321-11330. doi: 10.1021/bi036178q

Noguchi K, Go CS, Terashima I, Ueda S, Yoshinari T (2001a) Activities of the cyanide-resistant respiratory pathway in leaves of sun and shade species. Aust J Plant Physiol 28:27-35. doi:10.1071/PP00056

Noguchi K, Go CS, Miyazawa SI, Terashima I, Ueda S, Yoshinari T (2001b) Costs of protein turnover and carbohydrate export in leaves of sun and shade species. Aust J Plant Physiol 28:37-47. doi:10.1071/PP00057

Nowaczyk MM, Hebeler R, Schlodder E, Meyer HE, Warscheid B, Rögner M (2006) Psb27, a cyanobacterial lipoprotein, is involved in the repair cycle of photosystem II. Plant Cell 18:3121-3131. doi:10.1105/tpc.106.042671

Ögren E, Öquist G, Hällgren JE (1984) Photoinhibition of photosynthesis in *Lemna gibba* as induced by the interaction between light and temperature. I. Photosynthesis in vivo. Physiol Plant 62:181-186. doi:10.1111/j.1399-3054.1984.tb00368.x

Oguchi R, Terashima I, Chow WS (2009) The involvement of dual mechanisms of photoinactivation of photosystem II in *Capsicum annuum* L. plants. Plant Cell Physiol 50:1815-1825. doi: 10.1093/pcp/pcp123

Oguchi R, Douwstra P, Fujita T, Chow WS, Terashima I (2011) Intra-leaf gradients of photoinhibition induced by different color lights: implications for the dual mechanisms of photoinhibition and for the application of conventional chlorophyll fluorometers. New Phytol 191:146-159. doi:10.1111/j.1469-8137.2011.03669.x

Ohnishi N, Allakhverdiev SI, Takahashi S, Higashi S, Watanabe M, Nishiyama Y, Murata N (2005) Two-step mechanism of photodamage to photosystem II: step 1 occurs at the oxygen-evolving complex and step 2 occurs at the photochemical reaction center. Biochemistry 44:8494-8499. doi:10.1021/bi047518q

Ono T (2001) Metallo-radical hypothesis for photoassembly of $(Mn)_4$-cluster of photosynthetic oxygen evolving complex. Biochim Biophys Acta 1503:40-51. doi:10.1016/S0005-2728(00)00226-7

Ono T, Inoue Y (1982) Photoactivation of the water-oxidation system in isolated intact chloroplasts prepared from wheat leaves grown under intermittent flash illumination. Plant Physiol 69:1418-1422. doi:10.1104/pp.69.6.1418

Ono T, Inoue Y (1987) Reductant-sensitive intermediates involved in multi-quantum process of photoactivation of latent O_2-evolving system. Plant Cell Physiol 28:1293-1299.

Ono T, Noguchi T, Inoue Y, Kusunoki M, Matsushita T, Oyanagi H (1992) X-ray detection of the period-four cycling of the manganese cluster in photosynthetic water oxidizing enzyme. Science 258:1335-1337. doi:10.1126/science.258.5086.1335

Öquist G, Anderson JM, McCaffery S Chow WS (1992) Mechanistic differences in photoinhibition of sun and shade plants. Planta 188:422-431. doi:10.1007/BF00192810

Osmond CB (1994) What is photoinhibition? Some insights from comparison of shade and sun plants. In: Baker NR, Bowyer JR (ed) Photoinhibition of photosynthesis: from molecular mechanisms to the field. Bios Scientific Publishers, Oxford, pp 1-24

Park S, Khamai P, Garcia-Cerdan JG, Melis A (2007) REP27, a tetratricopeptide repeat nuclear-encoded and chloroplast-localized protein, functions in D1/32-kD reaction center protein turnover and photosystem II repair from photodamage. Plant Physiol 143:1547-1560. doi:10.1104/pp.107.096396

Park YI, Anderson JM Chow WS (1996) Photoinactivation of functional photosystem II and D1-protein synthesis *in vivo* are independent of the modulation of the photosynthetic apparatus by growth irradiance. Planta 198:300-309. doi:10.1007/BF00206257

Peng L, Ma J, Chi W, Guo J, Zhu S, Lu Q, Lu C, Zhang L (2006) LOW PSII ACCUMULATION1 is involved in efficient assembly of photosystem II in *Arabidopsis thaliana*. Plant Cell 18:955-969. doi:10.1105/tpc.105.037689

Porra RJ, Thompson WA, Kriedemann PE (1989) Determination of accurate extinction coefficients and simultaneous equations for assaying chlorophylls *a* and *b* extracted with four different solvents: verification of the concentration of chlorophyll standards by atomic absorption spectroscopy. Biochim Biophys Acta 975:384-394.

doi:10.1016/S0005-2728(89)80347-0

Powles SB (1984) Photoinhibition of photosynthesis induced by visible light. Annu Rev Plant Physiol 35:15-44. doi:10.1146/annurev.pp.35.060184.000311

Radmer R, Cheniae GM (1971) Photoactivation of the manganese catalyst of O_2 evolution. II. A two-quantum mechanism. Biochim Biophys Acta 253:182-186. doi:10.1016/0005-2728(71)90243-X

Raven JA (1989) Fight or flight: the economics of repair and avoidance of photoinhibition of photosynthesis. Funct Ecol 3:5-19. doi:10.2307/2389670

Raven JA (2011) The cost of photoinhibition. Physiol Plant 142:87-104. doi:10.1111/j.1399-3054.2011.01465.x

Rintamaki E, Kettunen R, Aro EM (1996) Differential D1 dephosphorylation in functional and photodamaged photosystem II centers. J Biol Chem 271:14870-14875. doi:10.1074/jbc.271.25.14870

Roose JL, Pakrasi HB (2004) Evidence that D1 processing is required for manganese binding and extrinsic protein assembly into photosystem II. J Biol Chem 279:45417-45422. doi:10.1074/jbc.M408458200

Schreiber U, Bilger W, Neubauer C (1994) Chlorophyll fluorescence as a nonintrusive indicator for rapid assessment of *in vivo* photosynthesis. In: Schulze E-D, Caldwell MM (eds) Ecophysiology of Photosynthesis. Springer, Berlin, pp 49-70

Shipton CA, Barber J (1991) Photoinduced degradation of the D1 polypeptide in isolated reaction centers of photosystem II: evidence for an autoproteolytic process triggered by the oxidizing side of the photosystem. Proc Natl Acad Sci USA88:6691-6695. doi:10.1073/pnas.88.15.6691

Shen JR, Terashima I, Katoh S (1990) Cause for dark, chilling-induced inactivation of photosynthetic oxygen-evolving system in cucumber leaves. Plant Physiol 93:1354-1357. doi:10.1104/pp.93.4.1354

Spetea C, Hundal T, Lohmann F, Andersson B (1999) GTP bound to chloroplast thylakoid membranes is required for light-induced, multienzyme degradation of the photosystem II D1 protein. Proc Natl Acad Sci USA 96:6547-6552. doi:10.1073/pnas.96.11.6547

Stefanov D, Terashima I (2008) Non-photochemical loss in PSII in high- and low-light-grown leaves of *Vicia faba* quantified by several fluorescence parameters including L_{NP}, F_0/ F_m', a novel parameter. Physiol Plant 133:327-338. doi:10.1111/j.1399-3054.2008.01077.x

Stengel A, Gügel IL, Hilger D, Rengstl B, Jung H, Nickelsen J (2012) Initial steps of photosystem II de novo assembly and preloading with manganese take place in biogenesis centers in *Synechocystis*. Plant Cell 24:660-675. doi:10.1105/tpc.111.093914

Takahashi S, Milward SE, Fan DY, Chow WS, Badger M (2009) How does cyclic electron flow alleviate photoinhibition in *Arabidopsis*? Plant Physiol 149:1560-1567 doi:10.1104/pp.108.134122

Takahashi S, Badger MR (2011) Photoprotection in plants: a new light on photosystem II damage. Trends Plant Sci 16:53-60. doi:10.1016/j.tplants.2010.10.001

Tamura N, Cheniae G (1987) Photoactivation of the water-oxidizing complex in photosystem II membranes depleted of Mn and extrinsic proteins. I. Biochemical and kinetic characterization. Biochim Biophys Acta 890:179-194. doi:10.1016/0005-2728(87)90019-3

Tamura N, Kamachi H, Hokari N, Masumoto H, Inoue H (1991) Photoactivation of the water-oxidizing complex of photosystem II core complex depleted of functional Mn. Biochim Biophys Acta 1060:51-58. doi:10.1016/S0005-2728(05)80118-5

Terashima I, Fujita T, Inoue T, Chow WS, Oguchi R (2009) Green light drives leaf photosynthesis more efficiently than red light in strong white light: revisiting the enigmatic question of why leaves are green. Plant Cell Physiol 50:684-697. doi:10.1093/pcp/pcp034

Terashima I, Huang LK, Osmond B (1989) Effects of leaf chilling on thylakoid functions, measured at room temperature, in *Cucumis sativus* L. and *Oryza sativa* L. Plant Cell Physiol 30:841-850.

Terashima I, Kashino Y, Katoh S (1991) Exposure of leaves of *Cucumis sativus* L. to low

temperatures in the light causes uncoupling of thylakoids I. Studies with isolated thylakoids. Plant Cell Physiol 32:1267-1274.

Terashima I, Masuzawa T, Ohba H (1993) Photosynthetic characteristics of a giant alpine plant, *Rheum nobile* Hook. f. et Thoms. and of some other alpine species measured at 4300 m, in the Eastern Himalaya, Nepal. Oecologia 95:194-201. doi:10.1007/BF00323490

Tikkanen M, Greaco M, Kangasjärvi S, Aro EM (2010) Thylakoid protein phosphorylation in higher plant chloroplasts optimizes electron transfer under fluctuating light. Plant Physiol 152:723-735. doi:10.1104/pp.109.150250

Tsonev TD, Hikosaka K (2003) Contribution of photosynthetic electron transport, heat dissipation, and recovery of photoinactivated photosystem II to photoprotection at different temperatures in *Chenopodium album* leaves. Plant Cell Physiol 44:828-835. doi:10.1093/pcp/pcg107

Tu W, Li Y, Zhang Y, Zhang L, Liu H, Liu C, Yang C (2012) Diminished photoinhibition is involved in high photosynthetic capacities in spring ephemeral *Berteroa incana* under strong light conditions. J Plant Physiol 169:1463-1470. doi:10.1016/j.jplph.2012.05.027

Tyystjärvi E, Ali-Yrkko K, Kettunen R, Aro EM (1992) Slow degradation of the Dl protein is related to the susceptibility of low-light-grown pumpkin plants to photoinhibition. Plant Physiol 100:1310-1317. doi:10.1104/pp.100.3.1310

Tyystjärvi E, Aro EM (1996) The rate constant of photoinhibition, measured in lincomycin-treated leaves, is directly proportional to light intensity. Proc Natl Acad Sci USA 93:2213-2218.

Umena Y, Kawakami K, Shen JR, Kamiya N (2011) Crystal structure of oxygen-evolving photosystem II at a resolution of 1.9 Å. Nature 473:55-60. doi:10.1038/nature09913

Vainonen JP, Hansson M, Vener AV (2005) STN8 protein kinase in *Arabidopsis thaliana* is specific in phosphorylation of photosystem II core proteins. J Biol Chem 280:33679-33686. doi:10.1074/jbc.M505729200

Vass I, Styring S, Hundal T, Koivuniemi A, Aro E, Andersson B (1992) Reversible and

irreversible intermediates during photoinhibition of photosystem II: stable reduced Q_A species promote chlorophyll triplet formation. Proc Natl Acad Sci USA 89:1408-1412. doi:10.1073/pnas.89.4.1408

von Caemmerer S (2000) Modelling C_3 photosynthesis. In: von Caemmerer S (ed) Techniques in plant science No 2. Biochemical models of leaf photosynthesis, CSIRO Publishing, Collingwood, pp 29-71

Wünschmann G, Brand JJ (1992) Rapid turnover of a component required for photosynthesis explains temperature dependence and kinetics of photoinhibition in a cyanobacterium, *Synechococcus* 6301. Planta 186:426-433. doi:10.1007/BF00195324

Yokthongwattana K, Melis A (2006) Photoinhibition and recovery in oxygenic photosynthesis: mechanism of a photosystem II damage and repair cycle. In: Demmig-Adams B, Adams III WW, Mattoo AK (eds) Photoprotection, Photoinhibition, Gene Regulation, and Environment, Springer Netherlands, Heidelberg, pp 175-191. doi:10.1007/1-4020-3579-9_12

Yoshioka M, Yamamoto Y (2011) Quality control of Photosystem II: where and how does the degradation of the D1 protein by FtsH proteases start under light stress? - Facts and hypotheses. J Photochem Photobiol B 104:229-235. doi:10.1016/j.jphotobiol.2011.01.016

Zhang L, Paakkarinen V, Suorsa M, Aro EM (2001) A SecY homologue is involved in chloroplast-encoded D1 protein biogenesis. J Biol Chem 27:37809-37814. doi:10.1074/jbc.M105522200

Zhang L, Paakkarinen V, van Wijk KJ, Aro EM (2000) Biogenesis of the chloroplast-encoded D1 protein: regulation of translation elongation, insertion, and assembly into photosystem II. Plant Cell 12:1769-1782. doi:10.1105/tpc.12.9.1769